## ABSTRACT

HESTER, DAVID BARRY. Land Cover Mapping and Change Detection in Urban Watersheds Using QuickBird High Spatial Resolution Satellite Imagery. (Under the direction of Drs. Siamak Khorram and Stacy A.C. Nelson.)

The objective of this research was to develop methods for urban land cover analysis using QuickBird high spatial resolution satellite imagery. Such imagery has emerged as a rich commercially available remote sensing data source and has enjoyed high-profile broadcast news media and Internet applications, but methods of quantitative analysis have not been thoroughly explored.

The research described here consists of three studies focused on the use of pan-sharpened 61-cm spatial resolution QuickBird imagery, the spatial resolution of which is the highest of any commercial satellite. In the first study, a per-pixel land cover classification method is developed for use with this imagery. This method utilizes a per-pixel classification approach to generate an accurate six-category high spatial resolution land cover map of a developing suburban area. The primary objective of the second study was to develop an accurate land cover change detection method for use with QuickBird land cover products. This work presents an efficient fuzzy framework for transforming map uncertainty into accurate and meaningful high spatial resolution land cover change analysis.

The third study described here is an urban planning application of the high spatial resolution QuickBird-based land cover product developed in the first study. This work both meaningfully connects this exciting new data source to urban watershed management and makes an important empirical contribution to the study of suburban watersheds. Its analysis of residential roads and driveways as well as retail parking lots

sheds valuable light on the impact of transportation-related land use on the suburban landscape.

Broadly, these studies provide new methods for using state-of-the-art remote sensing data to inform land cover analysis and urban planning. These methods are widely adaptable and produce land cover products that are both meaningful and accurate. As additional high spatial resolution satellites are launched and the cost of high resolution imagery continues to decline, this research makes an important contribution to this exciting era in the science of remote sensing.

Land Cover Mapping and Change Detection in Urban Watersheds Using QuickBird High Spatial Resolution Satellite Imagery

by
David Barry Hester

A dissertation submitted to the Graduate Faculty of
North Carolina State University
in partial fulfillment of the
requirements for the Degree of
Doctor of Philosophy

Forestry

Raleigh, North Carolina

2008

APPROVED BY:

| | |
|---|---|
| Dr. Siamak Khorram<br>Co-chair of Advisory Committee | Dr. Stacy A.C. Nelson<br>Co-chair of Advisory Committee |
| Dr. Halil I. Cakir | Dr. Heather Cheshire |

## DEDICATION

To my grandparents,

Ed and Louise Hester

and

Joe and Hazel Dakin

## BIOGRAPHY

I was born and raised in Atlanta, Georgia. Growing up I enjoyed fishing and camping as well as working as much as possible on my grandparents' cotton, rice, and soybean farm in Mississippi. I earned a B.S. in Ecology at the University of Georgia in 2001. Between high school and entering NCSU as a graduate student, I worked at a retail lawn and garden center, in a home improvement store, on an organic vegetable farm, in a stream ecology laboratory, and on a Marine Corps base, where I was an Americorps volunteer in endangered species management. The summer after my junior year of college, my friend Lane Seabolt and I kayaked the length of the Mississippi River in a pair of sea kayaks. Each of these pursuits solidified my professional interest in maps and the environment.

I met the greatest natural beauty of them all, my now-wife Leslie, in middle school. We were friendly academic rivals in a tenth-grade biology class but did not date until after we went on the same undergraduate study abroad trip to Costa Rica. She actually made three semesters of graduate statistics at NCSU fun. We have two black labs, May and Sport, and we are expecting our first child, Bruce Edward, later this year. As our family and friends know, marrying Leslie was the smartest thing I've ever done.

I entered NCSU as a Master's student in 2003 and developed my thesis work into this dissertation before entering law school. I am currently a second-year law student at the Georgia State University College of Law in Atlanta. In the summer after my first year of law school, I was a legal intern with the U.S. Environmental Protection Agency. I will be pursuing a career in real or intellectual property law.

## ACKNOWLEDGMENTS

I want to first thank my graduate committee members for their support and patience throughout my unconventional trek through this degree program. Dr. Khorram provided a steady and experienced hand to move things along when I was tempted to take two steps backward without at least taking one forward. Dr. Nelson's hands-on approach and enthusiasm assured me that I would reach the finish line. Dr. Cakir's extra efforts consistently rescued me from dead-ends and pitfalls, while Dr. Cheshire provided dispassionate constructive criticism that improved the research each step of the way.

I also wish to thank the North Carolina Water Resources Research Institute (WRRI) for its financial support of this work. Its grant money was primarily used to purchase the satellite imagery at the center of this study. In addition, WRRI gave us three different opportunities to present our work publicly, engagements which immeasurably enhanced both the research and my own professional development.

Finally, I want to thank friends and family for their patience, advice, and support. From my colleagues at the Center for Earth Observation to my parents Tim and Guy Hester and in-laws Max and Lillian Alexander, I enjoyed a widely branched support network. Linda Babcock at the CEO provided timely answers to a host of burning logistic questions and presented a much-needed sense of humor. My lovely wife Leslie has been an incredible advocate and coach throughout this process, and May and Sport have patiently waited out many a thirty-minute "five more minutes." Some rawhides and new tennis balls are in their future.

# TABLE OF CONTENTS

## LIST OF TABLES

## LIST OF FIGURES

# 1. INTRODUCTION

## 1.1. Overall research objectives

The broad objective of this research was to develop land cover analysis methods for use with high spatial resolution satellite imagery. The recent emergence of high spatial resolution satellite imagery on the commercial market has revolutionized the remote sensing landscape and introduced new research opportunities. Analysis methods for use with this imagery, however, are still in their infancy. In three component studies, the work described here develops methods for analyzing high spatial resolution QuickBird imagery in urban watersheds. QuickBird imagery is uniquely suited to form the centerpiece of this work because it currently has the highest spatial resolution of any commercially available satellite data. This research was funded in large part by two grants from the North Carolina Water Resources Research Institute and is oriented around the relationship between impervious surface and water quality.

## 1.2. Dissertation organization

This dissertation is composed of three stand-alone journal manuscripts introduced by a literature review and followed by a section of conclusions and recommendations. Slight formatting differences in each manuscript chapter reflect the different requirements of the peer-reviewed journals to which they have been submitted for publication. While the second and third chapters are still under review by the *International Journal of Remote Sensing* and the *Journal of Environmental Management*, respectively, the first manuscript was published in the April 2008 edition of *Photogrammetric Engineering and Remote Sensing*, and its citation is:

Hester, D. B., H. I. Cakir, S. A. C. Nelson, and S. Khorram, 2008. Per-pixel classification of high spatial resolution satellite imagery for urban land cover mapping. *Photogrammetric Engineering & Remote Sensing*, 74(4): 464-471.

# 2. LITERATURE REVIEW

## 2.1. Introduction

The research described here develops methods for using high spatial resolution to map urban land cover and adds to a large body of remote sensing and geographic information systems (GIS) research. In this chapter, background information is presented in three major parts expanding upon concepts underlying the research presented in the three substantive research chapters, Chapters 3-5. While those chapters are intended to stand alone, an understanding of the principles and achievements therein is deepened by the materials presented here.

## 2.2. Land cover classification using high spatial resolution satellite imagery

### *2.2.1.* Recent advances in remote sensing technology

Recent advances in the type and quality of remotely sensed data expanded its range of environmental monitoring applications. Available aerial photography has steadily increased in spatial resolution, and new sensors are capturing these data in digital format, eliminating the problematic and time-consuming hard- to soft-copy conversion necessary for previous imagery. For satellite sensors, the last decade has been an unprecedented period of increasing data abundance, diversity, and quality (see Table 2-1, adapted from Rogan and Chen (2004)). This has been a function of increases in research demand as well as the commercialization of satellite data. Inevitably, new research and processing challenges have emerged alongside these data improvements, and the remote

**Table 2-1. Characteristics of selected satellite sensors.**

| Sensor Mission | Organization | Operation period | Swath width (km) | Spatial res. | Temporal res. | Radiometric res. | Spectral res. (µm) | Spectral Channels |
|---|---|---|---|---|---|---|---|---|
| MSS (Landsat 1-5) | NASA, USA | 1972-1983 | 185 | 75 (MS) 240 (TIR) | 16-18 days | 8-bit | 0.5-12.6 | 4 |
| AVHRR (NOAA 6-15) | NOAA, USA | 1978- | 2700 | 1100 | 12 hours | 10-bit | 0.58-11.5 | 5 |
| TM (Landsat 5) | NASA, USA | 1984- | 185 | 30 (MS) 120 (TIR) | 16 days | 8-bit | 0.45-2.35 | 7 |
| HRV (SPOT 1-3) | SPOT Image, France | 1986- | 60 | 10 (PAN) 20 (MS) | 26 days | 8-bit | 0.50-0.89 | 3 |
| LISS-I (IRS-1A) | ISRO, India | 1988- | 148 | 72.5 | 24 days | | 0.45-0.86 | 4 |
| LISS-II (IRS-1B) | ISRO, India | 1991- | 146 | 36.25 | 24 days | | 0.45-0.86 | 4 |
| SAR, OPS (JERS-1) | NASDA, Japan | 1992- | 75 | 18 | 44 days | | 0.43-1.7 | 7 |
| LISS-III (IRS-1C, 1D) | ISRO, India | 1995- | 142 | 23, 70 188 (WiFS) | 24 days | 7-bit | 0.52-1.7 | 4 |
| SAR (RADARSAT-1) | Canada | 1995- | 45-500 | 8-100 | 24 days | 4-bit | N/A | 1 |
| Panchromatic (IRS-1D) | ISRO, India | 1997- | 70 | 5.8 | 24 days | 7-bit | 0.50-0.75 | 1 |
| GOES-8,10 | NESDIS, USA | 1994- | 8 | 1000 (VNIR) 8000 (SWIR) 4000 (TIR) | 0.25 - 3 hours | 10-, 13-bit | 0.52-12.5 | 5 |
| SAR OPS (ERS-2) | ESA | 1995- | 102 | 26 | 35 days | | N/A | N/A |
| HRVIR (SPOT 4,5) | SPOT Image, France | 1998- | 60 | 10 (PAN) 20 (MS) | 26 days | 8-bit | 0.50-1.75 | 3 |
| Vegetation (SPOT 4,5) | SPOT Image, France | 1998- | 2250 | 1150 | 26 days | 8-bit | 0.43-1.75 | 5 |
| SeaWiFS (OrbView-2) | GeoEye, USA | 1997- | 2800 | 1130 | 24 hours | | 0.40-0.88 | 8 |
| MODIS (EOS) | NASA, USA | 1999- | 2300 | 250 (PAN) 500 (VNIR) 1000 (SWIR) | 1-2 days | 12-bit | 0.620-2.155, 3.66-14.385 | 36 |
| ASTER (EOS Terra) | NASA and MITI, USA | 1999- | 60 | 15 (VNIR) 30 (SWIR) 90 (TIR) | 4-16 days | 8-, 8-, 12-bit | 0.52-0.86, 1.60-2.43, 8.125-11.65 | 14 |
| MISR (EOS Terra) | JPL and NASA, USA | 1999- | 360 | 275 | 16 days | | 0.425-0.886 | 4 |
| ETM+ (Landsat 7) | NASA, USA | 1999- | 185 | 15 (PAN) 30 (MS) 60 (TIR) | 16 days | | 0.45-2.35, 10.4-12.5 | 7 |
| IKONOS | Space Imaging, USA | 1999- | 11 | 1 (PAN) 4 (NIR) | 2-5 days | 11-bit | 0.45-0.90 | 4 |
| QuickBird | DigitalGlobe, USA | 2001- | 6, 30 | 0.61 (PAN) 2.44 (MS) | 1-4 days | 11-bit | 0.45-0.90 | 4 |
| Hyperion and ALI (EO-1) | NASA, USA | 2000- | 7.5, 185 | 10 (PAN) 30 (MS) | 16 days | | 0.433-2.35 | 242, 9 |
| MERIS (Envisat-1) | NASA, USA | 2001- | 1150 | 300, 1200 | 35 days | | 0.39-1.04 | Up to 15 |
| ASAR (Envisat-1) | NASA, USA | 2001- | 400 | 30 | 35 days | | Radar | 1 |
| HRG (Spot 5) | SPOT Image, France | 2002- | 60 | 5 (PAN) 10 (VNIR) 20 (SWIR) | 26 days | 8-bit | 0.48-1.75 | 3 |
| OrbView-3 | GeoEye, USA | 2003-2007 | 8 | 1 (PAN) 4 (MS) | 3 days | 11-bit | 0.45-0.90 | 4 |

sensing community has responded with continued innovation and growth. Specific gains in satellite-derived remote sensing data quality have occurred in each of the four components of its resolution: spectral, spatial, radiometric, and temporal. Advances in spectral resolution

There are three broad classes of data spectral resolution, a description of the range and partitioning of the electromagnetic reflectance recorded by a sensor. Three classes loosely divide sensors into general levels of spectral sensitivity as panchromatic (one spectral band), multispectral (multiple spectral bands), and hyperspectral (many spectral bands) data (Jensen, 2005). Traditional satellite-derived remote sensing data are captured in panchromatic or multispectral format, with the seven spectral channels of Landsat TM and ETM+ marking the high end of satellite data spectral resolution in recent years.

The emergence of space-borne platforms capturing more spectrally complex data during the last decade has been a revolutionary phenomenon. While its data are considered multispectral, the Moderate Resolution Imaging Spectroradiometer (MODIS) instrument aboard NASA's Terra (EOS AM) and Aqua (EOS PM) satellites is one example of this area of advancement. MODIS has been collecting data since 1999, and it provides 36 discrete spectral channels of information (NASA, 2003). Additionally, ASTER (Advanced Spaceborne Thermal Emission and Reflection radiometer) carried only by the Terra satellite records reflectance in 14 bands of spectral information (NASA, 2008). The first satellite equipped with actual hyperspectral-recording capability, however, was launched in 2000 by NASA. The EO-1 satellite carries Hyperion, a sensor which records data in 220 spectral channels and functions as a true imaging spectrometer

(USGS, 2006). Previous to Hyperion, the rich information content provided by hyperspectral data had only been produced by airborne or field instruments. Satellite-derived hyperspectral sources are more consistent, affordable, and repeatable than their aerial counterparts, and, thus, Hyperion represents a huge forward leap for remote sensing.

Imaging spectroscopy, as the analysis of the spectral profiles recorded in hyperspectral data is known, is a powerful tool for discriminating between different types of minerals or identifying stressed vegetation, for example. Challenges to the use of hyperspectral data include its volume and processing requirements. Before these data can be used for terrestrial characterization or environmental monitoring, unique spectral "endmembers" must be generated to represent the diverse reflectance or emittance behavior of potential scene features (Lillesand and Kiefer, 2004). These challenges are not unique to remotely sensed or space-derived hyperspectral data, but the scale and diversity of the landscapes studied with these data require particularly intense computations.

The increased availability and affordability of space-derived hyperspectral data has spawned broader interests in its application. Whereas its widespread use had previously been limited to relatively specific fields such as mineralogy, the space age of hyperspectral data is opening up new research area for which spectral profiles are not well-defined. For example, recent work has tried to develop a set of hyperspectral profiles for the complex urban landscape (Herold et al., 2004). Other new applications of these data include studies of marine and estuarine water quality in Australia (Brando and

Dekker, 2003), invasive species in China (Galvao et al., 2005), sugarcane species in Brazil (Ramsey et al., 2005), and forest classification in the United States' Pacific Northwest (Goodenough et al., 2003).

#### 2.2.1.1. Increases in spatial resolution

Increases in satellite spatial resolution, or the ground size of pixels, have been achieved in imagery provided by a number of American commercial ventures, a direct result of the U.S. Government's 1994 decision to allow such firms to collect and market this type of data (Rogan and Chen, 2004). In 1999, Space Imaging's IKONOS satellite was launched to deliver a landmark one-meter (panchromatic) and four-meter (multispectral) image product. Subsequently, sensors which have matched or exceeded the one-meter pixel size threshold have qualified among the new class of high spatial resolution platforms. Most notably, these include OrbView-3 and QuickBird-2 (Maktav et al., 2005). At the same time, aerial-based systems have steadily increased in spatial resolution, and many now capture imagery with pixel sizes as small as 30 cm (Thomas et al., 2003). High resolution satellite imagery has the potential, however, to be a more consistent and affordable data source of the same quality. In addition, satellite-derived satellite imagery can capture large areas under identical temporal and atmospheric conditions, a task for which aerial sources are not ideally suited (Carleer and Wolff, 2004). This is true even in areas that are difficult to service by aircraft.

Existing meter- or sub-meter spatial resolution satellite imagery is captured in panchromatic or, at its spectral best, in blue-green-red-near infrared multispectral imagery. This represents a potential limitation of this data type for applications that are highly sensitive to spectral response, such as automated species-level tree mapping. In general, the minimal spectral detail accompanying high spatial resolution imagery may make automated image land cover classification difficult because the high level of spatial detail will result in increased scene heterogeneity (Carleer et al., 2005). Spatially coarse data, in contrast, has a smoothing effect on variable spectral responses. In the same way, high spatial detail presents added classification complexity because this imagery can be replete with shadows (Dare, 2005; Thomas et al., 2003; Fisher and Goetz, 2001). Methods to deal with this image complexity are in their infancy; data storage and processing requirements are a concern with this kind of data, as well.

As is true for any data type, cost is an important factor in the use of high spatial resolution imagery. Tasked multispectral QuickBird data cost \$58/km$^2$ at its initial offering in 2000 (Read et al., 2003). This was more than 27,000 times the cost of acquiring Landsat ETM+ data in 2003, \$0.00213/ km$^2$ (Rogan and Chen, 2004). Archived bundled QuickBird data is currently available for \$20/km$^2$, however, and the cost of new tasked imagery has decreased to \$25/km$^2$. With several additional high spatial resolution satellite platforms expected to launch by 2009, the price of these data will only become increasingly competitive with traditional sources.

#### 2.2.1.2. Advances in radiometric resolution

Next-generation high spatial resolution sensors have ushered in another area of improvement in satellite remote sensing technology: increases in radiometric resolution. *Radiometric resolution*, also known as quantization, is a measure of the range of possible data values to which reflectance intensity can be assigned, and it is expressed as digital bit depth. Higher radiometric resolution means that a sensor is more sensitive to differences in brightness values (Jensen, 2005). Conventionally, satellite imagery has been stored as 8-bit data, although Advanced Very High Resolution Radiometer (AVHRR) and Geostationary Operational Environmental Satellite (GOES) data are stored in at least 10-bit format. These satellites, however, have coarse spatial resolutions (1000-4000 km) and are primarily used for monitoring global phenomena such as weather patterns. Higher radiometric resolution data has been reserved for spatially coarse sensors due to digital storage and processing requirements. As a result, some applications which would have required both high spectral and spatial resolutions have been hindered. Kutser et al. (2005) found that, while 8-bit Landsat 7 was not adequate to map colored dissolved organic matter (CDOM) in boreal lakes in Finland, 11-bit Advanced Land Imager (ALI) data from the EO-1 platform was sensitive enough to map CDOM at a wide range of concentrations.

The most recent generation of high spatial resolution satellites, including the commercial IKONOS by Space Imaging, Inc., QuickBird by DigitalGlobe, Inc., EROS A by ImageSat International N.V., and OrbView-3 by GeoEye all collect imagery in 11-bit radiometric depth. This aspect of this imagery's quality is often overshadowed by its spatial resolution, but analysts using these data have found that its radiometric quality is an extremely important element of its utility ( Kutser et al., 2005; Elvidge et al., 2004). High levels of radiometric resolution continue to present data storage and processing concerns, but Rogan and Chen (2004) point out that recent advances in remote sensing data quality have been matched with advances in computer hardware and image processing software.

#### 2.2.1.3. Increases in temporal resolution

As has been the case with high radiometric resolution, the highest temporal resolutions in satellite data have been limited to sensors with relatively low spatial resolution like GOES and AVHRR, whose revisit periods are 15 minutes to 12 hours, respectively (Rogan and Chen, 2004). This is appropriate to their functional purposes in monitoring ever-changing weather and oceanic conditions. Sensors such as the Landsat and SPOT series which have moderate spatial resolutions have revisit periods from 16 to 26 days.

Next-generation satellite sensors have achieved higher spatial resolution by orbiting at lower altitudes (705 km for Landsat 7 vs. 450 km for QuickBird), but this translates into much narrower at-nadir ground swaths (185 km for Landsat 7 vs. 16.5 km for QuickBird) and thus potentially less frequent overpass. More than compensating for this loss of revisit frequency, however, these sensors are pointable as much as 30° off-nadir, which means that their effective revisit period is from 1-3 days. Thus, recent increases in spatial and temporal resolution have been coupled in some sensors. This off-nadir acquisition capability also enables stereo-pair image capture, which can be used for stereoscopic feature and elevation extraction. The disadvantage of off-nadir image capture is that spatial resolution varies in the imagery captured by these pointable sensors, and geometric distortions can be severe. Furthermore, these stated revisit periods depend on the availability of cloud-free acquisition windows. Both of these complications can require extensive pre-processing time and can ultimately limit map accuracy.

### *2.2.2.* Defining land use and land cover

In the work described here, high spatial resolution satellite imagery was used to analyze urban land use and land cover. Although the terms are often used interchangeably, the concepts of land use and land cover are distinct and will be helpfully kept separate in considering this research. *Land cover* is the type of physical surface present at a given point on the earth (e.g., forest or water). *Land use*, on the other hand, denotes the type of human activity taking place at that point (e.g., agricultural or residential) (Lillesand and Kiefer, 2004). Barr and Barnsley (2000) articulate that land use is a matter of function and land cover a matter of form. Land cover has been described as a "fundamental variable" having local, regional, and global implications, and some researchers assert that land use/land cover (LU/LC) policy has the potential to significantly influence the effect of climate change on ecological systems (Pyke and Andelman, 2007; Foody et al., 2002).

The difference between land cover and land use importantly informs the research reported here. A predominant theme in this work is the analysis of impervious surface, a category of land cover that Arnold and Gibbons (1996) define as any material that prevents the infiltration of water into soil. The first two studies of the research presented here principally focus on land cover, while the third explores the interplay between suburban land cover and land use as it relates to water quality. Separating the concepts of land cover and land use is especially important in the context of remotely sensed image analyses such as that reported here because it uses *land cover* reflectance properties to generate maps meaningful to *land use* policy considerations.

#### *2.2.3.* Land cover classification categorization schemes

Broadly, land cover analyses can utilize field-based or remotely sensed data sources. Field-based land cover classification can extract detailed landscape information but is limited in its geographic scope. Time and labor constraints generally impact the extent of field data collection, and statistical analyses are used to determine the impact of sampling design on output significance. Remote sensing sources, such as satellite imagery or aerial photography, have a different set of output limitations, such as cost, spatial and spectral resolution, and interpretability (Jensen, 2005).

No matter what the input data, category definitions are central to LU/LC mapping. For example, a hypothetical field-based forest inventory is likely to be rich in information content; the analyst has the potential to identify and measure forest stand information that can be aggregated into an output map. Given this specificity and potential subjectivity, it is particularly important that this user develop clear class definitions before she develops this output map. This is because the output map's statistical defensibility or its applicability to future studies may depend on the ability of other users to repeat the categorization effort. If time or labor is a major constraint, this analyst may find from initial work that it is necessary to broaden or generalize one of her metrics (e.g., from species to genus) to reflect these considerations. Furthermore, generalization may be necessary when the analyst begins to share or present his/her findings because of visual or audience requirements. These adjustments to class definitions change the entire study process and map output.

When LU/LC products are derived from remote sensing data, the desired output information similarly drives the analysis process. Consider the widely-used National Land Cover Database 2001 (NLCD 2001) produced by the Multi-Resolution Land Characteristics Consortium (MRLC) in the United States. This hybrid LU/LC product was developed by the combined resources of nine federal agencies (such as EPA, USGS, and NOAA) in an effort to provide data for all 50 states that is flexible enough to meet the needs of a wide variety of end-users (Homer et al., 2004).

The ambitious MRLC land cover mapping goal of representing the entire United States informed both the categorization class definitions and the required input data. In general, the classification scheme is a modified version of the hierarchical Anderson Classification System (Anderson et al., 1976). This scheme provides a standardized template for LU/LC mapping that can be broadened or refined to suit study goals, which has made it particularly attractive for mapping large, diverse areas like the entire United States. A more rigorous classification scheme might have had less regional applicability and less end-user flexibility, two attributes which MRLC desired its land cover products to have. Furthermore, the wide availability and relative affordability of Landsat series data made it an obvious match with study needs.

In light of the large area MRLC attempted to map in NLCD 2001, it was not reasonable (using existing methods) to time- and cost-effectively map individual single-family homes or parking lots in their output products. This is especially true given the well-developed body of research which has developed automated or semi-automated means of rapidly deriving LU/LC information from Landsat data. Instead of mapping partitioned categories of impervious land uses, NLCD 2001 depicts "Developed" land of various aggregate intensities of imperviousness. "Developed, Low Intensity," for example is a NLCD 2001 category defined as areas in which "impervious surface account for 20-49 percent of total cover" (Homer et al., 2004). Unlike the previous MRLC land cover product, NLCD 1992, the 2001 version also includes a map of per-pixel imperviousness, reflecting a value-added derivative of the relatively coarse Landsat data that is very adaptable to a variety of potential research areas, such as urban planning or stormwater modeling. Both of the NLCD maps which represent developed land ultimately reflect the MRLC analysis goals for its 2001 products: comprehensive United States coverage and map output flexibility for a variety of end users.

At the other end of the remote sensing land cover analysis input data spectrum, class definitions in LU/LC mapping are equally important. Manual delineation is a predominant means of deriving LU/LC from aerial photography. While manual photointerpretation is possible using relatively spatially coarse satellite data, such as Landsat TM data, data that are high in spatial resolution can be readily delineated into LU/LC maps by hand and have been extensively used for that purpose since World War I (Lillesand and Kiefer, 2004).

This capacity implicates an important consideration of LU/LC mapping using any high spatial resolution remotely sensed data: LU/LC categories must be defined in a way that reflects the lack of discrete boundaries in nature. Except for certain anthropogenic land development, landscapes are often a mosaic of transitional land cover. A study of non-urban land cover, for instance, will need to accommodate mixed forest types, unless the minimum mapping unit is as small as individual tree trunks or crowns. A study like that of Oswald (2000) might only consider pine composition and therefore individual forest stands as the smallest unit of mapping interest. Alternatively, Miyamoto et al (2004) used balloon-mounted camera, 15-cm photography in a recent study of plant diversity within a Japanese wetland, visually interpreting the photography to successfully make genus-level identification between such individual features as dwarf shrubs and sedges. Undoubtedly, the choice of classification scheme categories will be limited by the spatial resolution of data at hand, but the choice of the image or photographic data itself should ideally have been a function of study goals.

#### *2.2.4.* Land cover classification and high spatial resolution satellite imagery

High spatial resolution data present a particular set of methodological challenges in its use for urban land cover classification. Urban areas are spatially complex, and they represent a mosaic of heterogeneous land uses and land covers. This detail has prompted some analysts to map the urban landscape indirectly by reference to the extent of development. For instance, McCauley and Goetz (2004) used Landsat TM data and a decision tree classifier to map residential land use along a low-high gradient of development intensity. Such an approach acknowledges that urban land use is diverse at scales smaller than 30 m TM data, but it does not attempt to directly map this diversity. This is a similar convention used in the recent Multi-Resolution Land Characteristics Consortium 2001 National Land Cover Database (Homer et al., 2004) to specify degrees of development in which impervious surfaces cover a specified percentage of total pixel land cover.

High spatial resolution data enables analysts to map heterogeneous urban land cover directly and precludes the need to aggregate. This capability, though, is fraught with challenges because of the spatial detail which enables it. As discussed earlier, the effective aggregation of landscape features (such as shadows or small features such as individual, isolated trees) by spatially coarse data may actually be desirable for LU/LC mapping purposes. The strategies that have previously been successful in LU/LC classification for coarse data, in turn, may not necessarily translate into classification success with spatially fine data (Thomas et al., 2003). These considerations have motivated a whole new range of textural (Johansen and Phinn, 2006), morphological (Cablk and Minor, 2003), and image segmentation (Carleer et al., 2005) classification approaches for use with high spatial resolution imagery. Many of these new methods are inspired by the mapping of urban places.

Conventional per-pixel classifiers, such as the maximum likelihood and minimum-distance-to mean algorithms, are spectral-based classification methods and constitute a historically dominant approach to remote sensing-based automated LU/LC derivation (Gao et al., 2004). The maximum likelihood classifier, in fact, is frequently used as a "benchmark" against which novel classification algorithms are evaluated (Song et al., 2005). Such classifiers are widely available in commercial image processing software packages and enjoy widespread user familiarity. It has been suggested that traditional per-pixel classification methods have limited applicability to high spatial resolution data because they cannot fully exploit its information content (Hu et al., 2005). Other analysts have reported that the detail of high spatial resolution imagery has confounded conventional automated land cover classification techniques, particularly in studies of heterogeneous urban environments. Problematic aspects have included shadows (Dare, 2005; Barr and Barnsley, 2000), high reflectance variability but limited spectral information (Carleer et al., 2005), general image complexity (Hu et al., 2005) and data volume (Fisher and Goetz, 2001).

Several spectral-based classification studies of high spatial resolution imagery have been more successful. Goetz et al. (2003) reported overall and per category accuracies of between 75 and 85 percent for supervised and unsupervised classifications of a leaf-on and leaf-off mosaic of 4 m IKONOS imagery. The researchers in that study also used decision tree classifiers that incorporated only spectral information, including band ratios, to map urban imperviousness and tree canopy with overall accuracies of 84.2 percent and 97.3 percent, respectively. Sawaya et al. (2003), also working with IKONOS data, adapted modeling approaches developed for Landsat TM data to accurately describe urban lake water clarity using unsupervised per-pixel classification ($r^2 = 0.94$) and developed regression equations between IKONOS-derived normalized difference vegetation index (NDVI) values and sample area percent imperviousness. These equations were used to estimate percent impervious surface with a reference-data correlation of 0.98. Thomas et al. (2003) concluded that their pixel-based approach to urban impervious surface mapping using high spatial resolution imagery had only moderate success due to the limited spectral content of those data. That study classified land cover in an urban desert ecosystem using 8-bit aerial scanner imagery. Notably, several high spatial resolution satellite image sensors, including IKONOS, QuickBird, and GeoEye's future OrbView-5 satellite, are designed to record reflectance data in 11-bit radiometric depth. A fundamental premise underlying the research reported here is that, in light of such qualities, the utility of familiar pixel-based approaches to mapping LU/LC using next-generation satellite imagery has not been fully exhausted.

*2.2.5.* Data fusion

The recent advances in the quality and diversity of remote sensing technology have been paralleled by innovations in image fusion that may also enhance the effectiveness of pixel-based classification. Using image fusion algorithms, lower resolution satellite imagery can be spatially sharpened with higher resolution imagery. Data fusion, in this sense, is the combination of the two image types that results in one image with panchromatic ground resolution and multispectral spectral resolution (Svab and Osti, 2006; Pohl and van Genderen, 1998). The Cakir-Khorram algorithm featured in the research reported here (Cakir and Khorram, 2004) achieves this combined resolution while preserving spectral integrity better than conventional image fusion algorithms, such as principal components analysis and intensity-hue-saturation fusion.

Other data fusion varieties may also be useful to high spatial resolution image classification. The integration of ancillary GIS data with per-pixel classification has long been a successful land cover derivation technique with a variety of medium- and low-resolution image types (Ludwig et al., 2003; Lunetta et al., 2003; Foody, 1995), but, as of yet, its applicability to high-resolution data has only been cursorily examined (Sawaya et al., 2003; Thomas et al., 2003). This is despite the inherent suitability of such imagery to these techniques, the efficacy of which depends on sufficient geographic alignment

(Cablk and Minor, 2003).

*2.2.6.* Summary

The type and quality of satellite-based remote sensing data sources has expanded dramatically during the last decade. Among these expansions, commercially available imagery has emerged at resolutions comparable to that of aerial photography and in inherently digital format, at 11-bit radiometric resolution, and with 1-3 day revisit periods. These advances make this imagery an exciting data source for the study of urban land cover. Although researchers have reported limitations to the applicability of conventional land cover classification methods to high spatial resolution imagery, these approaches enjoy widespread familiarity and should not be quickly dismissed if techniques to overcome such limitations are conceivable. Image fusion and the integration of ancillary GIS data are among the most promising of these techniques.

## 2.3. Remote sensing-based land cover change detection

*2.3.1.* Change detection methods

Change detection using remote sensing data is an attempt to record natural and anthropogenic transitions occurring on Earth (Jensen, 2005). The choice of input data for this purpose will depend on the application interests, study area size, and landscape features of concern, and the analysis can be done using either manual or automated methods or both. The spatial scale and information content of satellite-derived remote sensing data, though, has inspired a proliferation of automated change detection algorithms and methodologies, especially for evaluating and recording land use / land cover (LU/LC) change. In the broadest sense, these automated options can be categorized as pre-classification, post-classification, or advanced.

2.3.1.1. Pre-classification change detection

Pre-classification methods develop change maps from multitemporal data without first generating classified LU/LC maps from that data (Jensen, 2005). These change algorithms may transform or simplify the original data before creating a change map, but they do not rely on the generation of meaningful classifications of the individual image dates. One of the most critical aspects of any pre-classification change detection algorithm is the specification of a change threshold. This parameter, either derived by the analyst using initial algorithm output or by the analyst using only *a priori* knowledge, represents the interpretative mechanism by which the algorithm judges whether change has occurred.

The change threshold will have as many different forms as there are pre-classification methods. Some of the most notable of these methods include image differencing, image regression, imaging ratioing, vegetation index differencing, principal component analysis (PCA), and change vector analysis (Lu et al., 2004). In each of these methods, the analyst's major responsibility is to interface with the algorithm in defining the change threshold. If input imagery is suitably matched in terms of geometric, radiometric, and atmospheric quality, then the major advantage of pre-classification change detection is its theoretical simplicity; the implementation of these approaches may be computationally intensive but do not introduce a great deal of analyst interpretation as they evaluate the quantitative differences in image dates.

One notable drawback to pre-classification change analysis is that geometric and radiometric alignment between image dates may be difficult or even impossible to achieve. The most significant limitation, however, to all pre-classification approaches is that they cannot provide a complete "from-to" representation of change (Jensen, 2005). They are primarily equipped to identify either binary or scaled indicators of "change" or "no change." As such, they are particularly robust in measuring in-category and landscape-level change, as in the forest defoliation study by Muchoney and Haack (1994) and the analysis of continent-scale land cover change in Africa by Lambin and Ehrlich (1996).

#### 2.3.1.2. Post-classification change detection

Post-classification change detection provides a detailed matrix of "from-to" change and generally requires a great deal of preparatory analyst input. In this approach, the original study imagery is either thematically classified or otherwise used to derive a secondary input product. The change analysis occurs when the classified maps are compared by one or more of the diverse post-classification methods. These include the expectation-maximization algorithm, artificial neural networks (ANN), unsupervised change detection, and hybrid change detection (Lu et al., 2004). Each classification output introduces error into any post-classification change analysis, and this error is magnified in the final change map by the aggregate classification errors from each input image. Importantly, though, in addition to the advantage of the "from-to" output generated by these approaches, post-classification change detection can minimize the effect of atmospheric and environmental disparity between input images. These traits and its computational simplicity have made post-classification change analysis the most widely applied variety (Jensen, 2005).

2.3.1.3. Other approaches to remote sensing-based change detection

Advanced change analysis methods integrate ancillary Geographic Information System (GIS) data, statistical models, spatial analysis, textural metrics, or other alternative to pre- and post-classification approaches (Lu et al., 2004). These methods are too diverse to fit many general characterizations, but they are usually developed in response to specific research area issues or LU/LC categories of particular interest. Examples of advanced methods include those using measures of spatial dependence (Henebry, 1993), generalized linear models (Morisette et al., 1999), spatial-spectral structure (Zhang et al., 2002), and spatial statistics (Read and Lam, 2002).

*2.3.2.* Mapping urban land cover change using high spatial resolution satellite imagery

The dynamic nature of urban environments presents unique challenges to remote sensing-based change detection. Concern over the rate, permanence, and impact of certain land cover changes, such as forest conversion to impervious surface, has spawned a diverse research interest in mapping and understanding urban change (Wilson and Lindsey, 2005; Stone, 2004; Arnold and Gibbons, 1996). Urban change mapping efforts can focus on evaluating changes in the spatial boundary or extent of urban places or in the physical landscape changes that have occurred (Zhang et al., 2002). Furthermore, analysts of urban environments can choose to map changes in either land use (McCauley and Goetz, 2004), land cover (Dougherty et al., 2004; Jennings et al., 2004), or aggregate landscape-level metrics (Jin and Shepherd, 2005) and can accomplish this using a wide range of remote sensing data. Especially with respect to impervious residential and transportation features, however, urban change is characterized by disjointed, incremental change. These small changes are emerging as key elements of environmental and municipal degradation (Stone, 2004), but they may not be adequately represented in some data types.

Recent advances in sensor spatial resolution have made satellite data type a formidable media with which to map urban land cover and its change. DigitalGlobe's QuickBird sensor has provided imager with nominal spatial resolutions of 61 cm in the visible range (panchromatic) and 2.44 m multispectral (blue-green-red-infrared) since 2000 (DigitalGlobe, 2006). This type of data is of a spatial and radiometric quality suitable to capturing the irregular, small-increment LU/LC changes that occur in urban areas. High spatial resolution satellite imagery has already been used to accurately map single-image impervious surface extent and distribution (Goetz et al., 2003; Sawaya et al., 2003).

While the next-generation of high spatial resolution satellites such as QuickBird and IKONOS provide high quality 11-bit data with submeter ground pixel size and have been shown to have land cover mapping promise, their use in change analyses raises both familiar and unique trade-offs. One inherent limitation is the spectral resolution of these data. The heterogeneity of urban landscapes coupled with this imagery's spatial detail results in a complex spectral response. Four discrete spectral bands in the visible and near infrared wavelengths at a high spatial resolution may not be enough spectral specificity to statistically define distinct scene endmembers, especially when sunlit and shaded sides of the same feature will have such different spectral responses (Carleer et al., 2005). If this issue cannot be resolved by an attempted classification process for two image dates, then pre-classification change detection may be the only viable change mapping option. However, as described above, pre-classification algorithms rely primarily on quantifiable image statistics to generate change maps and will also be hindered by extreme spectral variability. The 11-bit depth of this imagery will be a positive attribute in this respect, but there are other challenges to the implementation here of pre-classification change detection.

Foremost among these is this difficulty of achieving the accuracy of image co-registration necessary to perform successful pre-classification change detection using high spatial resolution imagery. Because these sensors are pointable, they often acquire extreme off-nadir images in order to accomplish frequent revisit periods at their low orbit. This results in both slightly variable spatial resolutions as well as significant variations in image geometric distortion. Additionally, the high spatial resolution of these images approaches the limits even of highly accurate georeferencing data such as that of differentially corrected Global Positioning Systems (GPS). Thus, although pre-processing methods can aid in geo-registering multiple dates of these images, some misregistration is inevitable and will certainly degrade change detection accuracies. Change detection error due to image misregistration has already been noted as a particular problem with high spatial resolution data (Wang and Ellis, 2005).

While misregistration will negatively affect both pre- and post-classification change detection success and accurate image classification with these data are not computationally simple, a combination of post-classification and advanced methods of change detection will likely extract the most accurate and useful change maps from this imagery. One justification for this reasoning is that the creation of accurate individual date LU/LC maps with this imagery, as briefly detailed above, has been more thoroughly researched than has using these data for pre-classification image algebra or regression analysis. Furthermore, cleaning up spurious change regions may be a more straightforward process in evaluating post-classification change maps than pre-classification maps since a detailed “from-to” record is available. In urban areas, ancillary GIS data is also likely to exist, and this extra information could assist in all aspects of classification and change detection using this imagery.

#### *2.3.3.* Summary

While its spatial detail may be an obstacle to accurate image co-registration and the detection of true change, next-generation high spatial resolution satellite imagery is rich in information content and is a promising source of land cover change monitoring data. The integration of GIS data as well as simple reasoning about post-classification “from-to” indications of change may be highly feasible means of improving high spatial resolution change detection given the image detail it captures. In urban areas, where rapid and complex land use change is the norm, the research utility of accurate high spatial resolution satellite-based change detection is high.

### 2.4. An application of high spatial resolution land cover mapping: Impervious surface and suburban watersheds

#### *2.4.1.* The environmental impact of sprawl

In the research reported here, methods for using high spatial resolution imagery to map land cover were developed using QuickBird imagery of a suburban watershed in the

United States. The land use pattern in this area exemplifies a form of growth that might be referred to as *sprawl*. Galster (2001) notes that this term is not easily defined but generally refers to the patterns, processes, causes, and consequences of low-density and segregated-land use development in populated places. Sprawl has been criticized as having negative social impacts, such as increased racial and economic segregation (Yang and Jargowsky, 2006), and impacts on individual health, including increased childhood obesity (Ewing et al., 2006) and body mass index (Pendola and Gen, 2007; Ross et al., 2007) due to its influence on transportation choices. Sprawl has also been described as a comparatively costly design for municipalities to serve with public services such as water and sewer infrastructure (Speir and Stephenson, 2002) and roads (Burchell and Mukherji, 2003). Decreased air quality (Borrego et al., 2006) and the loss of open space, or pockets of undeveloped urban land (Torres et al., 2007), are often counted as among sprawl's environmental harms.

The potential of sprawling suburban development to impact water quality is well-documented ( Tu et al., 2007; Interlandi and Crockett, 2003; Bowen and Valiela, 2001). Some analysts have estimated that substantial declines in watershed health begin to occur with as little as 10% impervious cover (Arnold and Gibbons, 1996). Sprawl poses a unique threat to urban surface water quality in part because it incorporates an extensive array of impervious features, such as roads, rooftops, and parking lots. This threat can add to the fiscal strain placed on growing municipalities already financing stormwater management with special fees and utilities (Kasperson, 2001). On the other hand, low-density suburban areas can accommodate an arrangement of open space that actually mitigates stormwater volume and pollution (Moglen and Kim, 2007). Such a result is indicative of a proper understanding of the spatial relationship between suburban land use and surface water quality (Brabec et al., 2002).

*2.4.2.* Sprawl and high spatial resolution land cover mapping

High spatial resolution satellite imagery has a significant potential to assess the ecological impact of sprawl. Its spatial detail is inherently well-suited to integration with ancillary GIS data, such as stormwater infrastructure layers, that account for essential alterations to hydrologic function and are receiving increasing research attention (Walsh et al., 2004). Recent work has reinforced the related notion that the location of impervious surface may be determinative of watershed health than its extent ( Moglen and Kim, 2007; Snyder et al., 2005). This implicates the core strength of high spatial resolution data. These advantages build on those satellite imagery has conventionally had over aerial-derived imagery and field-based inventory, including its capacity for updated synoptic coverage and its inherently digital format ( Cablk and Minor, 2003; Barr and Barnsley, 2000).

*2.4.3.* Summary

Suburban development characterized as sprawling is closely tied to private automobile transportation and low-density residential development. Beyond its cultural critiques, sprawl is purported to have environmental impacts in growing metropolitan areas. In particular, its association with impervious surface implicates water quality degradation. This association, however, is not well-understood. Novel high spatial resolution satellite imagery is a promising source of data for the analysis of this relationship because suburban land use is an intricate array of land cover.

### 2.5. References

Anderson, J. R., E. E. Hardy, J. T. Roach, and R. E. Witmer. 1976. A land use and land cover classification system for use with remote sensor data. *U.S. Geological Survey Professional Paper 964*, 28 p.

Arnold, C., and C. Gibbons, 1996. Impervious surface coverage - The emergence of a key environmental indicator. *Journal of the American Planning Association*, 62: 243-258.

Barr, S., and M. Barnsley, 2000. Reducing structural clutter in land cover classifications of high spatial resolution remotely-sensed images for urban land use mapping. *Computers and Geosciences*, 26: 433-449.

Borrego, C., H. Martins, O. Tchepel, L. Salmim, A. Monteiro, and A. T. Miranda, 2006. How urban structure can affect city sustainability from an air quality perspective, *Environmental Modelling & Software*, 21(4): 461-467.

Bowen, J. L., and I. Valiela, 2001. The ecological effects of urbanization of coastal watersheds: historical increases in nitrogen loads and eutrophication of Waquoit Bay estuaries, *Canadian Journal of Fisheries & Aquatic Sciences*, 58(8): 1489-1500.

Brabec, E., S. Schulte, and P. L. Richards, 2002. Impervious surfaces and water quality: A review of current literature and its implications for watershed planning, *Journal of Planning Literature*, 16(4): 499-514.

Brando, V.E., and A.G. Dekker, 2003. Satellite hyperspectral remote sensing for estimating estuarine and coastal water quality. *IEEE Transactions on Geoscience and Remote Sensing*, 41: 1378-1387.

Burchell, R. W., and S. Mukherji, 2003. Conventional development versus managed growth: The costs of sprawl. *American Journal of Public Health*, 93(9): 1534-1540.

Cablk, M.E., and T.B. Minor, 2003. Detecting and discriminating impervious cover with high-resolution IKONOS data using principal component analysis and morphological operators. *International Journal of Remote Sensing*, 24: 4627-4645.

Cakir, H. I., and S. Khorram, 2004. Methods, systems and computer program products for fusion of high spatial resolution imagery with low-spatial but high-spectral resolution imagery using correspondence analysis. November 4, 2004, US Patent Appl. No. 10/982,054.

Carleer, A., and E. Wolff, 2004. Exploitation of very high resolution satellite data for tree species identification. *Photogrammetric Engineering and Remote Sensing*, 70: 135-140.

Carleer, A.P., O. Debeir, and E. Wolff, 2005. Assessment of very high spatial resolution satellite image segmentations. *Photogrammetric Engineering and Remote* Sensing, 71: 1285-1294.

Dare, P.M., 2005. Shadow analysis in high-resolution satellite imagery of urban areas. *Photogrammetric Engineering and Remote Sensing*, 71: 169-177.

Dougherty, M., R. Dymond, S. Goetz, C. Jantz, and N. Goulet, 2004. Evaluation of impervious surface estimates in a rapidly urbanizing watershed. *Photogrammetric Engineering and Remote Sensing*, 70: 1275-1284.

Elvidge, C.D., J.B. Dietz, R. Berkelmans, S. Andrefouet, W. Skirving, A.E. Strong, and B.T. Tuttle, 2004. Satellite observation of Keppel Islands (Great Barrier Reef) 2002 coral bleaching using IKONOS data, *Coral Reefs*, 23: 123-132.

Ewing, R., R. C. Brownson, and D. Berrigan, 2006. Relationship between urban sprawl and weight of United States youth, *American Journal of Preventative Medicine*, 31(6): 464-474.

Fisher, J., and S. Goetz, 2001. Considerations in the use of high spatial resolution imagery: an applications research assessment. American Society for Photogrammetry and Remote Sensing (ASPRS) Conference Proceedings, St. Louis, MO.

Foody, G.M., 1995. Land-cover classification by an artificial neural-network with ancillary information. *International Journal of Geographical Information Systems*, 9: 527-542.

Foody, G.M., 2002. Status of land cover classification accuracy assessment. *Remote Sensing of Environment*, 80: 185-201.

Galster, G., R. Hanson, M. R. Ratcliffe, H. Wolman, S. Coleman, and J. Freihage, 2001. Wrestling sprawl to the ground: Defining and measuring an elusive concept, *Housing Policy Debate*, 12(4): 681-717.

Galvao, L.S., A.R. Formaggio, and D.A. Tisot, 2005. Discrimination of sugarcane varieties in southeastern Brazil with EO-1 hyperion data. *Remote Sensing of Environment*, 94: 523-534.

Gao, J., H. F. Chen, Y. Zhang, and Y. Zha, 2004. Knowledge-based approaches to accurate mapping of mangroves from satellite data. *Photogrammetric Engineering and Remote* Sensing, 70: 1241-1248.

Goetz, S., R. Wright, A. Smith, E. Zinecker, and E. Schaub, 2003. IKONOS imagery for resource management: Tree cover, impervious surfaces, and riparian buffer analyses in the mid-Atlantic region. *Remote Sensing of Environment*, 88: 195-208.

Goodenough, D.G., A. Dyk, O. Niemann, J.S. Pearlman, H. Chen, and T. Han, M. Murdoch, M., and C. West, 2003. Processing Hyperion and ALI for forest classification. *IEEE Transactions on Geoscience and Remote Sensing*, 41: 1321-1331.

Henebry, G.M., 1993. Detecting change in grasslands using measures of spatial dependence with Landsat TM data. *Remote Sensing of Environment*, 46: 223-234.

Herold, M., D.A. Roberts, M.E. Gardner, and P.E. Dennison, 2004. Spectrometry for urban area remote sensing - Development and analysis of a spectral library from 350 to 2400 nm. *Remote Sensing of Environment*, 91: 304-319.

Homer, C., C.Q. Huang, L.M. Yang, B. Wylie, and M. Coan, 2004. Development of a 2001 National Land-Cover Database for the United States. *Photogrammetric Engineering and Remote Sensing*, 70: 829-840.

Hu, X. Y., C. V. Tao, and B. Prenzel, 2005. Automatic segmentation of high-resolution satellite imagery by integrating texture, intensity, and color features. *Photogrammetric Engineering and Remote* Sensing, 71: 1399-1406.

Interlandi, S. J., and C. S. Crockett, 2003. Recent water quality trends in the Schuylkill River, Pennsylvania, USA: A preliminary assessment of the relative influences of climate, river discharge and suburban development. *Water Research*, 37(8): 1737-1748.

Jennings, D., S. Jarnagin, and D. Ebert, 2004. A modeling approach for estimating watershed impervious surface area from national land cover data 92. *Photogrammetric Engineering and Remote Sensing*, 70: 1295-1307.

Jensen, J., 2005. *Introductory Digital Image Processing: A Remote Sensing Perspective*, 3rd ed. Prentice Hall, Upper Saddle River, NJ, 526 p.

Jin, M., and J.M. Shepherd, 2005. Inclusion of urban landscape in a climate model - How can satellite data help? *Bulletin of the American Meteorological Society,* 86: 681-689.

Johansen, K., and S. Phinn, 2006. Mapping structural parameters and species composition of riparian vegetation using IKONOS and landsat ETM plus data in Australian tropical savannahs. *Photogrammetric Engineering and Remote Sensing*, 72: 71-80.

Kasperson, J., 2001. The stormwater utility: Will it work in your community? *Stormwater* 1(1), available at http://www.stormcon.com/sw_0011_utility.html (last accessed Apr. 10, 2008).

Kutser, T., D. Pierson, L. Tranvik, A. Reinart, S. Sobek, and K. Kallio, 2005. Using satellite remote sensing to estimate the colored dissolved organic matter absorption coefficient in lakes. *Ecosystems*, 8: 709-720.

Lambin, E.F., and D. Ehrlich, 1996. The surface temperature-vegetation index space for land cover and land-cover change analysis. *International Journal of Remote Sensing*, 17: 463-487.

Lillesand, T.M., and Kiefer, R.W., 2004. *Remote Sensing and Image Interpretation*, 5th ed. John Wiley & Sons, Inc., New York, 724 p.

Lu, D., P. Mausel, E. Brondizio, and E. Moran, 2004. Change detection techniques. *International Journal of Remote Sensing*, 25: 2365-2407.

Ludwig, R., M. Probeck, and W. Mauser, 2003. Mesoscale water balance modelling in the Upper Danube watershed using sub-scale land cover information derived from NOAA-AVHRR imagery and GIS-techniques. *Physics and Chemistry of the Earth*, 28: 1351-1364.

Lunetta, R. S., J. Ediriwickrema, J. Iiames, D. M. Johnson, J. G. Lyon, A. McKerrow, and A. Pilant, 2003. A quantitative assessment of a combined spectral and GIS rule-based land-cover classification in the Neuse River Basin of North Carolina. *Photogrammetric Engineering and Remote* Sensing, 69: 299-310.

Maktav, D., F. Erbek, and C. Jurgens, 2005. Remote sensing of urban areas. *International Journal of Remote Sensing*, 26: 655-659.

McCauley, S., and S. Goetz, 2004. Mapping residential density patterns using multi-temporal Landsat data and a decision-tree classifier. *International Journal of Remote Sensing*, 25: 1077-1094.

Miyamoto, M., K. Yoshino, T. Nagano, T. Ishida, and Y. Sato, 2004. Use of balloon aerial photography for classification of Kushiro wetland vegetation, northeastern Japan, *Wetlands*, 24: 701-710.

Moglen, G. E., and S. Kim, 2007. Limiting imperviousness - Are threshold-based policies a good idea?, *Journal of the American Planning Association*, 73(2): 161-171.

Morisette, J.T., S. Khorram, and T. Mace, 1999. Land-cover change detection enhanced with generalized linear models. *International Journal of Remote Sensing*, 20: 2703-2721.

Muchoney, D.M., and B.N. Haack, 1994. Change detection for monitoring forest defoliation. *Photogrammetric Engineering and Remote Sensing*, 60: 1243-1251.

NASA, 2008. *ASTER Instrument Characteristics*, available at http://asterweb.jpl.nasa.gov/content/01_mission/03_instrument/01_Characteristics/default.htm (last accessed on Apr. 13, 2008).

NASA, 2003. *MODIS Data from the GES DISC DAAC*, available at http://daac.gsfc.nasa.gov/MODIS/documentation/brochure/MODIS-Brochure.1.pdf (last accessed Apr. 13, 2008).

Oswald, B.P., J.T. Fancher, D.L. Kulhavy, and H.C. Reeves, 2000. Classifying fuels with aerial photography in East Texas. *International Journal of Wildland Fire*, 9: 109-113.

Pendola, R., and S. Gen, 2007. BMI, auto use, and the urban environment in San Francisco, *Health Place*, 13(2): 551-556.

Pohl, C., and J. L. van Genderen, 1998. Multisensor image fusion in remote sensing: concepts, methods and applications. *International Journal of Remote Sensing*, 19: 823-854.

Pyke, C.R., and S.J. Andelman, 2007. Land use and land cover tools for climate adaptation. *Climatic Change*, 80(3-4): 239-51.

Ramsey, E., A. Rangoonwala, G. Nelson, and R. Ehrlich, 2005. Mapping the invasive species, Chinese tallow, with EO1 satellite Hyperion hyperspectral image data and relating tallow occurrences to a classified Landsat Thematic Mapper land cover map. *International Journal of Remote Sensing*, 26: 1637-1657.

Read, J., D. Clark, E. Venticinque, and M. Moreira, 2003. Application of merged 1-m and 4-m resolution satellite data to research and management in tropical forests. *Journal of Applied Ecology*, 40: 592-600.

Read, J.M., and N.S.N. Lam, 2002. Spatial methods for characterising land cover and detecting land-cover changes for the tropics. *International Journal of Remote Sensing*, 23: 2457-2474.

Rogan, J., and D.M. Chen, 2004. Remote sensing technology for mapping and monitoring land-cover and land-use change. *Progress in Planning*, 61: 301-325.

Ross, N. A., S. Tremblay, S. Khan, D. Crouse, M. Tremblay, and J. M. Berthelot, 2007. Body mass index in urban Canada: Neighborhood and metropolitan area effects. *American Journal of Public Health*, 97(3): 500-508.

Sawaya, K., L. Olmanson, N. Heinert, P. Brezonik, and M. Bauer, 2003. Extending satellite remote sensing to local scales: land and water resource monitoring using high-resolution imagery. *Remote Sensing of Environment*, 88: 144-156.

Snyder, M. N., S. J. Goetz, and R. K. Wright, 2005. Stream health rankings predicted by satellite derived land cover metrics. *Journal of the American Water Resources Association*, 41(3): 659-677.

Song, M., D. L. Civco, and J. D. Hurd, 2005. A competitive pixel-object approach for land cover classification. *International Journal of Remote Sensing*, 26: 4981-4997.

Speir, C., and K. Stephenson, 2002. Does sprawl cost us all? Isolating the effects of housing patterns on public water and sewer costs. *Journal of the American Planning Association*, 68(1): 56-70.

Stone, B., 2004. Paving over paradise: how land use regulations promote residential imperviousness. *Landscape and Urban Planning*, 69: 101-113.

Svab, A., and K. Osti, 2006. High-resolution image fusion: methods to preserve spectral and spatial resolution. *Photogrammetric Engineering and Remote Sensing*, 72: 565-572.

Thomas, N., C. Hendrix, and R. Congalton, 2003. A comparison of urban mapping methods using high-resolution digital imagery. *Photogrammetric Engineering and Remote Sensing*, 69: 963-972.

Torres, H., H. Alves, and M. A. De Oliveira, 2007. Sao Paulo peri-urban dynamics: some social causes and environmental consequences. *Environment and Urbanization*, 19(1): 207-223.

Tu, J., Z. G. Xia, K. C. Clarke, and A. Frei, 2007. Impact of urban sprawl on water quality in eastern Massachusetts, USA. *Environmental Management*, 40(2): 183-200.

USGS, 2006. EO-1 Website, available at http://eo1.usgs.gov (last accessed Apr. 13, 2008).

Walsh, C. J., P. J. Papas, D. Crowther, and J. Yoo, 2004. Stormwater drainage pipes as a threat to a stream-dwelling amphipod of conservation significance, Austrogammarus australis, in southeastern Australia. *Biodiversity and Conservation*, 13(4): 781-793.

Wang, H.Q., and E.C. Ellis, 2005. Image misregistration error in change measurements. *Photogrammetric Engineering and Remote* Sensing, 71: 1037-1044.

Wilson, J., and G. Lindsey, 2005. Socioeconomic correlates and environmental impacts of urban development in a central Indiana landscape. *Journal of Urban Planning and Development D-ASCE*, 131: 159-169.

Yang, R., and P. A. Jargowsky, 2006. Suburban development and economic segregation in the 1990s. *Journal of Urban Affairs*, 28(3): 253-273.

Zhang, Q., J. Wang, X. Peng, P. Gong, and P. Shi, 2002. Urban built-up land change detection with road density and spectral information from multi-temporal Landsat TM data. *International Journal of Remote Sensing*, 23: 3057-3078.

**Sensor and agency websites (last accessed Apr. 13, 2008)**:

European Space Agency (ESA): http://www.esrin.esa.it

IKONOS 2, OrbView-3: GeoEye http://www.geoeye.com

Indian Space Research Organisation: http://www.isro.org/

National Aeronautics and Space Administration (NASA): http://www.nasa.gov

QuickBird / DigitalGlobe: http://www.digitalglobe.com

RADARSAT:  http://ccrs.nrcan.gc.ca/radar/spaceborne/radarsat1/index_e.php

Restec: http://www.restec.or.jp

# 3. PER-PIXEL CLASSIFICATION OF HIGH SPATIAL RESOLUTION SATELLITE IMAGERY FOR URBAN LAND COVER MAPPING

## 3.1. Abstract

Commercial high spatial resolution satellite data now provide a synoptic and consistent source of digital imagery with detail comparable to that of aerial photography. In the work described here, per-pixel classification, image fusion, and GIS-based map refinement techniques were tailored to pan-sharpened 0.61 m QuickBird imagery to develop a six-category urban land cover map with 89.3 percent overall accuracy ($\kappa$ =0.87). The study area was a rapidly developing 71.5 $km^2$ part of suburban Raleigh, North Carolina, U.S.A., within the Neuse River basin. "Edge pixels" were a source of classification error as was spectral overlap between bare soil and impervious surfaces and among vegetated cover types. Shadows were not a significant source of classification error. These findings demonstrate that conventional spectral-based classification methods can be used to generate highly accurate maps of urban landscapes using high spatial resolution imagery.

## 3.2. Introduction

The recent emergence of high spatial resolution satellite image sensors has introduced an exciting new set of possibilities for analyzing imperviousness and other land cover types at fine levels of detail. Commercial satellites including GeoEye's IKONOS (1 m panchromatic ground resolution, **www.geoeye.com**) and DigitalGlobe's QuickBird (0.61 m panchromatic ground resolution, **www.digitalglobe.com**) acquire imagery at a spatial resolution previously possible to aerial platforms alone. Continuing this trend, the planned 2007 launch of the GeoEye-1 sensor will herald even higher spatial resolution (0.41 m panchromatic ground resolution, **www.geoeye.com**). This level of spatial quality builds on advantages satellite imagery has conventionally had over aerial-derived imagery, including its capacity for synoptic coverage and its inherently digital format (Barr and Barnsley, 2000; Cablk and Minor, 2003). Such high spatial resolution space-derived imagery has already been used successfully in a diverse array of environmental mapping efforts such as earthquake damage assessment (Miura and Midorikawa, 2006), orchard and vineyard identification (Warner and Steinmaus, 2005), rain forest tree mortality inventory (Clark *et al.*, 2004), and coral reef delineation (Maeder *et al.*, 2002).

Conventional per-pixel classifiers, such as the maximum likelihood and minimum distance-to-mean algorithms, are spectral-based classification methods and constitute a historically dominant approach to remote sensing-based automated land use/land cover (LU/LC) derivation (Gao *et al.*, 2004). The maximum likelihood classifier, in fact, is frequently used as a "benchmark" against which novel classification algorithms are evaluated (Song *et al.*, 2005). Such classifiers are widely available in commercial image processing software packages and enjoy widespread user familiarity. It has been suggested, however, that traditional per-pixel classification methods have limited applicability to high spatial resolution data because they cannot fully exploit its information content (Hu *et al.*, 2005). Other analysts have reported that the detail of high spatial resolution imagery has confounded conventional automated land cover classification techniques, particularly in studies of heterogeneous urban environments. Reportedly problematic aspects have included shadows (Barr and Barnsley, 2000; Dare, 2005), high reflectance variability but limited spectral information (Carleer *et al.*, 2005), general image complexity (Hu *et al.*, 2005) and data volume (Fisher and Goetz, 2001).

Several spectral-based classification studies of high spatial resolution imagery have been more successful. Goetz *et al.* (2003) reported overall and per category accuracies of between 75 and 85 percent for supervised and unsupervised classifications of a leaf-on and leaf-off mosaic of 4 m IKONOS imagery. The researchers in that study also used decision tree classifiers that incorporated only spectral information, including band ratios, to map urban imperviousness and tree canopy with overall accuracies of 84.2 percent and 97.3 percent, respectively. Sawaya *et al.* (2003), also working with IKONOS data, adapted modeling approaches developed for Landsat TM data to accurately describe urban lake water clarity using unsupervised per-pixel classification ($r^2 = 0.94$) and developed regression equations between IKONOS-derived normalized difference vegetation index (NDVI) values and sample area percent imperviousness. These equations were used to estimate percent impervious surface with a reference-data correlation of 0.98.

Thomas *et al.* (2003) concluded that their pixel-based approach to urban impervious surface mapping using high spatial resolution imagery had only moderate success due to the limited spectral content of that data. That study classified land cover in an urban desert ecosystem using 8-bit aerial scanner imagery. Notably, several high spatial resolution satellite image sensors, including IKONOS, QuickBird, and GeoEye's future GeoEye-1 satellite, are designed to record reflectance data in 11-bit radiometric depth. The result is imagery with a special blend of modest spectral resolution but rich reflectance storage capacity. This is particularly important in light of innovative data fusion methods that allow analysts to merge multispectral content with its higher spatial-resolution panchromatic corollary (Svab and Osti, 2006).

Other data fusion varieties may also be useful to high spatial resolution image classification. The integration of ancillary GIS data with per-pixel classification has long been a successful land cover derivation technique with a variety of medium- and low-resolution image types (Foody, 1995; Ludwig *et al.*, 2003; Lunetta *et al.*, 2003), but, as of yet, its applicability to high-resolution data has only been cursorily examined (Sawaya *et al.*, 2003; Thomas *et al.*, 2003). This is despite the inherent suitability of such imagery to these techniques, the efficacy of which depends on sufficient geographic alignment (Cablk and Minor, 2003).

The utility of per-pixel classification in analyzing high spatial resolution satellite data is an important research direction because pixel-based classification enjoys widespread familiarity and software accessibility due to its historical prominence. This paper describes a per-pixel classification approach used to accurately generate an urban land cover map using fused sub-meter high spatial resolution satellite imagery, and the incorporated methods are readily available in standard remote sensing and GIS analysis packages. In order to provide a more robust account of the applicability of these conventional methods to one promising use of high spatial resolution imagery in urban areas, the accuracies of output impervious surface maps were analyzed using both point- and area-based metrics.

### 3.3. Study Area

The study area incorporates 71.5 $km^2$ of adjacent drainage catchments and is located in the northeast part of Raleigh, North Carolina, USA. This area is composed of primarily urban and suburban land uses interspersed with large forested clusters and includes part of a major transportation corridor, US-1 (Figure 3-1). Raleigh is a part of Wake County and the Neuse River watershed, the third largest river basin in the state of North Carolina. This basin drains all or part of twenty-three counties into the Albemarle-Pamlico Sound; its ecological integrity has been the subject of numerous studies in recent decades (Burkholder *et al.*, 1992; McMahon and

Lloyd, 1995; Paerl *et al.*, 1998).

According to U.S. Census Bureau estimates, Wake County was among the nation's 100 fastest-growing counties between 01 April 2000 and 01 July 2006 of those ending the period with a population greater than 10,000 (2006). This rapid level of urban and population expansion has become a major concern of state, federal, and local agencies seeking to safeguard water quality in the Neuse River watershed. Indeed, both of the major streams within the study area, Marsh Creek and Perry Creek, have been included on North Carolina's federally-mandated Clean Water Act, Section 303 (d), Impaired Waters List every year since its inception. Each time, the state has cited "urban runoff/storm sewers" as the likely cause of impairment (North Carolina Division of Water Quality, 2004). The present study is part of a larger effort to describe the rapid land cover change occurring in the Raleigh area and to evaluate its potential impacts on water quality.

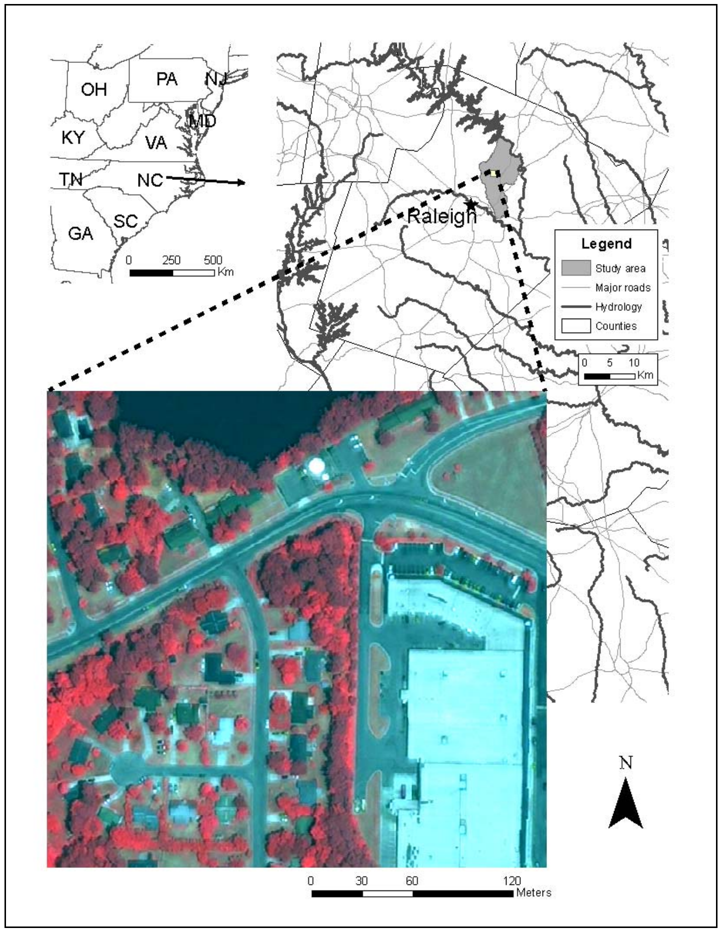


**Figure 3-1. Raleigh, NC, study area depicted regionally and locally. Study area is shown on local map in shaded gray, and inset figure is a large-scale QuickBird image subset. A color version of this figure is available on the ASPRS website (www.asprs.org).**

## 3.4. Data and Image Pre-Processing

For this study, multispectral and panchromatic QuickBird imagery was obtained from DigitalGlobe's image archives. The image was collected on 01 June 2002 under clear atmospheric conditions at 16:01 local time and at 10.1° off-nadir. The taskable QuickBird sensor is capable of collecting imagery up to 30.0° off-nadir. At the time of data collection, the sun azimuth was 126.5° and the sun elevation was 69.4°, while the satellite's azimuth and elevation metrics were 136.4° and 79.0°, respectively.

At nadir, the QuickBird sensor collects data in three visible channels (450-520 nm, 520-

600 nm, and 630-690 nm) and one near-infrared channel (760-900 nm) at 2.44 m spatial resolution. Its panchromatic (445-900 nm) sensor images scenes at 0.61 m spatial resolution. All data are recorded in 11-bit radiometric storage depth. Using image fusion algorithms, multispectral satellite imagery can be spatially sharpened with panchromatic imagery. Data fusion, in this sense, is the combination of the two image types that results in one image with panchromatic ground resolution and multispectral spectral resolution (Pohl and van Genderen, 1998). The Cakir-Khorram algorithm used in this study (Cakir and Khorram, 2004) achieves this combined resolution while preserving spectral integrity better than conventional image fusion algorithms, such as principal components analysis and intensity-hue-saturation fusion. The resulting pan-sharpened multispectral image has a ground resolution of 0.61 m.

In order to georeference the image, 32 ground control points were field-collected throughout the study area using differentially-corrected Trimble Pro XR Global Positioning System (GPS) data. These points, recorded with a sub-meter accuracy margin of error, were then used to resolve geometric distortion within the image using a first-order polynomial correction. This algorithm was applied systemically to the image and achieved a root-mean square error (RMSE) of 1.6 m. This RMSE was considered acceptable given the high spatial resolution of the imagery and the one-meter error limitation of the DGPS. The imagery was then projected to NC State Plane, NAD 83 datum, meters, to match existing ancillary GIS data including roads, hydrography, and Raleigh municipal zoning layers. All image processing was performed in Leica Geosystem's ERDAS IMAGINE® 8.7; all GIS analyses were performed in ArcGIS® 9.0.

## 3.5. Methods

### *3.5.1. Per-Pixel Land Cover Classification*

A hybrid per-pixel classification approach was developed for urban land cover mapping in this analysis. Such an approach acknowledges the benefits of both supervised and unsupervised classification (Kelly *et al.*, 2004). Six categories of land cover, including impervious surface, were selected for mapping within the study area (Table 3-1). These categories were chosen based on their applicability to water quality analysis as well as their relevance to high spatial resolution image analysis. For example, discrete impervious land cover features in this imagery include sidewalks, roads, and buildings. Thus, in contrast to many analyses of coarser-resolution data, it is not necessary to indirectly represent impervious features by mapping aggregate classes of land cover which specify, for example, a broad range of impervious surface coverage within a land use class. This approach is often adopted in light of sensor resolution limitations, although innovative recent work has sought to estimate impervious surface area at sub-pixel levels using medium-resolution data such as that of Landsat (Yang *et al.*, 2003; Jennings *et al.*, 2004) The possibility of directly mapping land cover extent, such as imperviousness, is a primary allure of using high spatial resolution imagery (Jensen and Cowen, 1999; Barr and Barnsley, 2000).

**Table 3-1. Urban land cover categorization scheme for hybrid classification.**

| Class | Land cover type | Description |
|---|---|---|
| 1 | Impervious | Transportation infrastructure (roads, parking lots, etc.), rooftops, recreational areas (i.e., tennis courts), and all other manmade impervious surfaces that are paved or built |
| 2 | Water | Lakes, ponds, rivers, streams, pools, and all other natural and artificial surface waters |
| 3 | Bare/Disturbed soil | Construction sites, landfills, gravel areas, or any other unpaved non-vegetated surface |
| 4 | Deciduous | Trees or shrubs that shed their leaves before the winter (mostly hardwood species). |
| 5 | Evergreen | Trees or shrubs that keep their leaves throughout the winter (mostly coniferous species) |
| 6 | Herbaceous | Urban grasses (yards, recreational fields, vegetated road medians, etc.) of varying degrees of maintenance |

The hybrid classification process employed for the present study is summarized in Figure 3-2. As an initial step in this process, a supervised classification was performed using the maximum likelihood algorithm and 25 classes. A total of 138 training sites were digitized throughout the study area following well-established manual training site generation protocols (Jensen, 2005). These training sites included at least five examples of each representative feature type within the six broad land cover categories described in Table 3-1. Furthermore, illuminated and shaded versions of relevant land cover feature types were represented by separate training site groups. For example, the impervious category was represented by five homogeneous training sites for the following feature types: concrete-like, concrete-like (shaded), asphalt-like, asphalt-like (shaded), green roofs, white roofs, red roofs, brown roofs, red recreational court surfaces, and green recreational court surfaces. This training site assemblage was taken to be exhaustive only with respect to the dominant land cover feature types within a given category. Certain features with highly variable reflectance, such as vehicles, or features with isolated representation, such as railroad tracks, were not included in the training site scheme, a limitation addressed by the unsupervised element of this hybrid classification approach.

After the output from the supervised classification was aggregated into the six classes of land cover interest, categories that evidenced classification confusion based on visual inspection were subset. Within each of these image subsets, an unsupervised classification was performed using 25 classes, ISODATA (Iterative Self-Organizing Data Analysis Technique) clustering, principal axis means computing, 25 maximum iterations, and a 95 percent convergence threshold. Ultimately, this second classification step was carried out for each of the initial supervised classification outputs except the two categories of woody vegetation, evergreen and deciduous. After the unsupervised classifications were completed and pixels were recategorized, these results were combined with the evergreen and deciduous pixels from the original classification. Finally, a 3 x 3 majority filter was applied to eliminate "salt-and-pepper" pixels and complete the thematic map. Such post-classification filters are commonly used to remove land cover clusters that are smaller than an analyst's minimum mapping unit of interest (Jensen, 2005).

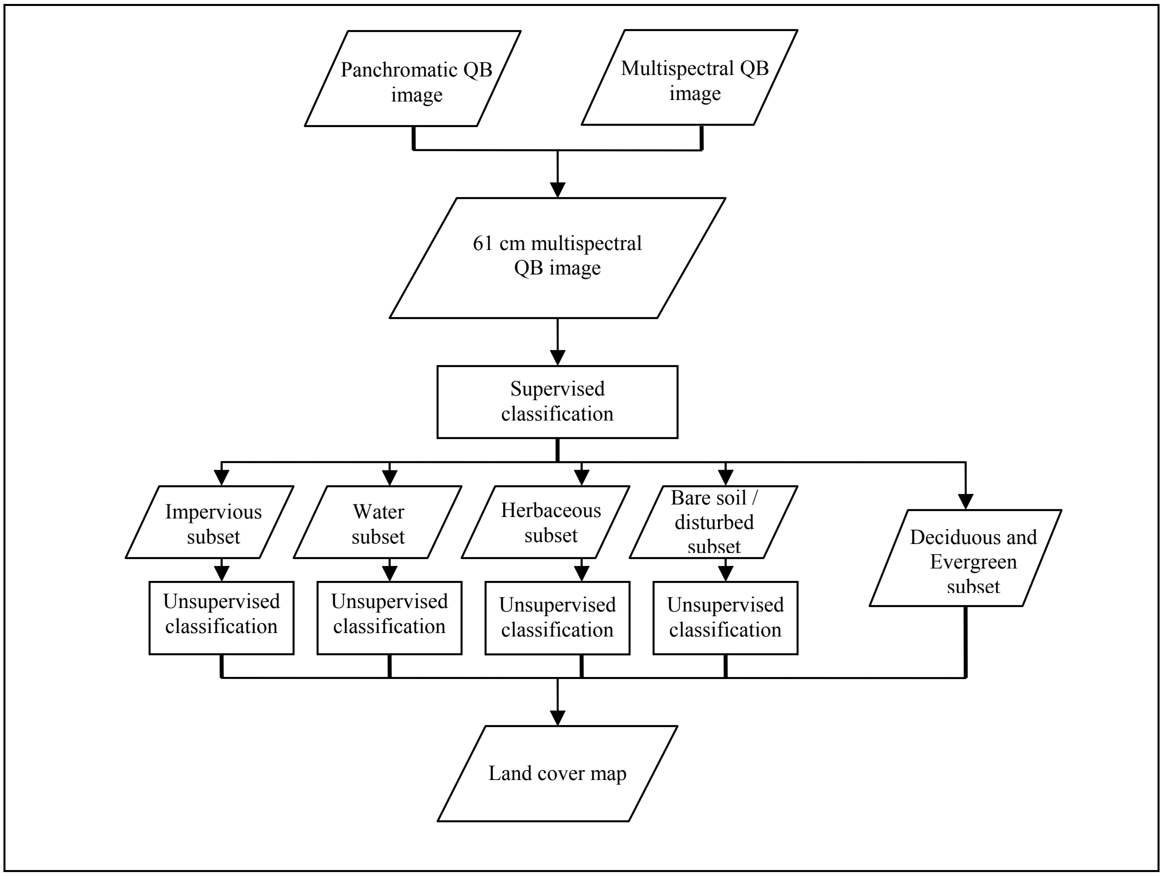


**Figure 3-2. Flow chart summarizing hybrid per-pixel classification method.**

### *3.5.2. Point-Based Thematic Accuracy Assessment*

To assess the thematic accuracy of the hybrid land cover classification using a traditional point-based technique, a reference dataset was created consisting of 300 randomly selected points. The land cover at each point was photointerpreted using the fused QuickBird image and the land cover classes described in Table 3-1. Fifty points were evaluated within each of these classes using a 3 x 3 pixel majority interpretation centered on the point. In general, a reference data set for accuracy assessment of any thematic map must adequately represent the scale, detail, and classification scheme of the map itself (Khorram *et al.*, 1999). This has special implications for high spatial resolution image analysis that will be discussed later in this paper. In order to assess the integrity of QuickBird photointerpretation for these particular land cover types, a separate field-based reference dataset was generated and indicated 100 percent photointerpretation accuracy (27/27). Using the image-based reference data, classification validity was reported in terms of producer's accuracy, user's accuracy, and overall classification accuracy as well as through category and overall Kappa ($\kappa$) statistics.

### *3.5.3. Area-based Thematic Accuracy Assessment*

In order to further assess the quality of this land cover product, land cover was digitized within a random sample of 50 residential property parcels, 10 commercial parcels, and 10 five-meter buffers of road segments throughout the study area. Within each of these regions, polygons were manually delineated based on the six-category classification scheme. Features were digitized based on their appearance in the pan-sharpened QuickBird image displayed as a color-infrared composite. Any impervious feature obscured by overhanging vegetation such as tree canopy would be delineated from that vertical perspective without deference to ground-level boundaries. The minimum mapping unit (MMU) for this effort was 3 x 3 (0.61 m) pixels or 3.35 $m^2$. The digitized area totaled 9.1 ha (residential), 8.1 ha (commercial), and 1.1 ha (road buffer), with a linear total of 970 road-segment meters digitized. Foody (2002), in tracing the history of thematic accuracy assessment, states that area-based accuracy assessment has limited utility because, in reality, mapped area is correct only if it is mapped in the right place. This critique is well-founded. Accordingly, area-based accuracy assessment was intended here to supplement point-based assessment in evaluating mapping accuracy at the localized scale of individual land parcels and road buffers. Comparisons here were made using measures of Pearson's correlation between per-region percent land cover as well as mean and standard deviation percent land cover error (reference minus classified) for all three region types. Additionally, for imperviousness, areal estimates based on all regions within each type were aggregated and compared to summary reference area figures.

## 3.6. Results

### *3.6.1. Land Cover Map and Conventional Accuracy Assessment Results*

Table 3-2 presents the error matrix for the initial hybrid classification. The overall accuracy of this classification was 83.0 percent and the κ statistic was 0.796. Within the six-category scheme, producer's accuracies ranged from 69.1 percent to 97.6 percent while user's accuracies ranged from 66.0 percent to 94.0 percent. All category κ statistics were between 0.61 and 0.92. For four of the categories in this six-category scheme, user's and producer's accuracy were both above 75 percent and κ was above 0.75.

**Table 3-2. Error matrix for initial land cover map (Overall κ statistics=0.796, σ=0.0265, and 0.95 CI: 0.7441 - 0.8479).**

| Category | 1 | 2 | 3 | 4 | 5 | 6 | Row total | User's Accuracy (%) | Kappa (κ) |
|---|---|---|---|---|---|---|---|---|---|
| 1. Impervious | **47** | 0 | 2 | 0 | 1 | 0 | 50 | 94.0 | 0.92 |
| 2. Water | 8 | **40** | 0 | 0 | 0 | 2 | 50 | 80.0 | 0.77 |
| 3. Bare/disturbed | 7 | 0 | **41** | 0 | 0 | 2 | 50 | 82.0 | 0.79 |
| 4. Deciduous | 0 | 0 | 0 | **44** | 5 | 1 | 50 | 88.0 | 0.85 |
| 5. Evergreen | 2 | 0 | 0 | 4 | **44** | 0 | 50 | 88.0 | 0.85 |
| 6. Herbaceous | 4 | 1 | 2 | 8 | 2 | **33** | 50 | 66.0 | 0.61 |
| Column Total | 68 | 41 | 45 | 56 | 52 | 38 | 300 | | |
| Producer's Accuracy (%) | 69.1 | 97.6 | 91.1 | 78.6 | 84.6 | 86.8 | | **83.0** | |

Two accuracy metrics in this matrix demonstrating the greatest areas of classification confusion were herbaceous user's accuracy and impervious producer's accuracy. With respect to the 34 percent herbaceous commission error, confusion was found with all other categories although commission of deciduous cover to herbaceous was the most pronounced. With respect to the impervious category, a producer's accuracy of 69.1 percent and user's accuracy of 94.0 percent was achieved. The two areas of greatest confusion for the impervious category were the water and herbaceous categories, with omission errors of 11.8 percent and 10.3 percent, respectively, as part of a total percent omission error of 30.8 percent.

Of this confusion, it was evident that, while omission of impervious pixels with respect to the herbaceous category had no readily available resolution, the erroneous assignment of impervious pixels to the water category had a promising GIS-based method of minimization. This was a simple image segmentation based on a GIS overlay of the lakes features and subsequent unsupervised classification within the lake-subset portion of this image. During the unsupervised phase of the initial hybrid classification, no probability weighting was used for assigning pixel clusters to either the impervious or water categories despite the *a priori* knowledge that there was comparatively little water in the study area. In this GIS-based classification refinement step, the "water" unsupervised cluster from the initial Table 3-3 land cover map was re-evaluated using an additional 25-class unsupervised classification of this image subset. In this pixel re-assignment process, heavy *a priori* weight was given to the impervious category. The output from this stage was then integrated into the initial land cover map, forming an intermediate land cover map. Next, in the 25-cluster output from the separate lake-subset unsupervised classification, heavy *a priori* weight was given to water in assigning pixels to one of the six land cover categories. When this image was combined with the initial thematic map, its "water" pixels supplanted intermediate land cover map pixels where this assignment was not already made, resulting in the final land cover map.

The thematic accuracy of this final land cover map was assessed using the same methods described for use with the initial map. The resulting error matrix is presented in Table 3-3. Pairwise comparison of error matrices based on the Z-test of κ values (Congalton and Green, 1999) showed that the initial (Table 3-2) and final accuracy (Table 3-3) matrices were significantly different (Z = 2.190274491, 95% confidence level) and there was a significant improvement from the initial classification. Relative to the initial map, measures of overall accuracy and κ statistic were improved to 89.3 percent and 0.87, respectively. Producer's accuracy for the impervious category, 69.1 percent, was improved to 81.8 percent; this increase reflects the elimination of impervious confusion with water, a category classified perfectly according to this assessment, in which user's and producer's accuracies were both 100 percent and κ was 1.0. Numeric improvements in impervious producer's accuracy and water user's accuracy were the only category accuracy changes that exceeded the standard error of the corresponding accuracies in the initial land cover map assessment. This statistical difference reinforced qualitative findings of this impervious/water refinement. Overall, all categories in the final land cover map exhibited user's and producer' accuracies greater than 75 percent and κ statistics greater than 0.70. According to this final land cover map, the study area is primarily composed of herbaceous cover (33.6 percent), followed by approximately equal amounts of impervious and deciduous cover (23.6 percent each) and a smaller extent of evergreen vegetation (14.2 percent), bare/disturbed soil (4.2 percent), and water (0.8 percent).

**Table 3-3. Error matrix for final land cover map after GIS-based refinement (Overall κ statistics=0.872, σ=0.0224, and 0.95 CI: 0.8282 - 0.9158).**

| Category | 1 | 2 | 3 | 4 | 5 | 6 | Row total | User's Accuracy (%) | Kappa (κ) |
|---|---|---|---|---|---|---|---|---|---|
| 1. Impervious | **45** | 0 | 4 | 0 | 0 | 1 | 50 | 90.0 | 0.88 |
| 2. Water | 0 | **50** | 0 | 0 | 0 | 0 | 50 | 100 | 1.00 |
| 3. Bare/disturbed | 4 | 0 | **45** | 0 | 0 | 1 | 50 | 90.0 | 0.88 |
| 4. Deciduous | 0 | 0 | 0 | **46** | 2 | 2 | 50 | 92.0 | 0.90 |
| 5. Evergreen | 0 | 0 | 0 | 5 | **44** | 1 | 50 | 88.0 | 0.86 |
| 6. Herbaceous | 6 | 0 | 0 | 3 | 3 | **38** | 50 | 76.0 | 0.72 |
| Column Total | 55 | 50 | 49 | 54 | 49 | 43 | 300 | | |
| Producer's Accuracy (%) | 81.8 | 100 | 91.8 | 84.9 | 89.8 | 88.4 | | **89.3** | |

### *3.6.2. Area-Based Accuracy Assessment Results*

Table 3-4 presents the results of area-based accuracy assessment within the random sample of residential and commercial parcels and the road-segment buffers. Pearson's correlation coefficients between classified and digitized percent land cover were at least 0.80 for all land cover categories in all digitized regions. For the impervious category, all correlation coefficients were at least 0.90. The highest correlation coefficient for any category was 0.997 with respect to impervious surface percentage within the commercial parcels. As evidenced by the mean percent error (classified minus digitized percent land cover, per sample), classified impervious percentage estimates were generally lower than reference percentages, but only by an average error across all region types of 5.6 percent. By contrast, classified herbaceous percentage estimates were generally higher than reference percentages, again by a small across-region type average of 8.9 percent. The herbaceous class, incidentally, also evidenced the highest mean percent error for any category, 12.1 percent within the residential parcels.

**Table 3-4. Agreement between classified and digitized percent land cover values within sampled land use regions by region type.**

| Land cover category | Statistic | Residential | Commercial | Road segments |
|---|---|---|---|---|
| | | Samples =50<br>Total area=21.7 ac | 10<br>19.9 ac | 10<br>2.6 ac |
| Impervious | Percent error, mean | - 6.9 | - 2.1 | - 7.9 |
| | Percent error, standard deviation | 5.7 | 2.0 | 6.9 |
| | Pearson's coefficient of correlation | 0.905 | 0.997 | 0.942 |
| Water | Percent error, mean | - 0.1 | 0.0 | 0.0 |
| | Percent error, standard deviation | 0.7 | 0.0 | 0.0 |
| | Pearson's coefficient of correlation | 0.980 | ---* | ---* |
| Bare/Disturbed | Percent error, mean | 0.2 | 0.0 | 0.8 |
| | Percent error, standard deviation | 0.8 | 0.5 | 4.3 |
| | Pearson's coefficient of correlation | 0.099** | 0.963 | - 0.099** |
| Deciduous | Percent error, mean | - 4.3 | - 5.0 | - 0.9 |
| | Percent error, standard deviation | 8.1 | 6.1 | 2.2 |
| | Pearson's coefficient of correlation | 0.912 | 0.991 | 0.833 |
| Evergreen | Percent error, mean | - 1.0 | 1.1 | - 0.4 |
| | Percent error, standard deviation | 7.2 | 2.6 | 2.1 |
| | Pearson's coefficient of correlation | 0.928 | 0.993 | 0.973 |
| Herbaceous | Percent error, mean | 12.1 | 6.1 | 8.5 |
| | Percent error, standard deviation | 8.0 | 4.0 | 7.1 |
| | Pearson's coefficient of correlation | 0.885 | 0.938 | 0.932 |

Aggregate estimates of impervious surface area from the classification within digitized regions are presented in Table 3-5. For all three region types, impervious surface area was underestimated, a function of the consistently low per-region percent estimates. For the commercial parcels and road segments, however, this error was less than 10.0 percent. The high accuracy in these regions (96.9 percent and 92.4 percent, respectively) is contrasted by that within the residential parcels (63.0 percent). This latter figure is distinctly lower than the two former, despite similar mean percent impervious error values, because impervious surfaces were much more extensive in commercial parcels (mean coverage, 74 percent) and road segments (mean coverage, 84 percent) than in residential parcels (mean coverage, 22 percent). Thus, the same mean percent error for this land cover type represented a proportionally larger accounting deficiency overall for residential parcels. Representative map results are presented in Figure 3-3.

Table 3-5. Area-based producer's accuracy of impervious surface mapping by land use region type.

| Region type | Classification area, $m^2$ | Reference area, $m^2$ | Difference, $m^2$ | Percent accuracy |
|---|---|---|---|---|
| Residential | 9674 | 15354 | -5680 | 63.0 |
| Commercial | 86107 | 88862 | -2755 | 96.9 |
| Road segments | 8146 | 8819 | -673 | 92.4 |


(a) (b) (c)

**Figure 3-3. Land cover mapping results within selected (a) residential, (b) commercial, and (c) road-corridor regions and corresponding true-color QuickBird imagery. A color version of this figure is available on the ASPRS website (www.asprs.org).**

### 3.7. Discussion

The land cover maps produced by the hybrid per-pixel classification employed in this study illustrate some, but not all, of the complications purported to plague traditional approaches to high spatial resolution image classification. There were three vegetation categories and three non-vegetation categories in the six-category land cover scheme used here. In general, classification error in the final land cover map was partitioned by these two groupings. Within the deciduous category, for example, confusion only existed with other vegetated cover types. This is the type of error that suggests that, despite its high spatial and radiometric resolution, the limited spectral content of QuickBird imagery was an obstacle to per-pixel classification. It was qualitatively apparent, however, that there were significant textural differences between, for example, the appearance in this imagery of forested and herbaceous vegetation. Just as Chubey *et al.* (2006) used texture metrics successfully in a high spatial resolution imagery-based forest classification within an undeveloped landscape, this approach could be a partial answer to spectral overlap in urban vegetation studies.

Spectral overlap was also a factor limiting discrimination between impervious surfaces and bare/disturbed soil cover types. These categories were confused in 9.0 percent and 8.0 percent of respective reference data in the initial and final land cover maps. These two land cover types both have diverse representations in urban landscapes, and bare or disturbed soil in urban watersheds can have ecological implications paramount to those of impervious surface coverage (Singh *et al.*, 2003; Faucette *et al.*, 2005; Hayes *et al.*, 2005). Herold *et al.* (2003a) catalogued urban reflectance and found that bare soil was confused with asphalt surfaces because neither surface type has distinct absorption features. Compounding this spectral overlap, the irregular shape of disturbed soil regions may mean that object-oriented analyses will also struggle to distinguish this cover type from developed surfaces. Bare or disturbed surfaces, though, are generally not extensive in urban landscapes except in extremely arid regions and their extent can perhaps be manually delineated without undue burden. This was the approach of Cablk and Minor (2003) in their IKONOS-based morphological analysis of urban impervious surface. If this is not suitable for a particular urban application, it may be useful for analysts to further borrow soil reflectance knowledge from agricultural remote sensing, such as that of moisture content analyses (Alvarez-Mozos *et al.*, 2005).

It was expected that shadows would compound spectral overlap among several land cover types, and that this complication would severely limit per-pixel classification. This expected result was not encountered here. Confusion among vegetated feature types, the reflectance of which is inherently heterogeneous, was exacerbated by shadowing. Additionally, accurate classification within herbaceous and impervious surfaces was also substantially prevented in areas adjacent to tree coverage due to shadows. Nonetheless, shadows were not considered an overall classification issue because they did not constitute a proportionally extensive part of the particular QuickBird image used here. Shadows were minimized by the mid-afternoon, summer time of collection, plus the similarity between the sun's elevation and azimuth and those of the satellite. These variables should be of high concern to analysts interested in purchasing high spatial resolution satellite imagery. Quantitatively, only 2 of the 15 errors associated with impervious surface in the final land cover map were definitively due to the presence of shadows: one impervious reference point classified as herbaceous and one herbaceous reference point classified as impervious.

As seen in the accuracy analysis for the initial land cover map, spectral overlap was a problem between water and impervious surface, although not because of shadows. Simple integration of ancillary GIS data minimized the effect of this problem. In the final land cover map, the water category was perfectly classified. The substantial commission of impervious reference points to water in the first land cover classification was essentially eliminated in this second output. Furthermore, this successful classification did not appreciably degrade the initial success of impervious surface accounting. While this particular application of GIS data integration was specific to a distinct confusion area and depended heavily on suitable data co-registration, it demanded only basic *a priori* knowledge of water features that is likely to be true of many potential urban study areas.

The initially counterintuitive finding of commission of impervious reference points to the herbaceous category was explained by a simple examination of those erroneous points. This confusion represented the greatest single source of error in the final land cover map. Of the six impervious reference points incorrectly classified as herbaceous, all six were located along boundary lines between herbaceous and impervious features. Such boundary lines are common in urban watersheds, as they are found along roads, driveways, parking lots, and buildings. Indeed, these transitions make up much of the patchwork that is the urban landscape. Even in high spatial resolution imagery, such contrasts are delineated by historically problematic "mixed pixels" (Foody, 1997), and these pixels posed classification difficulties as they have in other high spatial resolution studies (Segl *et al.*, 2003).

The "edge pixel" problem is central to understanding the results of the area-based analysis of error (Table 3-4) of the study's final land cover map. Overall, the level of accuracy determined here suggests that per-pixel classification is capable of mapping urban land cover at high levels of detail. As mentioned above, Pearson's correlation coefficients (when available) were at least 0.80 for all land cover categories for each type of region (residential, commercial, and transportation). This high level of agreement between classified and reference land cover percentages is a notable achievement for per-pixel classification. In the commercial parcels, this correlation was determined to be nearly perfect for impervious surface percentage. Total area imperviousness calculations from classified and reference outputs matched to a substantial extent for each land use type, although this match was markedly better in commercial and transportation (97 percent and 92 percent match, respectively) regions than for residential regions (63 percent match).

Taken as a whole, however, these results are very informative as to the limiting effect of "edge pixels" on per-pixel, high spatial resolution image classification. The accuracy data indicate that, while, impervious features were mapped here with moderate success, linear boundaries were not mapped very accurately, and discrete image objects, such as buildings and roads, were not depicted in the final land cover map with much real-world geometry. These conclusions are drawn on the basis of the significant impervious/herbaceous "edge pixel" error as well as the consistent under-estimation of imperviousness and over-estimation of herbaceous cover in all three types of digitized land use regions. In commercial and roads areas, where area-based impervious accuracy was high, the ratio of real-world imperviousness to vegetated features was also high. In residential areas, where vegetated features and their boundaries with impervious features were extensive, area-based impervious accuracy was low. In addition, houses and driveways in residential parcels were frequently and considerably obscured by overhanging tree canopy.

In sum, the highly heterogeneous nature of residential parcel land cover was a challenge for the per-pixel classification methods used here. Much of this heterogeneity was expressed in the form of "edge pixels," and, as mapped, real-world impervious geometry was eroded in company with falsely expanded vegetated cover. In contrast to the classification methods used here, the goal behind object-oriented classification is to isolate image objects, not pixels. Thus, land cover shape is not just preserved in a successful object-oriented classification but is, in fact, a primary basis for such classification. The advantage of such an approach is empirically suggested by the "edge pixel" complications reported here. In this urban study area, however, per-pixel classification was wholly effective wherever vegetated/non-vegetated boundaries were less extensive, such as in commercial areas. The predominance of impervious surfaces in these land uses, as well as their size, makes them important inputs for environmental modeling efforts (Butcher, 1999; Gillies *et al.*, 2003).

The "edge pixel" limitation of this land cover map was significant but not fully characterized by traditional point-based accuracy assessment. One reason for this is that, in generating the reference dataset for this traditional accuracy assessment, mixed pixels were a challenge to interpret, although this concern is not new to the development of thematic map reference data (Khorram, 1999). For high spatial resolution data, field-generated data may be especially appropriate despite the difficulties its acquisition often poses (Cablk and Minor, 2003). In general, the heterogeneous nature in which features are represented by high spatial resolution imagery may not be adequately tested by conventional accuracy methods. Barr and Barnsley (2000) discussed this problem and addressed it in their study by examining morphological accuracy, the goal of which was to evaluate the accuracy of land cover shape- as well as total area-mapping results. Previously, it has been noted that a limitation of the traditional error matrix is that it does not describe the spatial distribution of classification error (Morisette *et al.*, 1999). This may have unique implications for the detail that is sought through high spatial resolution image classification.

### 3.8. Conclusions

This paper has examined the use of conventional per-pixel image classifiers, the maximum likelihood and ISODATA algorithms, in developing an urban land cover map using pan-sharpened 0.61 m QuickBird imagery. An exclusively spectral-based classification approach, coupled with a simple GIS masking step, was used to generate a six-category land cover map with 89.3 percent overall accuracy. Impervious surfaces were mapped particularly well ($\kappa = 0.88$). Total impervious surface estimates matched reference figures with 96.9 percent and 92.4 percent agreement in commercial and road buffer reference regions. Area-based imperviousness accuracy estimates reinforced qualitative findings, however, that real-world geometry was not well-represented among certain land use types. In highly heterogeneous residential areas, for example, the misrepresentation of linear boundaries between impervious surfaces and vegetated cover types was pronounced.

An ancillary GIS layer depicting study area lakes was used to virtually eliminate an initial area of confusion between impervious surfaces and water. Such ready integration of GIS data is inherent advantage to the analysis of high spatial resolution imagery. A solution to another classification problem, the lack of discriminatory power among vegetated cover types, was not so readily apparent. Importantly, though, none of the classification difficulties reported here was extensively due to the effects of shadows, as had been expected. In fact, confusion was more commonly due to image heterogeneity and reflectance overlap among illuminated versions of different cover types. Analysts are encouraged to carefully consider high spatial resolution image acquisition parameters to minimize the potential effects of shadowing.

Future work should continue to investigate the use of familiar spectral-based approaches to mapping high spatial resolution imagery, and the results of this study indicate that, for mapping particular urban land cover types, these approaches can be highly efficient and accurate. In this study, impervious surface mapping accuracy was higher in areas where reference data indicated that it was more extensive and continuous, such as in commercial parcels. The distribution and shape of such cover types in heterogeneous areas may be more accurately mapped by emerging object-oriented approaches customized to exploit detailed object morphology. Traditional spectral-based approaches, however, are comparatively simple and well-documented. In this light, the results of this study suggest that existing per-pixel classification methods present an efficient, widely available, and familiar means of land cover map derivation for particular applications of this exciting new data source.

### 3.9. References


Al-Khudhairy, D. H. A., I. Caravaggi, and S. Glada, 2005. Structural damage assessments from Ikonos data using change detection, object-oriented segmentation, and classification techniques. *Photogrammetric Engineering and Remote Sensing*, 71:825-837.

Alvarez-Mozos, J., J. Casali, M. Gonzalez-Audicana, and N. E. C. Verhoest, 2005. Correlation between ground measured soil moisture and RADARSAT-1 derived backscattering coefficient over an agricultural catchment of Navarre (North of Spain). *Biosystems Engineering*, 92:119-133.

Barr, S., and M. Barnsley, 2000. Reducing structural clutter in land cover classifications of high spatial resolution remotely-sensed images for urban land use mapping. *Computers and Geosciences,* 26:433-449.

Burkholder, J. M., E. J. Noga, C. H. Hobbs, and H. B. Glasgow, 1992. New Phantom Dinoflagellate Is the Causative Agent of Major Estuarine Fish Kills. *Nature*, 358:407-410.

Butcher, J. B., 1999. Forecasting future land use for watershed assessment. *Journal of the American Water Resources Association*, 35:555-565.

Cablk, M. E., and T. B. Minor, 2003. Detecting and discriminating impervious cover with high-resolution IKONOS data using principal component analysis and morphological operators. *International Journal of Remote Sensing*, 24:4627-4645.

Cakir, H. I., and S. Khorram, 2004. Methods, systems and computer program products for fusion of high spatial resolution imagery with low-spatial but high-spectral resolution imagery using correspondence analysis. November 4, 2004, US Patent Appl. No: 10/982,054.

Carleer, A. P., O. Debeir, and E. Wolff, 2005. Assessment of very high spatial resolution satellite image segmentations. *Photogrammetric Engineering and Remote Sensing,* 71:1285-1294.

Cheng, H. D., X. H. Jiang, Y. Sun, and J. L. Wang, 2001. Color image segmentation: advances and prospects. *Pattern Recognition*, 34:2259-2281.

Chubey, M. S., S. E. Franklin, and M. A. Wulder, 2006. Object-based analysis of Ikonos-2 imagery for extraction of forest inventory parameters. *Photogrammetric Engineering and Remote Sensing,* 72:383-394.

Clark, D. B., C. S. Castro, L. D. A. Alvarado, and J. M. Read, 2004. Quantifying mortality of tropical rain forest trees using high-spatial-resolution satellite data. *Ecology Letters*, 7:52-59.

Congalton, R. G., K. Birch, R. Jones, and J. Schriever, 2002. Evaluating remotely sensed techniques for mapping riparian vegetation. *Computers and Electronics in Agriculture*. 37:113-126.

Congalton, R. G., and K. Green, 1999. *Assessing the Accuracy of Remotely Sensed Data: Principles and Practices*, Lewis Publishers, Boca Raton, Florida, 137 p.

Dare, P. M., 2005. Shadow analysis in high-resolution satellite imagery of urban areas. *Photogrammetric Engineering and Remote Sensing,* 71:169-177.

Faucette, L.B., C. F. Jordan, L. M. Risse, M. Cabrera, D. C. Coleman, and L. T. West, 2005. Evatuation of stormwater from compost and conventionat erosion control practices in construction activities. *Journal of Soil and Water Conservation*, 60:288-297.

Fisher, J., and S. Goetz, 2001. Considerations in the use of high spatial resolution imagery: an applications research assessment. *Proceedings of the ASPRS 2001 annual convention*, 23-27 April, St. Louis, Missouri (American Society for Photogrammetry and Remote Sensing, Bethesda, Maryland), unpaginated CD-ROM.

Foody, G.M., 1995. Land-Cover Classification by an Artificial Neural-Network with Ancillary Information. *International Journal of Geographical Information Systems*, 9:527-542.

Foody, G.M., 1997. Fully fuzzy supervised classification of land cover from remotely sensed imagery with an artificial neural network. *Neural Computing and Applications*, 5:238-247.

Foody, G.M., 2002. Status of land cover classification accuracy assessment. *Remote Sensing of Environment*, 80:185-201.

Gao, J., H. F. Chen, Y. Zhang, and Y. Zha, 2004. Knowledge-based approaches to accurate mapping of mangroves from satellite data. *Photogrammetric Engineering and Remote Sensing,* 70:1241-1248.

Gillies, R. R., J. B. Box, J. Symanzik, and E. J. Rodemaker, 2003. Effects of urbanization on the aquatic fauna of the Line Creek watershed, Atlanta - a satellite perspective. *Remote Sensing of Environment*, 86:411-422.

Goetz, S., R. Wright, A. Smith, E. Zinecker, and E. Schaub, 2003. IKONOS imagery for resource management: Tree cover, impervious surfaces, and riparian buffer analyses in the mid-Atlantic region. *Remote Sensing of Environment,* 88:195-208.

Hayes, S. A., R. A. McLaughlin, and D. L. Osmond, 2005. Polyacrylamide use for erosion and turbidity control on construction sites. *Journal of Soil and Water Conservation*, 60:193-199.

Herold, M., M. E. Gardner, and D. A. Roberts, 2003a. Spectral resolution requirements for mapping urban areas. *IEEE Transactions on Geoscience and Remote Sensing*, 41:1907-1919.

Herold, M., X. H. Liu, and K. C. Clarke, 2003b. Spatial metrics and image texture for mapping urban land use. *Photogrammetric Engineering and Remote Sensing,* 69:991-1001.

Hu, X. Y., C. V. Tao, and B. Prenzel, 2005. Automatic segmentation of high-resolution satellite imagery by integrating texture, intensity, and color features. *Photogrammetric Engineering and Remote Sensing,* 71:1399-1406.

Jennings, D., S. Jarnagin, and D. Ebert, 2004. A modeling approach for estimating watershed impervious surface area from national land cover data 92. *Photogrammetric Engineering and Remote Sensing,* 70:1295-1307.

Jensen, J., 2005. *Introductory Digital Image Processing: A Remote Sensing Perspective, edition*. Prentice Hall, Upper Saddle River, NJ.

Jensen, J. R., and D. C. Cowen, 1999. Remote sensing of urban suburban infrastructure and socio-economic attributes. *Photogrammetric Engineering and Remote Sensing,* 65:611-622.

Kelly, M., D. Shaari, Q. H. Guo, and D. S. Liu, 2004. A comparison of standard and hybrid classifier methods for mapping hardwood mortality in areas affected by "sudden oak death". *Photogrammetric Engineering and Remote Sensing,* 70:1229-1239.

Khorram, S., G. S. Biging, N. R. Chrisman, D. R. Colby, R. G. Congalton, J. E. Dobson, R. L. Ferguson, M. F. Goodchild, J. R. Jensen, and T. H. Mace, 1999. *Accuracy Assessment of Remote Sensing-Derived Change Detection*, Monograph. Maryland: American Society for Photogrammetry and Remote Sensing.

King, R. S., M. E. Baker, D. F. Whigham, D. E. Weller, T. E. Jordan, P. F. Kazyak, and M. K. Hurd, 2005. Spatial considerations for linking watershed land cover to ecological indicators in streams. *Ecological Applications*, 15:137-153.

Ludwig, R., M. Probeck, and W. Mauser, 2003. Mesoscale water balance modelling in the Upper Danube watershed using sub-scale land cover information derived from NOAA-AVHRR imagery and GIS-techniques. *Physics and Chemistry of the Earth*, 28:1351-1364.

Lunetta, R. S., J. Ediriwickrema, J. Iiames, D. M. Johnson, J. G. Lyon, A. McKerrow, and A. Pilant, 2003. A quantitative assessment of a combined spectral and GIS rule-based land-cover classification in the Neuse River Basin of North Carolina. *Photogrammetric Engineering and*

*Remote Sensing,* 69, 299-310.

Maeder, J., S. Narumalani, D. C. Rundquist, R. L. Perk, J. Schalles, K. Hutchins, and J. Keck, 2002. Classifying and mapping general coral-reef structure using Ikonos data. *Photogrammetric Engineering and Remote Sensing,* 68:1297-1305.

McMahon, G., and O. Lloyd, 1995. Water Quality Assessment of the Albemarle-Pamlico Drainage Basin, North Carolina and Virginia:  Environmental Setting and Water-Quality Issues.. *U. S. Geological Survey Open File Report* 95-136. U. S. Geological Survey, Raleigh, North Carolina, 72p.

Miura, H., and S. Midorikawa, 2006. Updating GIS building inventory data using high-resolution satellite images for earthquake damage assessment: Application to Metro Manila, Philippines. *Earthquake Spectra*, 22:151-168.

Morisette, J. T., S. Khorram, and T. Mace, 1999. Land-cover change detection enhanced with generalized linear models. *International Journal of Remote Sensing*, 20:2703-2721.

North Carolina Division of Water Quality, 2004.  *North Carolina 303 (d) Impaired Waters List*. URL:  http://h2o.enr.state.nc.us/tmdl/General_303d.htm (last date accessed: 05 May 2006).

Paerl, H. W., J. L. Pinckney, J. M. Fear, and B. L. Peierls, 1998. Ecosystem responses to internal and watershed organic matter loading: consequences for hypoxia in the eutrophying Neuse river estuary, North Carolina, USA. *Marine Ecology-Progress Series*, 166:17-25.

Pohl, C., and J. L. van Genderen, 1998. Multisensor image fusion in remote sensing: concepts, methods and applications. *International Journal of Remote Sensing*, 19:823-854.

Sawaya, K., L. Olmanson, N. Heinert, P. Brezonik, M. Bauer, 2003. Extending satellite remote sensing to local scales: land and water resource monitoring using high-resolution imagery. *Remote Sensing of Environment*, 88:144-156.

Segl, K., S. Roessner, U. Heiden, and H. Kaufmann, 2003. Fusion of spectral and shape features for identification of urban surface cover types using reflective and thermal hyperspectral data. *ISPRS Journal of Photogrammetry and Remote Sensing*, 58:99-112.

Singh, V., T. Piechota, and D. James, 2003. Hydrologic impacts of disturbed lands treated with dust suppressants. *Journal of Hydrologic Engineering*, 8:278-286.

Song, M., D. L. Civco,  and J. D. Hurd, 2005. A competitive pixel-object approach for land cover classification. *International Journal of Remote Sensing*, 26:4981-4997.

Svab, A., and K. Osti, 2006. High-resolution image fusion: methods to preserve spectral and spatial resolution. *Photogrammetric Engineering and Remote Sensing,* 72:565-572.

Thomas, N., C. Hendrix, and R. Congalton, 2003. A comparison of urban mapping methods using high-resolution digital imagery. *Photogrammetric Engineering and Remote Sensing,* 69:963-972.

Walsh, C.J., T. D. Fletcher, and A. R. Ladson, 2005. Stream restoration in urban catchments through redesigning stormwater systems: looking to the catchment to save the stream. *Journal of the North American Benthological Society*, 24:690-705.

Wang, L.Z., J. Lyons, and P. Kanehl, 2001. Impacts of urbanization on stream habitat and fish across multiple spatial scales. Environmental Management. 28, 255-266.

Warner, T.A., and K. Steinmaus, 2005. Spatial classification of orchards and vineyards with high spatial resolution panchromatic imagery. *Photogrammetric Engineering and Remote Sensing,* 71:179-187.

Williams, E. S., and W. R. Wise, 2006. Hydrologic impacts of alternative approaches to storm water management and land development. *Journal of the American Water Resources Association*, 42:443-455.

U. S. Census Bureau, 2006. Population Estimates for the 100 U.S. Counties with the Largest Numerical Increase from April 1, 2000 to July 1, 2005. URL: http://www.census.gov/popest/counties/CO-EST2006-08.html, U. S. Department of Commerce, Washington, D. C. 20233 (last date accessed: 09 January 2008).

Yang, L., G. Xian, J. Klaver, and B. Deal, 2003. Urban land-cover change detection through sub-pixel imperviousness mapping using remotely sensed data. *Photogrammetric Engineering and Remote Sensing,* 69:1003-1010.

# 4. HIGH SPATIAL RESOLUTION LAND COVER CHANGE DETECTION BASED ON FUZZY UNCERTAINTY ANALYSIS AND CHANGE REASONING

## 4.1. Abstract

Land cover change detection is an important research and application area for analysts of remote sensing data. The primary objective of the research described here was to develop a change detection method capable of accommodating spatial and classification uncertainty in generating an accurate map of land cover change. As a secondary objective, this method was designed to facilitate the mapping of particular types and locations of change based on specific study goals. Urban land cover change pertinent to surface water quality in Raleigh, North Carolina, was evaluated using land cover classifications derived from pan-sharpened, 0.61 m QuickBird images from 2002 and 2005. A "from-to" change map had an overall accuracy of 78.9% ($\kappa = 0.747$) and effectively mapped land cover changes posing a threat to water quality, including increases in impervious surface. This work presents an efficient fuzzy framework for transforming map uncertainty into accurate and meaningful change analysis.

## 4.2. Introduction

Because of its synoptic coverage, cost-effective update potential, and increasingly digital format, remote sensing data have become a primary means of generating land cover change maps (Lu *et al.* 2004). In generating these maps, analysts seek to represent the transformation of the earth's biophysical and man-made features over a period of time (Jensen 2005). Such accounts provide a basis for understanding the causal phenomena behind land transformations and for planning the improved management and use of natural resources (Lu *et al.* 2004).

Like all maps, remote sensing-derived change maps generalize the shape, size, location, and distribution of real-world objects (Khorram 1999). This makes them models of the real world and therefore limited in value by their accuracy. Unfortunately, error in spatially-explicit or map data is not always fully assessed or reported. Missing or incomplete quantification of error occurs in part because map accuracy, relative to that of other model types, can be difficult to express in a way that is meaningful to users (Foody 2002). Dominant accuracy reporting practices for change map products have been criticized on these grounds (Khorram 1999; Foody 2002).

There are a variety of methods for deriving change maps from remotely sensed data, many of which were reviewed by Lu *et al.* (2004) who indicated that post-classification map comparison is among the most commonly used methods and has the advantages of providing from-to change information and minimizing the impact of sensor and environmental differences. The major disadvantages of this method are that it requires an analyst to generate or acquire individual-date input maps and, more pointedly, the accuracy of the change map depends on the quality and alignment of these individual-date maps (Khorram 1999). Much remote sensing-based change detection research has focused on the elimination of error in post-classification change mapping (Jensen *et al.* 1993; Zhang 2001; Liu and Zhou 2004; Prenzel and Treitz 2004). This has been a persistent research area despite the fact the sources of this error are well-known: inconsistent semantics, imperfect image alignment, and individual-date misclassification (Van Oort 2005). While error due to semantics is eliminated when consistent classification schemes are used (Achard *et al.* 2002), the latter two sources are more difficult to entirely eliminate.

The goal of eliminating post-classification change map error is grounded in classical set theory, a view which conceives of objects having membership in only one category of land cover (Jensen 2005). It has been suggested that land cover and its change are more appropriately viewed as *fuzzy* phenomena, however, because a point in space may exhibit membership in multiple land cover categories and because change does not always occur along discrete lines (Khorram 1999). By extension, post-classification change map error can also be seen as having a fuzzy composition. This view contemplates such "error" as *uncertainty* arising from imperfect image alignment and individual-date classification.

The present study adopts a fuzzy approach to dealing with post-classification map error with the goal of *characterizing*, not eliminating, uncertainty in the change map. This paradigm has two theoretical advantages: (1) existing post-classification error elimination methods are imperfect and risk introducing additional map uncertainty when operating under strict logical rules and (2) by viewing uncertainty as additional "soft" data rather than error, there is no inherent information loss. Specifically, the research described here develops a "change index", a quantitative gradient along which land cover change is characterized by both *certainty* and *relevance*. The result is a continuous representation of change, a product that retains more information and flexibility than discrete maps of change (Morisette *et al.* 1999). Change index parameters are quantified using either well-established procedures or subjective measures particular to the application area of this study. Broadly, the methods proposed here integrate several fuzzy techniques into an approach that can be customized to any change mapping application.

### 4.3. Study area and data

The study area is a 71.5 $km^2$ portion of suburban Raleigh, North Carolina, USA (Figure 4-1). This area encompasses a series of adjacent watersheds within the Neuse River Basin. All of suburban Raleigh is contained within Wake County, which was recently cited by the U.S. Census

Bureau as one of the sixty fastest-growing counties in the country (2003). Much of the growth in Wake County has occurred in suburban Raleigh. Both of the major watersheds within the study area have been listed on North Carolina's Clean Water Act Section 303(d) Impaired Waters List each time it has been produced (NCDENR 2007; NCDENR 2006). On both occasions, the cause of water quality impairment has been cited as "urban runoff/storm sewers". The present study was designed to highlight potential areas of urban land cover change that may be contributing to the deterioration of water quality within this growing suburban region.

Two leaf-on QuickBird images were used to derive individual-date land cover maps for this analysis. These images, captured in June of 2002 and 2005, provide four-band multispectral data at 2.44 m spatial resolution and panchromatic data in 0.61 m spatial resolution (www.digitalglobe.com). This exceptionally high spatial resolution makes this imagery a promising data source for mapping change in complex urban areas. Other data utilized in this study were GIS files for roads, tax parcels, and hydrology, all available from the Wake County iMAPS server.

### 4.4. Methods

Broadly, the approach described here integrates fuzzy logic and change reasoning to develop a land cover change index map. A raw post-classification change map was separately generated for comparison purposes and for transformation into the final change map. In generating the final map, the two individual-date land cover maps were first compared on the basis of fuzzy spatial agreement. Next, the uncertainty of the indicated change was further characterized according to classification accuracy and change type reasoning. This methodology is briefly outlined below and then discussed in further detail:

1. The raw 2002 QuickBird image was georeferenced using field-generated ground control points, and the raw 2005 QuickBird image was geo-registered to it using image control points.

2. Individual-date land cover maps were generated using the hybrid per-pixel classification method described in Hester *et al.* (2008). These maps were compared using simple map subtraction to develop the "raw post-classification change map".

3. Fuzzy logic was used to compare the individual-date maps and qualify land cover change by uncertainty in location (misregistration).

4. Fuzzy logic and change-type reasoning were used to qualify land cover change by uncertainty in categorization (misclassification).

5. The change detection process was attuned to the water quality goals of this study by weighting the most relevant types and locations of potential change.

6. Fuzzy logic and change reasoning results were integrated into a binary change/no change map that quantified the most certain, likely, and relevant change regions within the study area. A "from-to" change map was developed from this binary map inserting the type of change identified in the raw post-classification map.

7. Binary and from-to maps were assessed using "special effort sampling" described in Khorram (1999).

#### *4.4.1. Pre-processing of QuickBird imagery*

For both dates of QuickBird imagery, the multispectral and panchromatic components were fused using the Cakir-Khorram algorithm (Cakir and Khorram 2008). This is an image pan-sharpening method that achieves the spectral resolution of the multispectral image and the spatial resolution of the panchromatic image without compromising spectral integrity. The fused imagery retained red, green, blue, and near-infrared content at 0.61 m pixel size. Next, using a Trimble ProXR Global Positioning System (GPS) unit, 32 ground control points were collected in the field. These real-time differentially-corrected GPS data had a one-meter margin of horizontal positional error. These points were used in a first-order polynomial correction to georeference the 2002 image to a root-mean square error (RMSE) of 1.6 m. After projecting the 2002 and 2005 images to the North Carolina State Plane, NAD 83, meters, coordinate system, the 2005 image was geo-registered to the 2002 image using a second-order polynomial correction with an RMSE of 1.1 m. In light of the sensor spatial resolution, these measures of geometric accuracy were deemed acceptable despite exceeding the standard 0.5 pixel literature benchmark (Khorram 1999). For this imagery, an RMSE of 0.5 pixels would have been an error margin of less than 25 cm, a figure far smaller than the one-meter limitation of the GPS data would generally permit. Although further post-processing may have removed additional geometric registration error, this level of precision satisfied this study's goal of developing a change detection method capable of accommodating such typical image misalignment.

#### *4.4.2. Generation of individual-date land cover maps*

Two land cover maps were separately derived from the 0.61-meter multispectral QuickBird images covering the study area. Classification methodology developed for use with these high-resolution images is described in Hester *et al.* (2008). In short, this methodology combines supervised and unsupervised classification algorithms in an iterative, layered procedure. Using this approach, a six-category land cover map was developed for both images. All land cover was mapped as Impervious, Water, Bare/Disturbed, Deciduous, Evergreen, or

Herbaceous. The overall accuracy and Kappa statistics for the 2002 and 2005 land cover maps, respectively, was 89.3 percent ($\kappa$=0.872) and 85.0 percent ($\kappa$=0.820). Figure 4-2 presents these two land cover maps, and Figure 4-3 compares the mapped land cover at each date.

#### *4.4.3. Characterization of change uncertainty: fuzziness of location*

The primary goal of this research was to create a change map that quantified the most certain and relevant change regions in the study area. The first step toward the creation of this map was generating a *spatially fuzzy* map of change. The pernicious effects of image misregistration on the accuracy of conventionally derived land cover change maps have been well-documented (Dai and Khorram 1998; Khorram 1999; Verbyla and Boles 2000; Bruzzone and Cossu 2003). As suggested by Power *et al.* (2001), conventional pixel-by-pixel map comparison methods are systemically vulnerable to misregistration noise; these procedures record any pixel misalignment between maps as change. This exemplifies the rigid processing framework of *crisp logic*. Within this paradigm, the decision-making rubric in many automated or semi-automated remote sensing analyses, land cover and land cover change classes are treated as discrete sets (Khorram 1999). Human observers conducting visual inspection for change detection, in contrast, can typically resolve map misregistration by perceiving global similarities, logical coherence, and patterns (Hagen 2003). This exemplifies the use of *fuzzy logic*, a reasoning framework first identified by Zadeh (1965). The integration of fuzzy set theory into land cover analyses has become a popular strategy in light of the uncertainty inherent to geographic modeling and mapping (Shackelford and Davis 2003; Arnot *et al.* 2004; Nemmour and Chibani 2005).

Researchers affiliated with the Research Institute for Knowledge Systems (RIKS BV) in the Netherlands have recently developed novel fuzzy set tools for map comparison. With respect to map misalignment, Power *et al.* (2001) used fuzzy land use categories and polygon boundaries to evaluate global agreement between imperfectly aligned maps. Hagen (2003) formulated a measure of *fuzziness of location* to account for the imprecision with which identical map features may be represented in different maps. Expansions to that formulation were later incorporated into the Map Comparison Kit (MCK), a freeware program developed by RIKS in conjunction with the Netherlands Environmental Assessment Agency (Hagen-Zanker *et al.* 2005). This stand-alone software package is freely available for download at http://www.riks.nl/mck/ and described in detail by Visser and de Nijs (2006).

The MCK fully integrates a variety of fuzzy map comparison tools, including Hagen's (2003) fuzziness of location. This metric was selected for use in the present study because it provides a simple, efficient means of addressing change mapping uncertainty resulting from the comparison of misaligned land cover maps. *Fuzzy location* describes the land cover of a particular raster pixel, or cell, not just in isolation but in light of the neighborhood of cells around it. This description accommodates the fact that, in practice, a cell's location can only be specified in individual maps and aligned between maps with limited certainty. Thus, the similarity between the categorical values of the same cell location in different maps is more accurately assessed as a function of both the central cell and its neighborhood.

Within the Map Comparison Kit, an analyst can perform a fuzzy change analysis between individual land cover maps using the *Fuzzy kappa* algorithm by specifying the desired size and impact of a cell's neighborhood using a distance decay function. This function defines the degree to which neighborhood cells contribute to a central cell's fuzzy membership in each land cover category. The highest contribution for each category sets the membership value in that category. In the aggregate, these membership values form the "Fuzzy Neighborhood Vector" for each cell. The Fuzzy Neighborhood Vectors of each pixel in each map are then compared to evaluate map differences. This process, described in full by Hagen (2003), establishes the extent to which the central pixel has either matching category values or similar neighborhoods in the two maps being compared. The result is a single similarity value, ranging from 0-1, at the location of each cell. In this comparison product, the value 1 denotes that the two depictions of the central cell match in category, while, at a value of 0, the two depictions of the central cell do not match and have completely dissimilar neighborhoods.

Hagen (2003) states that there is no theoretically best parameter set for the membership distance decay function and that analysts should experiment with its size and form. In the present study, an exponential decay function with a 1.5-pixel halving distance and a five-pixel radius was utilized. At these settings, areas of true and false change due to apparent misregistration were distributed along a relatively even distribution of similarity values between 0-1.

For the purposes of this study, output similarity values were interpreted as a measure of the degree of spatial certainty with which land cover change was mapped. In other words, the similarity values were inverted such that the 0 values (those pixels with the least inter-map similarity) denoted pixels for which *change* was most spatially certain and 1 values (those pixels with inter-map category match at the central pixel) indicated that land cover could be characterized as *unchanged* with the highest degree of spatial certainty. To make this transformation, the 0-1 values were binned and reclassed as integer values (1-5) according to the scheme depicted in Table 4-1. This step advanced the goal of qualifying change mapping results in terms of *uncertainty*.

#### *4.4.4. Characterization of change uncertainty: fuzziness of category*

In order to further qualify the certainty of regions of change identified on the basis of spatial fuzziness, measures of *category fuzziness* were developed. This step addressed the change map uncertainty inevitably propagated from error in the individual-date classifications (Khorram 1999; Power *et al.* 2001). Lunetta and Elvidge (1999) proposed multiplying individual map classification accuracies in order to approximate the accuracy of post-classification change maps. While this measure of change map validity is intuitive and easy to calculate, it ignores local variability in change error as well as *a priori* knowledge about study area change. In some cases, the result of map classification error propagated in change products is unlikely from-to change types. Liu and Zhou (2004) used rationality tests for particular change types in order to identify mapped land use transitions that were deemed improbable, such as change from built-up urban use to another cover type. Fuzzy classification is inherently well-suited to incorporating change reasoning techniques. Tang *et al.* (2005), for example, employed logical rules in order to characterize the degree of change per pixel according to the extent of difference in each pixel's inter-date fuzzy category membership and crisp image spectral values.

In the study described here, category fuzziness was accommodated into the final change map using individual-map date classification accuracy as well as reasoning about the likelihood of particular land cover change type occurrence. With respect to individual-date classification accuracy, the product of map user's accuracies for each from-to change type was generated. Since each input map used the same six-category scheme, there were a total of thirty-six possible types of change and non-change pixels and resulting map user's accuracy products. These products were arranged in ascending order and partitioned into one-third bins. Adjusting for a tied value at the first breakpoint, the three bins were twelve, thirteen, and eleven values in size. This step again transformed change map information into integer measures of certainty, as the change types in each bin were then assigned, in ascending order, a value of 1, 2, or 3. Thus, those change pixels assigned a value of 3 were mapped with the most category-fuzzy confidence. Notably, non-change pixels were assigned values inversely related to user's accuracy products to reflect that high mapping confidence in these pixel types represents a decreased likelihood of change there. This potential source of omission error was specifically addressed in the accuracy assessment sampling strategy. Category fuzziness change index factors are displayed in Table 4-2.

#### *4.4.5. Specification of priority/improbable change categories and change-type relevance*

Land cover change reasoning was further used to accommodate the *relevance* of particular changes. This index factor presumes the purported change occurred (a presumption qualified by the category-product confidence factor and specifically tested in the accuracy assessment design) and identifies the relevance of that type of change. In the case of this study, relevance was determined in relation to urban water quality analysis, and, again, categorical mapping values were set as 1, 2, or 3 in order of increasing relevance. Highest priority change types (values here of 3) included transitions to the Impervious category from any other cover type. This specification derives from the well-documented impact of even small amounts of watershed impermeable surface on non-point source pollution and water quality (Schueler 1994;

Arnold and Gibbons 1996). Similarly, pixels indicating a change from any vegetated category (Herbaceous, Deciduous, or Evergreen) in the 2002 map to the Bare/Disturbed category in the 2005 map were also assigned a relevance value of 3. While this designation may not be justified in agricultural or coastal areas, *a priori* knowledge of the Raleigh study area suggested that most bare- or disturbed-soil surfaces were associated with construction sites, emerging roads, or other urban development in progress. This land cover type also has important implications for the composition and volume of urban stormwater (Faucette *et al.* 2005; Hayes *et al.* 2005). The only exceptions to this rule were change to Bare/Disturbed from Impervious (set as a low-priority 1) and from Water (set as 2 since, in this study area, this change occurs most commonly along the banks of lakes and streams and with little environmental consequence).

The relevance metric was also used to set change mapping priorities for improbable or trivial land cover change types relative to water quality management. Specifically, in concert with the reasoning of Liu and Zhou (2004) described above, any purported change from Impervious to any vegetated cover type was deemed improbable and assigned the minimum mapping priority of 0. Other change types designated as having a relevance of 0 to and/or priority for study water quality monitoring goals were changes between tree categories (Deciduous and Evergreen) and changes from Herbaceous to either of those categories. Non-change combinations were assigned a 0 priority, while all change types not detailed here were assigned a relevance factor of 1. The full derivation of fuzzy category change map index values is displayed in Table 4-2.

In a final refinement to the change map based on waste quality management *priorities*, study watershed catchments that had experienced the most significant summary change in land cover composition between 2002 and 2005 were identified. Of the 32 sub-catchments within the study area, only four experienced a total areal change in land cover in excess of 15% of total catchment area (Figure 4-4). All four of these high-change catchments were located in the northernmost extent of the study area, the region furthest from downtown Raleigh. This area was known *a priori* to be undergoing land cover change during the study period due to the construction of new residential development. To each change pixel within these four catchments, an additional change index factor of 1 was added to add a mapping "margin of error" in favor of identifying change in this dynamic area.

### *4.4.6. Generation of change index and change map*

For each pixel in the change index map, the degree of change certainty and relevance was generated by summing the change index factor values described above. This calculation is summarized in Table 4-3 and resulted in an index with values ranging from 2-12. The higher a pixel's index value, the greater the map *certainty* in the change indicated there and the greater the *relevance* of that change to water quality management. A visual inspection was used to determine a threshold of change index value above which change is deemed certain and relevant enough to be mapped as change, a step used to transform the interim change index map product into discrete change/no change and "from-to" change maps. In generating the "from-to" map, change was mapped at locations identified in the change/no change map and in the "from-to" type identified by the raw post-classification change map.

### *4.4.7. Accuracy assessment methods*

The challenges of assessing the accuracy of land use/land cover change map were described in detail by Khorram (1999) and echoed by Foody (2002). Khorram (1999) encouraged "special effort sampling" to test the accuracy of these maps given the rarity of true land cover change in most study area scenarios. *A priori* knowledge of the present study area supported the presumption that change was rare even in this growing population center. A random 100-point sample was used to empirically evaluate this theory (Khorram 1999).

Assuming the rarity of change and considering the change index factors, the "special effort sampling" accuracy assessment regime was designed to test aspects of change index development that most risked errors of change pixel omission and commission. The sample constituted of 350 photointerpreted points, and its distribution is detailed in Table 4-4. The areas sampled because of high omission risk were areas in which change was either deemed *likely* based on study area knowledge or, alternatively, areas in which change was *assumed to be unlikely* in the development of the change index. In both areas, the risk of omitting areas of true change was inherently elevated. Similarly, the areas sampled because of high commission risk were areas in which either change was deemed *unlikely* based on study area knowledge or, alternatively, areas in which change was *assumed to be likely* in the development of the change index.

## 4.5. Results

### *4.5.1. Likelihood of study area change and raw post-classification change detection accuracy*

Only 8% (8/100) of the "change rarity" evaluation points were interpreted as having experienced true 2002-2005 land cover change. Nearly half (3/8) of these change points were fixed on a point of transition from Deciduous to Herbaceous cover, *all maintained lawn grass*, and one-quarter (2/8) fell on locations at which Deciduous cover was converted to Impervious cover. At two other change points, Bare/Disturbed cover was developed into Impervious and Herbaceous cover, and, at the final point of randomly selected change, Evergreen cover became Bare/Disturbed. Thus, this random sample confirmed both the rarity of true change in this study area during the 2002-2005 period of analysis as well as the tendency of this change to occur in the direction of developed land cover types. Contrasting this result, the raw post-classification change map (Figure 4-5) suggests that change occurred in 31.5% of the study area. Evaluating this map using the 350 point sampling array developed for the change index map, the overall change/no change accuracy of this map was calculated as 64.0% and the "from-to" accuracy was 47.7%. Notably, the commission error in the change/no change binary form of this map was 34.0% (119/350) compared to its limited omission error (2.0% or 7/350).

### *4.5.2. Land cover change detection using the change index map*

A histogram of pixel change index values is displayed in Figure 4-6. After visual inspection of the change index map, a threshold consistently representing true change was identified at pixels with index values greater than 8. On this basis, the change index map presented in Figure 4-7 represents 2002 to 2005 "change" as any pixel with an index value of 9-12. According to this output, only 7.2% of the study area experienced land cover change between the two image dates. This comports with the results of the random 100-point "change rarity" evaluation in which 8.0% of sampled points were in areas of true change. The raw post-classification change map, in contrast, depicted that nearly four times as much change occurred. Figure 4-8 depicts a representative region of land cover change as depicted by QuickBird imagery in 2002 and 2005, and Figure 4-9 presents corresponding raw post-classification and change index maps for comparative purposes.

For purposes of “from-to” change mapping, land cover was interpreted to remain as mapped in the 2002 classification at pixels with change index values ranging from 2-8. Where change index values greater than 8 were interpreted to indicate that true land cover change occurred, “from-to” land cover change was presumed to be present in the form indicated by the raw post-classification change detection map. Under this interpretation, 79.4% of the mapped change was a transition from a vegetation category to Impervious. Another 18.8% of mapped change was some form of conversion to Bare/Disturbed from vegetation. Together, conversion from vegetated land cover in 2002 to Impervious or Bare/Disturbed cover in 2005 accounted for 98.2% of the change mapped using the change index method. The largest single type of mapped change was from Herbaceous to Impervious (33.5% of mapped change).

### *4.5.3. Land cover change index map and accuracy assessment*

As a binary map, with all pixels with index values from 9-12 representing “change” and all others representing “no change”, the index map had an accuracy of 85.4% with omission and commission errors of 7.4% and 7.1%, respectively. The “from-to” map error matrix is presented in Table 4-5, and overall from-to accuracy was 78.9% ($\kappa = 0.747$). Producer’s accuracy for non-change combinations was generally high, ranging from 84.8% to 100.0%. The same generalization is true for user’s accuracy for non-change classes except for Bare/Disturbed (37.0%). Among change types, producer’s accuracies were all above 60.0% while user’s accuracies were as low as 19.4%. Categories of change to Impervious in 2005 generally had the lowest user’s accuracies, ranging from 19.4% (Herbaceous-Impervious) to 65.5% (Bare/Disturbed-Impervious).

### 4.6. Discussion and Conclusions

The goal of this study was to develop a land cover change map that is meaningful, complete, and realistic using fuzzy logic and change reasoning. Specifically, this change map was designed to highlight urban land cover change pertinent to water quality management in a rapidly developing urban study area. Results showed that this change map minimized spurious indications of change by exploiting, not eliminating, inherent sources of map uncertainty. In change/no change format, this map included far less commission error than the raw post-classification change map (7.1% versus 34.0%) and comparable omission error percentage (7.4% versus 2.0%). In addition, this map indicated an extent of study area change comparable to that estimated using the 100-point "change rarity" survey (7.2% versus 8.0%) and in conformity with *a priori* study area knowledge. The change map developed here correctly characterized reference data as either change or no change in 299/350 points (85.4%).

In general, the methods described here effectively addressed the two major sources of post-classification change detection error identified *supra*: individual-date map misclassification and misregistration. Calculated "from-to accuracy", 78.9%, exceeds the nominal upper limit of such accuracy contemplated by Lunetta and Elvidge (1999), the product of the individual-date map accuracies (75.9%). This primarily reflects the capacity of category fuzziness characterization to reduce change detection error resulting from *misclassification*. Similarly, the accuracy of the raw post-classification change map was degraded due to image *misalignment*. This is plain from the spurious indications of change along roads and sidewalks in Figure 4-9, as is the capacity of fuzzy logic to overcome this limitation. Misalignment error is particularly limiting to change detection involving high spatial-resolution imagery such as QuickBird data

(Wang and Ellis 2005). This makes the "from-to" change detection accuracy achieved here especially notable.

As the change index was designed to heavily weight changes to Impervious or Bare/Disturbed land cover, it is not surprising that these categories dominate the land cover to which most of the mapped change pixels converted (98.2%). For the same reason, the decreased user's accuracies (higher errors of commission) seen in these from-to change types are also to be expected. Nonetheless, these are the predominant types of land cover change known to be occurring in the study area, and overall commission error was kept to a minimum. Thus, this map is a spatially-explicit depiction of 2002-2005 increases in impervious and bare land cover, the changes most likely to impacting surface water quality, and it errs on the side of mapping these changes without significantly sacrificing map accuracy. Quantitatively, the change index exemplified here adds such a "margin of error" to mapping change types of interest through change *relevance* and *priority* factors while *fuzziness of location* and *fuzziness of category* factors qualify indications of mapped change. This is exactly the kind of balancing test human observers conduct intuitively when performing map comparison that fuzzy analyses are intended to simulate (Hagen 2003).

The success of the approach described here was dependent to some extent on *a priori* knowledge of the study area. Conversion of vegetated land cover to impervious surfaces, for example, was known to be the dominant form of true land cover change. Thus, heavily weighting these types of change pixels was not likely to result in high errors of commission. Although this is a constraint on the use of this specific approach, it also demonstrates the flexibility of a fuzzy approach to change mapping capable of incorporating available information to address map uncertainty (Woodcock and Gopal 2000; Power *et al.* 2001). Moreover, category fuzziness-weighting only required knowledge of input map accuracy, and fuzziness of location weighting required no extrinsic information whatsoever. The methods described here generally rely on modest assumptions and inferences that can be customized for any change mapping application and are computationally easy to apply.

Future work should consider uses of semi-continuous depictions of land cover change such as that developed here as an interim map. As discussed *supra*, land cover change is not in reality a discrete phenomenon (Khorram 1999), and continuous change maps have previously been developed using novel pre-classification change detection methods (Morisette *et al.*, 1999). The interim post-classification change index map produced here represented change along a gradient from 2-12. It was used to develop binary and "from-to" change maps after estimating a threshold beyond which true change was unlikely or irrelevant to the water quality management goals of this study. Other uses might retain the entire gradient of change index values as a driver of sampling efforts, for example. Field verification of potential change might be allocated inversely proportional to change index value, or middle-range values might be subjected to further analysis while extreme values may be relied upon with more confidence. Broadly, a semi-continuous or continuous change index may be a more effective means of mapping the spatial contours of natural land cover change, such as gradual changes in forest composition (Southworth 2004).

Analysts should also continue to explore fuzzy logic as a means of accommodating the rich information content of high spatial-resolution remote sensing imagery, such as that acquired by the QuickBird sensor. This imagery is an exciting medium for analyzing land cover change, although its complexity has frustrated some applications of conventional processing techniques (Dare 2005; Hu *et al.* 2005). In this study, for example, slight image misalignment had a dramatic negative effect on post-classification map accuracy due in part to the irregular spatial details, such as sidewalks, depicted in the imagery. Nonetheless, the characterization of *fuzziness of location* largely eliminated this error source in the final change map. This is a powerful demonstration of how fuzzy logic coupled with change reasoning can improve land cover change detection by transforming map uncertainty into information.

## 4.7. Figures and figure legends

**1. Figures**

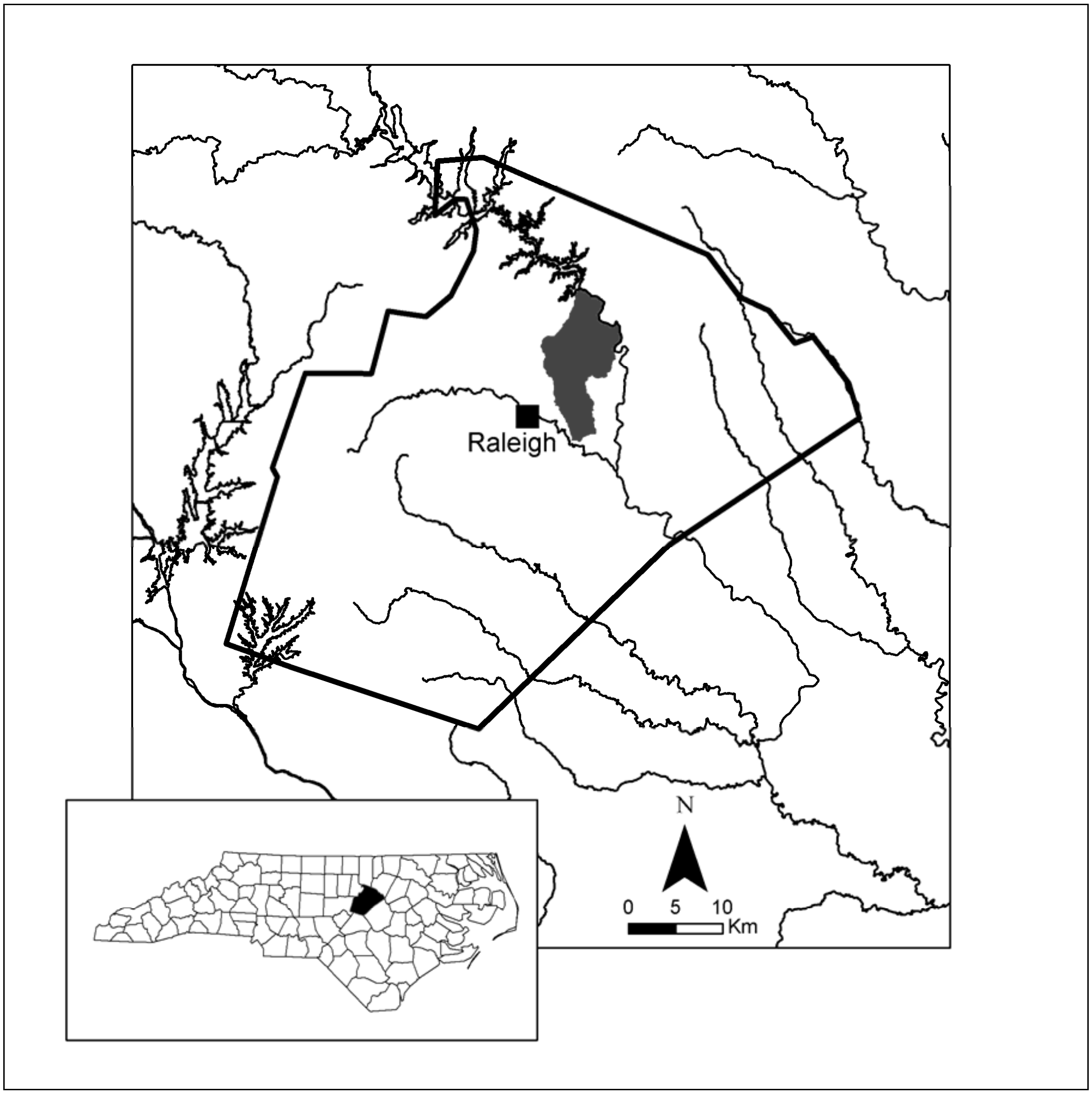


**Figure 4-1. Study area in northeast Raleigh, Wake County, North Carolina, USA.**

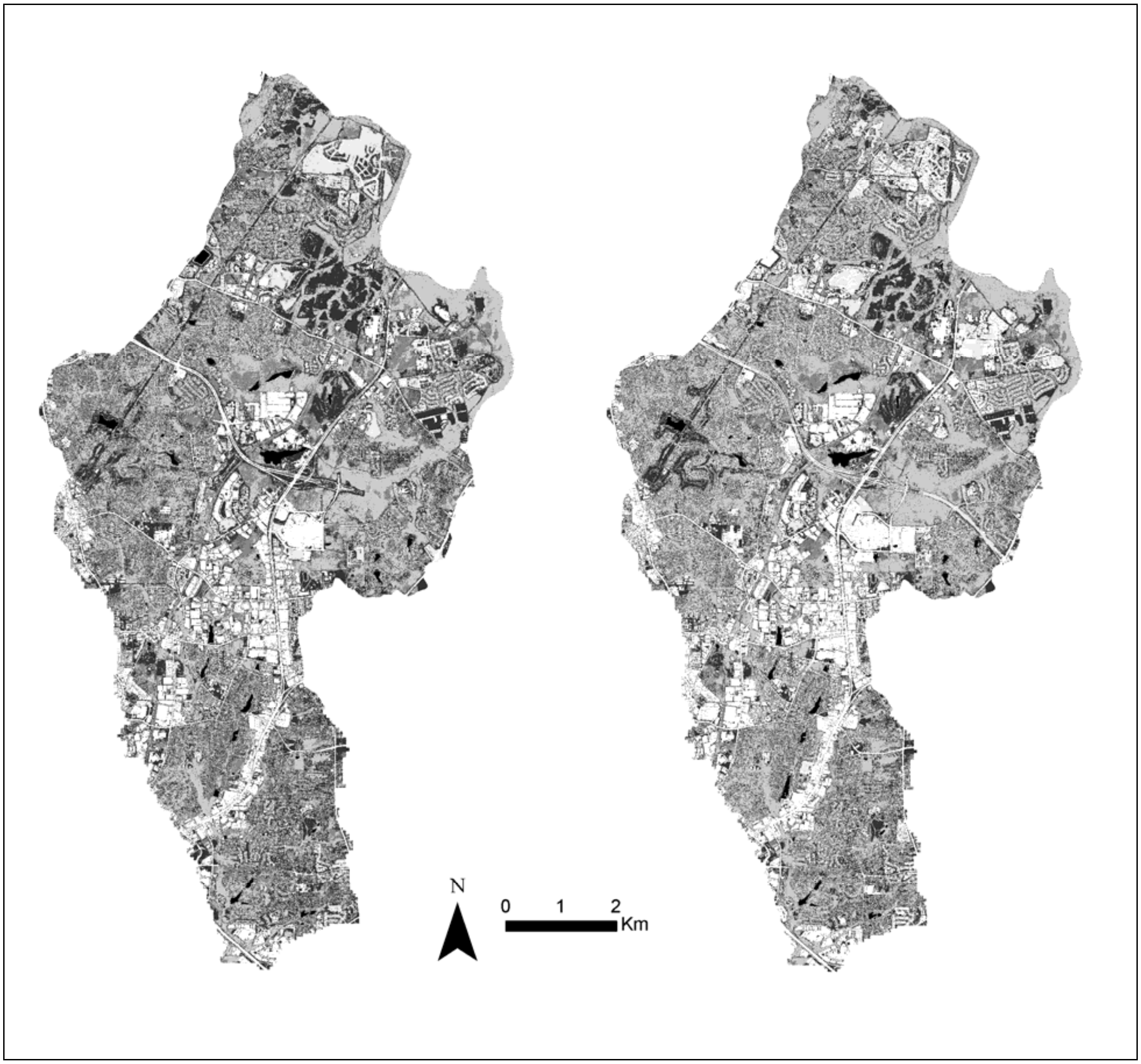


**Figure 4-2. Study area land cover classifications, 2002 (left) and 2005.**

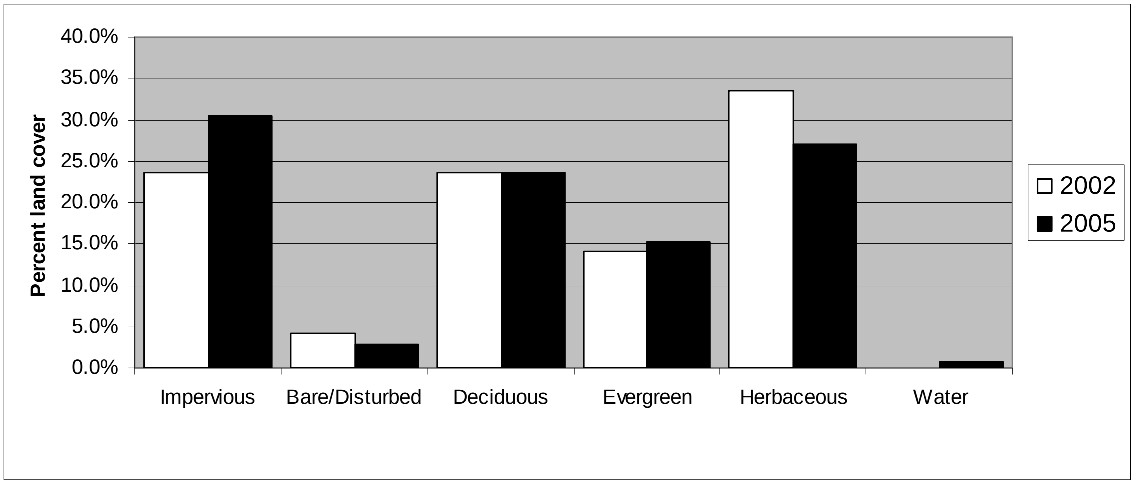


**Figure 4-3. Study area land cover classification histograms, 2002 and 2005.**

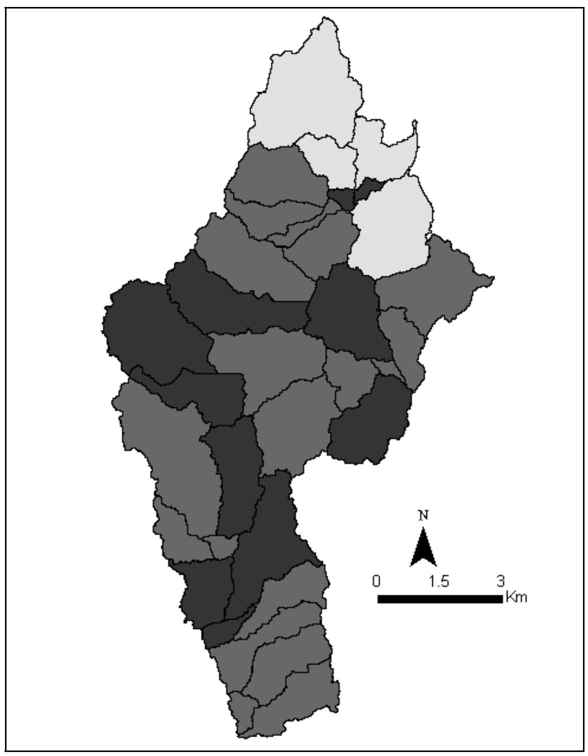


**Figure 4-4. Percent land cover change, 2002-2005, by catchment.**

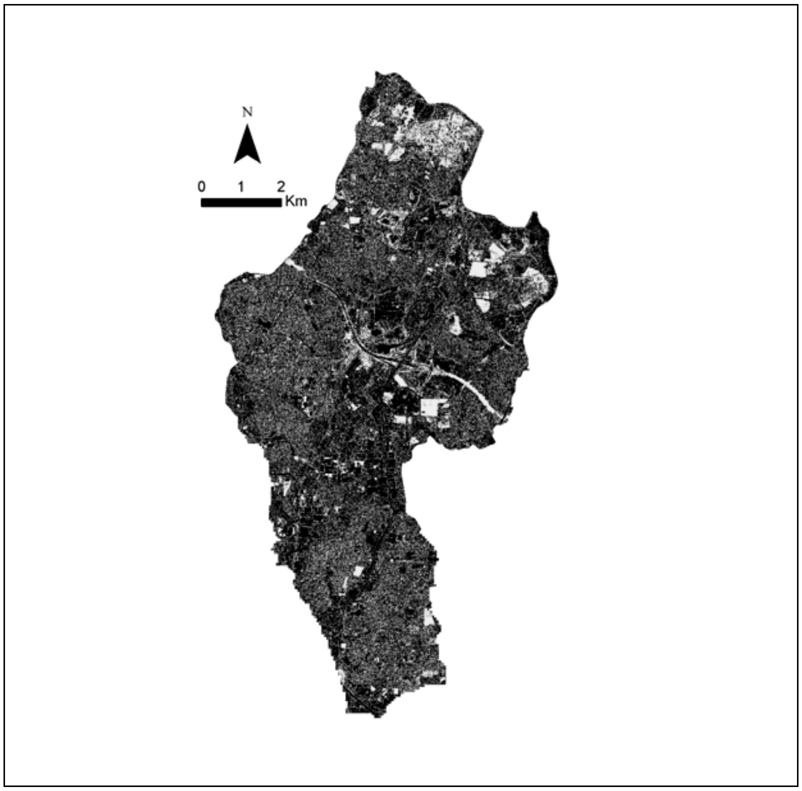


**Figure 4-5. Raw land cover change map, 2002-2005.**

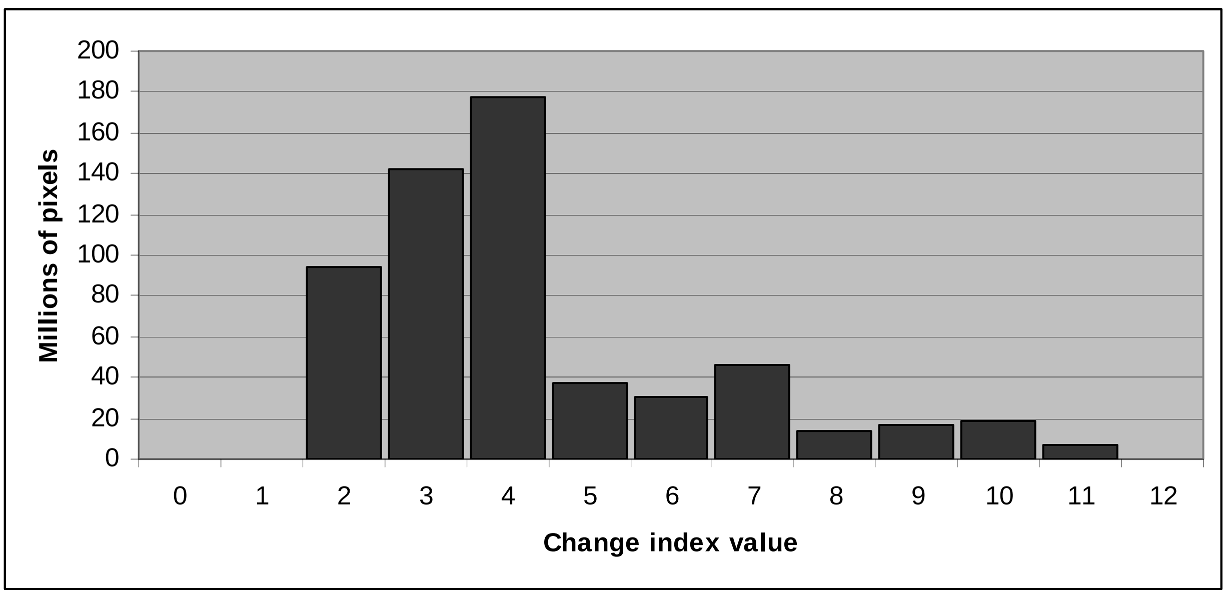


**Figure 4-6. Histogram of change index values in millions of pixels.**

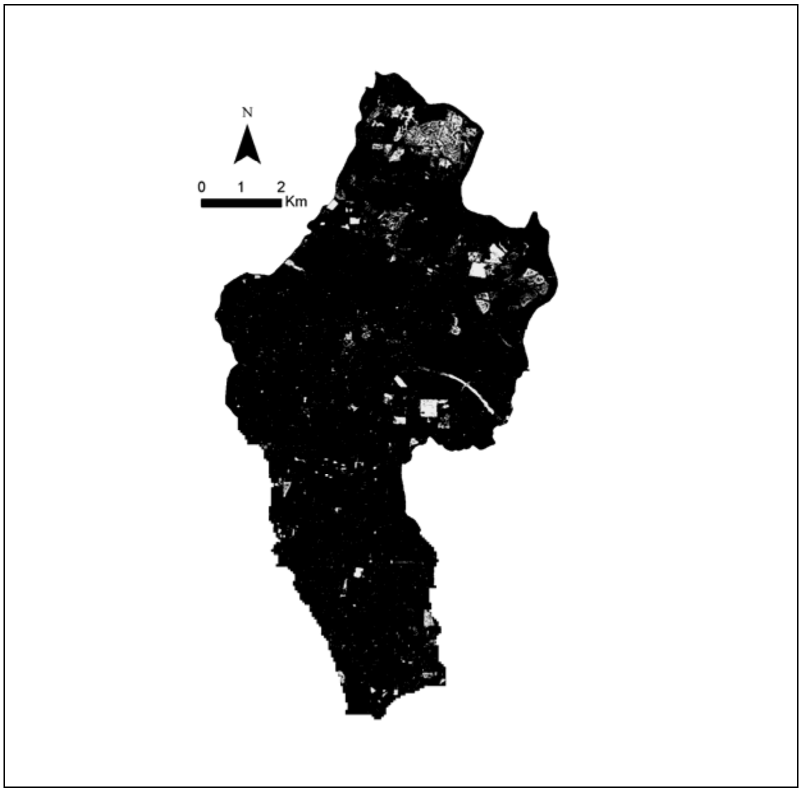


**Figure 4-7. Land cover change index map, 2002-2005, with 2-8 values mapped as "no change" and 9-12 values mapped as "change".**

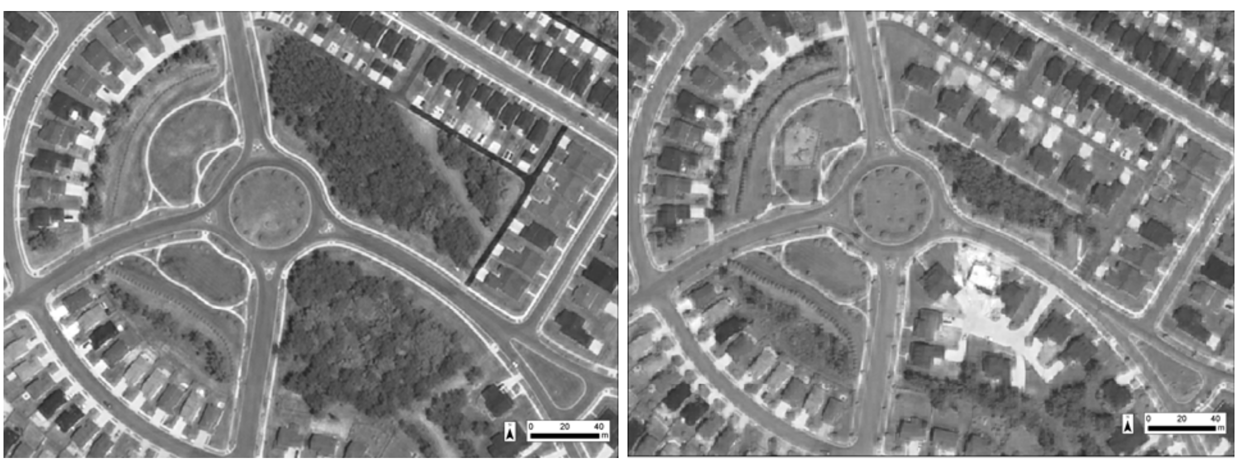

**Figure 4-8. 2002 (left) and 2005 (right) QuickBird imagery of example change region.**

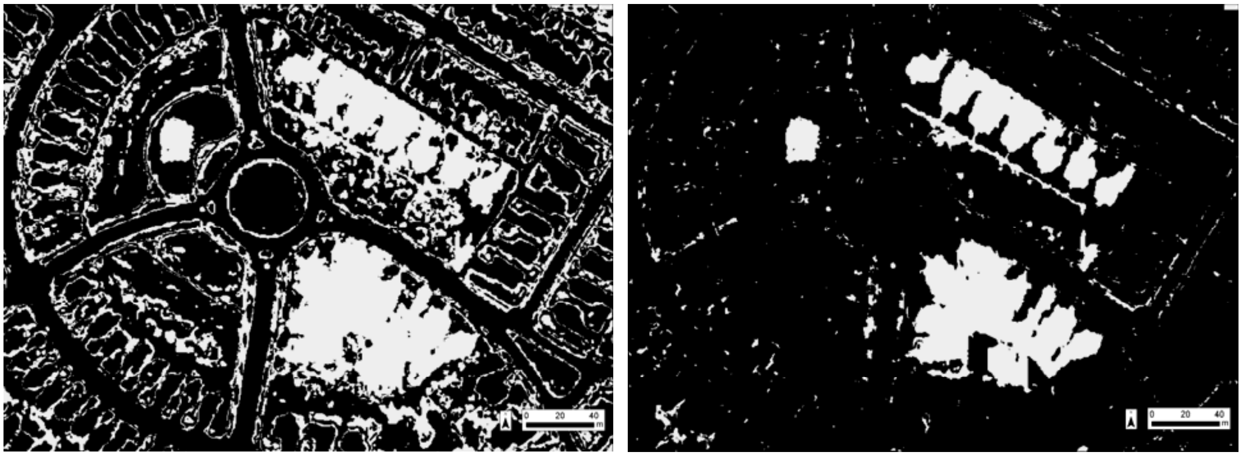

**Figure 4-9. Raw land cover change map (left) and change index-derived map (right) corresponding to the example change region depicted in Figure 4-8.**

## 2. Legends

Legend to Figure 4-1:

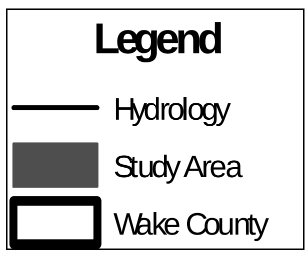


Legend to Figure 4-2:

Legend to Figure 4-4:

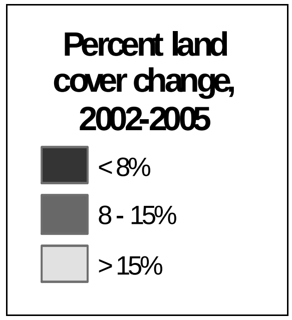


Legend to Figure 4-5:


Legend to Figure 4-7:


Legend to Figure 4-9 (same for both images):

## 4.8. Tables

.

**Table 4-1. Conversion of spatial similarity values into change index factors**

| Spatial similarity value | Change index factor |
|---|---|
| 0.0 | 5 |
| 0.01-0.14 | 4 |
| 0.15-0.49 | 3 |
| 0.50-0.74 | 2 |
| 0.75-1.0 | 1 |

Table 4-2. Derivation of change index value factors from category fuzziness and relevance.

| Change type | User's accuracy product | Change confidence | Change relevance | Change index factor |
|---|---|---|---|---|
| Water to Impervious | 0.88 | 3 | 3 | 6 |
| Deciduous to Impervious | 0.81 | 2 | 3 | 5 |
| Evergreen to Impervious | 0.77 | 2 | 3 | 5 |
| Bare/Disturbed to Impervious | 0.79 | 2 | 3 | 5 |
| Deciduous to Bare/Disturbed | 0.75 | 2 | 3 | 5 |
| Evergreen to Bare/Disturbed | 0.72 | 2 | 3 | 5 |
| Water to Bare/Disturbed | 0.82 | 3 | 2 | 5 |
| Herbaceous to Bare/Disturbed | 0.62 | 1 | 3 | 4 |
| Herbaceous to Impervious | 0.67 | 1 | 3 | 4 |
| Deciduous to Water | 0.92 | 3 | 1 | 4 |
| Evergreen to Water | 0.88 | 3 | 1 | 4 |
| Bare/Disturbed to Water | 0.90 | 3 | 1 | 4 |
| Water to Deciduous | 0.92 | 3 | 1 | 4 |
| Bare/Disturbed to Deciduous | 0.83 | 3 | 1 | 4 |
| Herbaceous to Water | 0.76 | 2 | 1 | 3 |
| Impervious to Water | 0.90 | 3 | 0 | 3 |
| Impervious to Bare/Disturbed | 0.74 | 2 | 1 | 3 |
| Impervious to Deciduous | 0.83 | 3 | 0 | 3 |
| Water to Evergreen | 0.74 | 2 | 1 | 3 |
| Water to Herbaceous | 0.74 | 2 | 1 | 3 |
| Deciduous to Herbaceous | 0.68 | 1 | 1 | 2 |
| Evergreen to Herbaceous | 0.65 | 1 | 1 | 2 |
| Bare/Disturbed to Herbaceous | 0.67 | 1 | 1 | 2 |
| Bare/Disturbed to Evergreen | 0.67 | 1 | 1 | 2 |
| Evergreen to Deciduous | 0.81 | 2 | 0 | 2 |
| Herbaceous to Deciduous | 0.70 | 2 | 0 | 2 |
| Impervious to Herbaceous | 0.67 | 1 | 0 | 1 |
| Herbaceous to Evergreen | 0.56 | 1 | 0 | 1 |
| Deciduous to Evergreen | 0.68 | 1 | 0 | 1 |
| Impervious to Evergreen | 0.67 | 1 | 0 | 1 |
| Evergreen to Evergreen | 0.65 | 3* | 0 | 3 |
| Deciduous to Deciduous | 0.85 | 1* | 0 | 1 |
| Herbaceous to Herbaceous | 0.56 | 3* | 0 | 3 |
| Water to Water | 1.00 | 1* | 0 | 1 |
| Impervious to Impervious | 0.79 | 2* | 0 | 2 |
| Bare/Disturbed to Bare/Disturbed | 0.74 | 2* | 0 | 2 |

*The "no change" pixel types warranted inverse change confidence weighting because the greater the user's accuracy product, the smaller the likelihood of change.

**Table 4-3. Summary of change index calculation.**

| Index factor | Range of Values |
|---|---|
| Spatial fuzziness | 1-5 |
| Category fuzziness | 1-3 |
| Relevance | 0-3 |
| Priority | 0-1 |
| *Total change index* | 2-12 |

**Table 4-4. Sampling strategy for accuracy assessment of land cover change index map.**

| Error type tested | Number of points | Location | Justification |
|---|---|---|---|
| Omission | 25 | Four catchments in the northern portion of study area | Area known *a priori* to be experiencing change (residential development) |
| | 25 | Within 10-m buffers of roads present in 2002 image | Fuzzy spatial metrics were designed to tolerate slight misregistration such as would have a large impact along road features |
| | 25 | Within residential property parcels | True change possibly masked by heterogeneous nature of residential land cover due to the misregistration tolerance of fuzzy spatial metrics |
| | 25 | At locations classified as Bare/Disturbed in 2002 | This land cover type, often associated with new construction, had a greater probability of experiencing change |
| | 25 | At change pixels indicating transition from Impervious to any other cover type | In growing urban areas, an improbable type of change; these pixels were assigned small weights of likelihood |
| | 25 | At indicated change pixels having lowest one-third change type UA product *and* not sampled elsewhere | Certainty of change at these pixels doubted and penalized in processing; includes only two change types (those between Herbaceous and Evergreen categories) |
| | 25 | At change pixels where raw post-classification analysis indicated no change | Change doubted at these pixels and weighted minimally in processing |
| | 25 | At change pixels having low to moderate values change index (0-8) | Change deemed highly doubtful to doubtful here after inspection of change index map and individual-date maps |
| *Subtotal* | 200 | | |
| Error type tested | Number of points | Location | Justification |
| Commission | 50 | At change pixels indicating change to Impervious from any other cover type | Highest priority change with respect to the water quality monitoring goals of this study; processing weight risked over-commitment to this category |
| | 50 | From catchments other than those four in the northern extreme of the study area | Area was known *a priori* to be stable and, at some places, built-out in 2002 |
| | 50 | At change pixels having high change index values (9-12) | Change deemed highly likely here after inspection of change index map and individual-date maps |
| *Subtotal* | 150 | | |
| ***Total*** | **350** | | |

**Table 4-5. From-to error matrix of change index map, 0-8 values as "no change" pixels and 9-12 values as change depicted in raw change map. From-to types are depicted by two-digit numbers where the first number represents 2002 and the second 2005 land cover, where 1 = Impervious, 3 = Deciduous, 4 = Water, 5 = Evergreen, 6 = Herbaceous, and 8 = Bare/Disturbed (overall κ = 0.757).**

| | Reference Data | | | | | | | | | | | | | | | | | | | | |
|---|---|---|---|---|---|---|---|---|---|---|---|---|---|---|---|---|---|---|---|---|---|
| Classified Data | 11 | 13 | 31 | 33 | 36 | 38 | 44 | 51 | 54 | 55 | 56 | 58 | 61 | 64 | 66 | 68 | 81 | 86 | 88 | Totals | Percent user's accuracy |
| 11 | **67** | 1 | | | | | | | | | | | | | | | | | | 68 | 98.5 |
| 13 | | - | | | | | | | | | | | | | | | | | | 0 | n/a |
| 31 | | | **7** | 1 | 2 | | | | | 1 | | | | | | | | | | 11 | 63.6 |
| 33 | | | | **67** | 5 | | | | | | | | | | | | | | | 72 | 93.0 |
| 36 | | | | | - | | | | | | | | | | | | | | | 0 | 0.0 |
| 38 | | | | | | **3** | | | | | | | | | | | | | | 3 | 100 |
| 44 | | | | | | | **3** | | | | | | | | | | | | | 3 | 100 |
| 51 | 1 | | | | | | | **3** | 1 | 1 | 1 | 1 | | | | | | | | 8 | 37.5 |
| 54 | | | | | | | | | - | | | | | | | | | | | 0 | n/a |
| 55 | | | | | | | | | | **31** | 2 | | | | | | | | | 33 | 93.9 |
| 56 | | | | 1 | | | | | | | - | | | | | | | | | 1 | 100 |
| 58 | | | | | | | | | | | | - | | | | | | | | 0 | n/a |
| 61 | 9 | | 1 | | | | | 2 | | | | | **6** | 1 | 9 | 3 | | | | 31 | 19.4 |
| 64 | | | | | | | | | | | | | | - | | | | | | 0 | n/a |
| 66 | | | | | | | | | | | | | 1 | | **55** | | | | | 56 | 98.2 |
| 68 | 1 | | | | | | | | | | | | 1 | | | **5** | | 1 | | 8 | 62.5 |
| 81 | 1 | | | | | | | | | | | | | | | | **19** | 9 | | 29 | 65.5 |
| 86 | | | | | | | | | | | | | | | | | | - | | 0 | n/a |
| 88 | | | | | | | | | | | | | | | | | 4 | 13 | **10** | 27 | 37.0 |
| Totals | 79 | 1 | 8 | 69 | 7 | 3 | 3 | 5 | 1 | 33 | 3 | 1 | 8 | 1 | 64 | 8 | 23 | 23 | 10 | ***350*** | |
| Percent producer's accuracy | 84.8 | 100 | 87.5 | 97.1 | 0.0 | 100 | 100 | 60.0 | 0.0 | 93.9 | 0.0 | 0.0 | 75.0 | 0.0 | 85.9 | 62.5 | 82.6 | 0.0 | 100 | | **Overall 78.9** |

## 4.9. References


ACHARD, F., H. D. EVA, H. J. STIBIG, P. MAYAUX, J. GALLEGO, T. RICHARDS, and J. P. MALINGREAU, 2002, Determination of deforestation rates of the world's humid tropical forests, *Science*, **297**, 999 - 1002.

ARNOLD, C., and C. GIBBONS, 1996, Impervious surface coverage: the emergence of a key environmental indicator, *Journal of the American Planning Association*, **62**, 243 - 258.

ARNOT, C., P. F. FISHER, R. WADSWORTH, AND J. WELLENS, 2004. Landscape metrics with ecotones: pattern under uncertainty, *Landscape Ecology*, **19**, 181 - 195.

BRUZZONE, L., and R. COSSU, 2003, An adaptive approach to reducing registration noise effects in unsupervised change detection, *IEEE Transactions on Geoscience and Remote Sensing*, **41**, 2455-2465.

CAKIR, H. I., and S. KHORRAM, 2008, Pixel level fusion of panchromatic and multispectral images based on correspondence analysis, *Photogrammetric Engineering & Remote Sensing*, **74**, 183 - 192.

DAI, X. L., and S. KHORRAM, 1998, The effects of image misregistration on the accuracy of remotely sensed change detection, *IEEE Transactions on Geoscience and Remote Sensing*, **36**, 1566 - 1577.

DARE, P. M., 2005, Shadow analysis in high-resolution satellite imagery of urban areas, *Photogrammetric Engineering & Remote Sensing*, **71**, 169 - 177.

FAUCETTE, L. B., C. F. JORDAN, L. M. RISSE, M. CABRERA, D. C. COLEMAN, and L. T. WEST, 2005, Evaluation of stormwater from compost and conventional erosion control practices in construction activities, *Journal of Soil and Water Conservation*, **60**, 288 - 297.

FOODY, G. M., 2002, Status of land cover classification accuracy assessment, *Remote Sensing of Environment*, **80**, 185 - 201.

HAGEN-ZANKER, A., B. STRAATMAN, and I. ULJEE, 2005, Further developments of a fuzzy set map comparison approach, *International Journal of Geographical Information Science*, **19**, 769 - 785.

HAGEN, A., 2003, Fuzzy set approach to assessing similarity of categorical maps, *International Journal of Geographical Information Science*, **17**, 235 - 249.

HAYES, S. A., R. A. MCLAUGHLIN, and D. L. OSMOND, 2005, Polyacrylamide use for erosion and turbidity control on construction sites, *Journal of Soil and Water Conservation*, **60**, 193 - 199.

HESTER, D. B., H. I. CAKIR, S. A. C. NELSON, AND S. KHORRAM, 2008, Per-pixel classification of high spatial resolution satellite imagery for urban land cover mapping, *Photogrammetric Engineering and Remote Sensing*, **74**, 463 - 471.

HU, X. Y., C. V. TAO, and B. PRENZEL, 2005, Automatic segmentation of high-resolution satellite imagery by integrating texture, intensity, and color features, *Photogrammetric Engineering & Remote Sensing*, **71**, 1399 - 1406.

JENSEN, J., 2005, *Introductory Digital Image Processing: A Remote Sensing Perspective*, 3rd ed. (Upper Saddle River, NJ: Prentice Hall).

JENSEN, J. R., D. J. COWEN, J. D. ALTHAUSEN, S. NARUMALANI, and O. WEATHERBEE, 1993, An evaluation of the Coastwatch Change Detection Protocol in South Carolina, *Photogrammetric Engineering and Remote Sensing*, **59**, 1039 - 1046.

KHORRAM, S. (ed), 1999, *Accuracy Assessment of Remote Sensing-Derived Change Detection* (Bethesda, MD: American Society for Photogrammetry and Remote Sensing).

LIU, H., and Q. ZHOU, 2004, Accuracy analysis of remote sensing change detection by rule-based rationality evaluation with post-classification comparison, *International Journal of Remote Sensing*, **25**, 1037 - 1050.

LU, D., P. MAUSEL, E. BRONDIZIO, and E. MORAN, 2004, Change detection techniques, *International Journal of Remote Sensing*, **25**, 2365 - 2407.

LUNETTA, R. A., and C. D. ELVIDGE, 1999 (eds), *Remote Sensing Change Detection: Environmental Monitoring Methods and Applications* (London, UK: Taylor & Francis).

MORISETTE, J. T., S. KHORRAM, and T. MACE, 1999, Land-cover change detection enhanced with generalized linear models, *International Journal of Remote Sensing*, **20**, 2703 - 2721.

North Carolina Department of Environment and Natural Resources (NCDENR), 2007. *Final North Carolina Water Quality Assessment and Impaired Waters List (2006).* Available online at http://h2o.enr.state.nc.us/tmdl/documents/303d_Report.pdf (last date accessed: 07 Oct 2007).

North Carolina Department of Environment and Natural Resources (NCDENR), 2006, *Final North Carolina Water Quality Assessment and Impaired Waters List (2004).* Available online at http://h2o.enr.state.nc.us/tmdl/documents/2004IRCategories4-7.PDF (last accessed: 07 Oct 2007).

NEMMOUR, H., and Y. CHIBANI, 2005, Neural network combination by fuzzy integral for robust change detection in remotely sensed imagery, *EURASIP Journal on Applied Signal Processing*, **2005**, 2187 - 2195.

POWER, C., A. SIMMS, and R. WHITE, 2001, Hierarchical fuzzy pattern matching for the regional comparison of land use maps, *International Journal of Geographical Information Science*, **15**, 77 - 100.

PRENZEL, B., and P. TREITZ, 2004, Remote sensing change detection for a watershed in north Sulawesi, Indonesia, *Progress in Planning*, **61**, 349 - 363.

SCHUELER, T. R., 1994, The importance of imperviousness, *Watershed Protection Techniques*, **1**, 100 - 111.

SHACKELFORD, A. K., and C. H. DAVIS, 2003, A hierarchical fuzzy classification approach for high-resolution multispectral data over urban areas, *IEEE Transactions on Geoscience and Remote Sensing*, **41**, 1920 - 1932.

SOUTHWORTH, J., 2004, An assessment of Landsat TM band 6 thermal data for analysing land cover in tropical dry forest regions, *International Journal of Remote Sensing*, **25**, 689 - 706.

TANG, X. M., W. KAINZ, and Y. FANG, 2005, Reasoning about changes of land covers with fuzzy settings, *International Journal of Remote Sensing*, **26**, 3025 - 3046.

U.S. CENSUS BUREAU, 2003, *Table HU-EST2002-07 - County Housing Unit Estimates*. Available online at http://www.census.gov/popest/archives/2000s/vintage_2002/HU-EST2002-07.html (last accessed: 24 October 2007).

VAN OORT, P. A. J., 2005, Improving land cover change estimates by accounting for classification errors, *International Journal of Remote Sensing*, **26**, 3009 - 3024.

VERBYLA, D. L., and S. H. BOLES, 2000, Bias in land cover change estimates due to misregistration, *International Journal of Remote Sensing*, **21**, 3553 - 3560.

VISSER, H., and T. DE NIJS, 2006, The Map Comparison Kit, *Environmental Modelling & Software*, **21**, 346 - 358.

WANG, H. Q., and E. C. ELLIS, 2005, Image misregistration error in change measurements, *Photogrammetric Engineering and Remote Sensing*, **71**, 1037 - 1044.

WOODCOCK, C. E., and S. GOPAL, 2000, Fuzzy set theory and thematic maps: accuracy assessment and area estimation, *International Journal of Geographical Information Science*, **14**, 153 - 172.

ZADEH, L. A., 1965, Fuzzy sets, *Information and Control*, **8**, 338-353.

ZHANG, Y., 2001, Detection of urban housing development by fusing multisensor satellite data and performing spatial feature post-classification, *International Journal of Remote Sensing*, **22**, 3339 - 3355.

# 5. AN ANALYSIS OF IMPERVIOUS SURFACE AND SUBURBAN FORM IN RALEIGH, NC, USING HIGH SPATIAL RESOLUTION SATELLITE IMAGERY

## 5.1. Abstract

Sources of impervious surface in suburban areas include roads, houses, buildings, parking lots, and driveways, and the arrangement and extent of these features are critical urban planning variables. The study described here used high spatial resolution satellite imagery to quantify the contribution of suburban imperviousness from sources closely associated with private automobile usage. Specifically, in a 71.5 $km^2$ study area in suburban Raleigh, NC, USA, QuickBird satellite image data were used to quantify the extent of imperviousness from low-density residential roads and driveways and from retail parking lots. These landscape features constituted only 14.3% of overall study area imperviousness but 58.8% of the imperviousness associated with low-density residential land use. Retail parking lots constituted 5.8% of study area impervious surface. A compact New Urban development within the study area was compared to a conventional low-density neighborhood in order to frame these findings within the context of contemporary urban planning and design. This study empirically documents the connections between conventional suburban form, private automobile-oriented transportation infrastructure, and watershed imperviousness, and it demonstrates the continuing synergy between remote sensing and landscape planning.

## 5.2. Introduction

Urban areas are spatially and ecologically complex, and planning for their growth is data-intensive. This is particularly true in suburban areas dominated by *sprawl*. Galster (2001) notes that this term is not easily defined but generally refers to the patterns, processes, causes, and consequences of low-density and segregated-land use development in populated places. Sprawl has been criticized as having negative social impacts, such as increased racial and economic segregation (Yang and Jargowsky, 2006), and impacts on individual health, including increased childhood obesity (Ewing et al., 2006) and body mass index (Pendola and Gen, 2007; Ross et al., 2007) due to its influence on transportation choices. Sprawl has also been described as a comparatively costly design for municipalities to serve with public services such as water and sewer infrastructure (Speir and Stephenson, 2002) and roads (Burchell and Mukherji, 2003). Decreased air quality (Borrego et al., 2006) and the loss of open space, or pockets of undeveloped urban land (Torres et al., 2007), are often counted as among sprawl's environmental harms.

The potential of sprawling suburban development to impact water quality is well-documented (Tu et al. 2007; Interlandi and Crockett, 2003; Bowen and Valiela, 2001). Some analysts have estimated that substantial declines in watershed health begin to occur with as little as 10% impervious cover (Arnold and Gibbons, 1996). Sprawl poses a unique threat to urban surface water quality in part because it incorporates an extensive array of impervious features, such as roads, rooftops, and parking lots. This threat can add to the fiscal strain placed on growing municipalities already financing stormwater management with special fees and utilities (Kasperson, 2001). On the other hand, low-density suburban areas can accommodate an arrangement of open space that actually mitigates stormwater volume and pollution (Moglen and Kim, 2007). Such a result is indicative of a proper spatial understanding of the relationship between suburban land use and surface water quality (Brabec et al. 2002).

The objective of this study was to evaluate the degree to which suburban imperviousness is derived from three different landscape features associated with sprawl: driveways in low-density residential lots, roads serving only low-density residential areas, and commercial retail parking lots. These impervious features reflect the broad orientation of sprawling land use around individual automobile travel. Nonetheless, their contribution to suburban imperviousness, and thus their relevance to suburban planning, has not been the subject of extensive analysis. Manville and Shoup (2005) even discussed this data gap with respect to the infamous urban landscape of Los Angeles, criticizing as unsubstantiated a widely repeated estimate that as much as two-thirds of that city is "consumed" by the automobile.

This study used state-of-the-art high spatial resolution satellite imagery to examine these important elements of the urban "microlandscape." The study area, a portion of suburban Raleigh, North Carolina, USA, is experiencing rapid development and related water quality problems typical of many growing urban areas. In estimating the contribution of low-density residential streets, low-density residential driveways, and retail parking lots to suburban imperviousness, this study provides an empirical framework for discussing alternatives to suburban land use. The use of this framework is illustrated in this paper by reference to one emerging alternative to sprawl, compact mixed use development.

*5.2.1. Low-density residential streets and driveways and impervious surface*

While there are gaps in the data explaining the relationship between the two, urban impervious surface is undoubtedly linked to individual automobile usage. Planners make transportation and traffic primary considerations as they zone for and approve of new development (Moudon et al., 2005). Critics of contemporary suburban planning deride this dynamic as "the tail wagging the dog," claiming that design with individual automobile usage in mind encourages low-density urban development and, in turn, sprawling suburbs (Handy, 2005). The connection is so pronounced that some researchers describe sprawl principally in terms of the human-automobile relationship (Galster et al., 2001).

This portion of the study sought to evaluate the commitment of low-density residential land use to driveways and roads. These are standard features of the suburban residential landscape, and they primarily serve the needs of private automobile travel, although both serve a variety of other purposes, such as recreation, commercial transport, and emergency response. Like the other suburban landscape features discussed in this study, conventional suburban road and driveway designs are such planning staples that their cumulative environmental footprint has not been thoroughly scrutinized.

A growing number of researchers, however, motivated by the fact that roads and driveways lie unused much of the time, are reconsidering these ordinary landscape features. Investigations have evaluated ways to reduce the environmental impact of these impervious surfaces without comprising their social utility, and research efforts have focused on both composition and form. Composition research, for example, has examined permeable pavement systems (Brattebo and Booth, 2003). Form research has analyzed the feasibility of narrower roads as well as smaller driveways through decreased street setbacks (Stone, 2004). Increasingly popular New Urban or Traditional Neighborhood Development (TND) designs have incorporated some of these alternative forms, and their proponents tout aesthetic and cultural benefits in addition to their environmental gains (Brander et al., 2004; Garde, 2004; Thompson-Fawcett and Bond, 2003). Relevant design elements include mixed use, smaller lots, reduced street setbacks, and private residential parking in shared alleyways and along streets (Berke et al., 2003). One such development, Bedford at Falls River, is located within the present study area, and its design will be discussed in this paper for comparative purposes.

The specific goal of this part of this analysis was to quantify study area imperviousness from low-density residential roads and driveways. Remote sensing studies have been relatively successful performing semi-automated extractions of roads as *land cover* features, keying in on their texture (Gamba et al., 2006) and reflectance properties (Zhu et al., 2005). For the purposes of this study, however, residential roads were manually extracted as *land use* features because of the narrow focus of this analysis and because manual delineation was feasible in light of the study area's size.

The extraction of driveway surfaces in this study, by contrast, was semi-automated and represents a simple but novel methodological approach. When derived from remote sensing data, driveways are often delineated manually (Lee and Heaney, 2003). Jennings et al. (2004) manually developed a "driveway impervious area percent" estimate for a calculation of watershed imperviousness using a random sample of driveways associated with relevant rooftops as seen in aerial photography. Stone (2004) estimated residential parcel impervious surface area from driveways by multiplying the city-required street setback by an average driveway width per garage stall (based on a 100-parcel visual analysis of aerial photography) and number of garage stalls. The present study introduces a semi-automated analysis of remote sensing data to estimate the contribution of low-density residential driveways to overall study area imperviousness.

Additionally, this portion of the study compares imperviousness in a low-density residential neighborhood to part of the compact Bedford neighborhood.

### *5.2.2. Retail parking lots and suburban impervious surface*

The commitment of suburban land to retail parking lots is even more poorly documented than its devotion to roads and driveways despite the fact that most U.S. municipalities include *minimum* parking space requirements for new commercial and retail development (Manville and Shoup, 2005; Shoup, 1999). This has important environmental implications as parking lots are typically contiguous expanses of impervious surface. Parking supply can also have a powerful effect on transportation and commuting behavior (de Cerreño, 2004; Mildner et al., 1997). Developers of commercial or retail space have economic incentives to avoid parking shortages, and, because they can externalize all of the costs of parking oversupply, they are often built to accommodate a peak volume that is rarely if ever seen. Advocates of mass transit, bicycling, pedestrianism, and other modes of alternative transportation see such oversupply an impediment to those causes (Deakin et al., 2004).

Some critics of suboptimal parking supply argue that it generates negative environmental and economic externalities such that it should be specially taxed in order to mitigate its cost to communities and municipalities (Feitelson and Rotem, 2004). Developers, on the other hand, may in fact prefer to build far less parking than local regulations require (Levine and Inam, 2004). Shoup (1999) quoted urban planner William Fulton as observing that minimum parking requirements force developers to first build a parking lot and then get permission from the local government to build something that will pay for it. Compounding this planning dilemma, local governments have traditionally had little data upon which to base the minimum parking requirements to which they are committed (Shoup, 1999).

The present use of data derived from high-spatial resolution satellite imagery represents a unique approach to empirically analyzing this suburban land use issue. Previous studies have either failed to specifically map parking lots or have not relied heavily on automated GIS and remote sensing methods in doing so. Satellite imagery has frequently been used to map urban commercial and industrial land uses separate from residential and other areas (Lu and Weng, 2006; Lu and Weng, 2005; McCauley and Goetz, 2004), but these studies, although highly automated, have not typically attempted to map parking lots. Even related studies utilizing high spatial resolution imagery have distinguished rooftops from paved surfaces but have stopped short of mapping parking lots (Thomas et al., 2003). On the other hand, Albanese and Matlack (1999) studied urban stream degradation adjacent to parking lots measuring lot size on-site by foot pacing. The authors also concluded that those parking lots were chronically underutilized, even during peak holiday season usage, suggesting that the runoff problems they caused were extraneous. Although total study area imperviousness was not determined, the mean parking area size for the ten sampled commercial and retail land uses was calculated as 5.86 ha.

In a more efficient but less precise analysis, Akbari et al. (2003) used Monte Carlo statistical sampling to analyze the fabric of urban imperviousness in Sacramento, CA. Those authors visually inspected 400-600 random point locations using 0.3-m color digital orthophotos and classified the land use at each point as one of thirty explicit types, such as “sidewalk,” “tree covering grass,” and “parking area.” They determined that in two sampled commercial areas, an exposition and shopping center, parking areas covered 62.8 and 38.0 percent of all paved surfaces, respectively. The present study uses remote sensing and GIS-based methods in an even more automated approach in mapping suburban Raleigh's retail parking land use.

### 5.3. Study Area and Materials

The study area incorporates 71.5 $km^2$ of adjacent drainage catchments and is located in the northeast part of the city of Raleigh, North Carolina, USA (Figure 5-1). This area, representing roughly 31% of Raleigh's incorporated land area, is composed of residential, commercial, and industrial land uses interspersed with large forested clusters and includes part of a major transportation corridor, US-1. The U.S Census Bureau recently listed Wake County, which encompasses Raleigh, as one of the 100 fastest-growing counties in the United States (2003). Raleigh is located within the Neuse River watershed, the third largest river basin in the state of North Carolina. This basin drains all or part of twenty-three counties into the Albemarle-Pamlico Sound; its ecological integrity has been the subject of numerous studies in recent decades (Paerl et al., 1998; McMahon and Lloyd, 1995; Burkholder et al., 1992). Both of the major streams within the study area, Marsh Creek and Perry Creek, have been included on North Carolina's federally-mandated Clean Water Act, Section 303(d), Impaired Waters List each year it has been compiled. Each time, the state has cited "urban runoff/storm sewers" as the likely cause of impairment (NCDENR, 2007 and 2006).

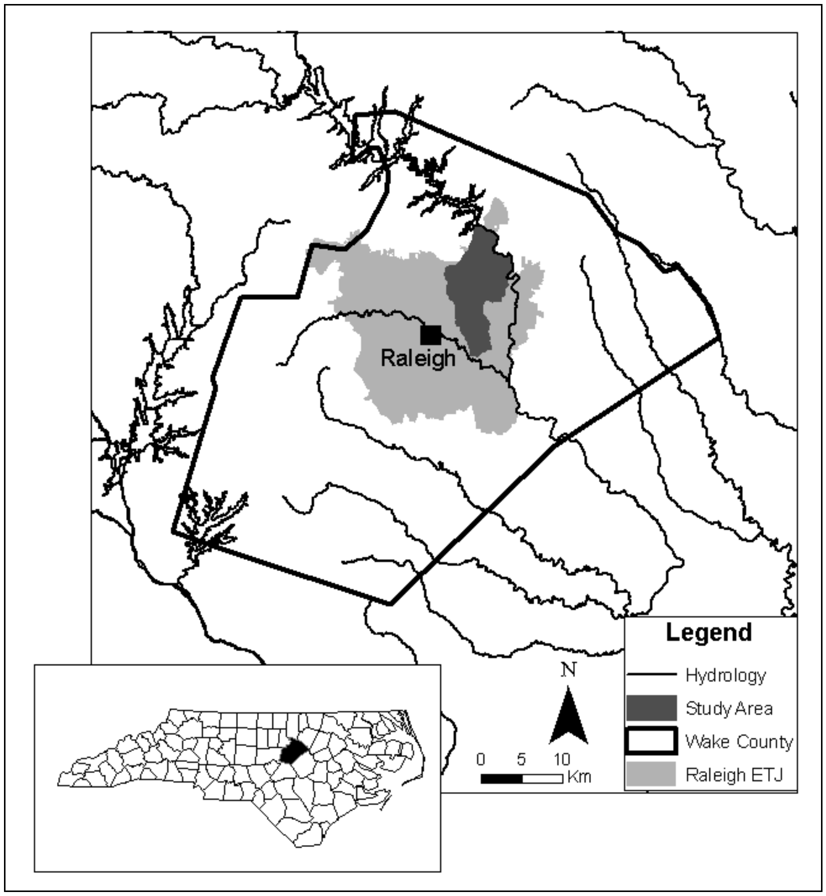

**Figure 5-1. Study area in northeast Raleigh, Wake County, North Carolina, USA, and Raleigh's extraterritorial jurisdiction (ETJ).**

The land use/land cover (LU/LC) data used and generated in this study were based on QuickBird satellite imagery, a DigitalGlobe, Inc., product (www.digitalglobe.com). Collecting panchromatic imagery at 0.61 m at nadir and multispectral imagery at 2.44 m at nadir, the QuickBird sensor currently produces the highest spatial resolution satellite data available on the commercial market. Multispectral and panchromatic study area imagery was collected in June, 2002, and the data fusion algorithm developed by Cakir and Khorram (2008) was used to enhance the spatial resolution of a multispectral image to 0.61 m. Applied to this fused image, land cover classification methods described in Hester et al. (2008) were used to produce a six-category, 0.61 m-resolution land cover map with an 89% overall accuracy and 90% user's accuracy for the impervious category. The five other mapped categories were water, bare/disturbed, deciduous, evergreen, and herbaceous and are described in Table 5-1. In ten selected commercial parcels, impervious surface area matched reference data with 96.9% accuracy. The resulting study area land cover map is presented in Figure 5-2. The study area is primarily composed of vegetation (71%) but is substantially covered by impervious surface (24%).

**Table 5-1. Land cover categorization scheme for QuickBird image classification.**

| Class | Land cover type | Description |
|---|---|---|
| 1 | Impervious | Transportation infrastructure (roads, parking lots, etc.), rooftops, recreational areas (i.e., tennis courts), and all other manmade impervious surfaces that are paved or built |
| 2 | Water | Lakes, ponds, rivers, streams, pools, and all other natural and artificial surface waters |
| 3 | Bare/Disturbed soil | Construction sites, landfills, gravel areas, or any other unpaved non-vegetated surface |
| 4 | Deciduous | Trees or shrubs that shed their leaves before the winter (mostly hardwood species). |
| 5 | Evergreen | Trees or shrubs that keep their leaves throughout the winter (mostly coniferous species) |
| 6 | Herbaceous | Urban grasses (yards, recreational fields, vegetated road medians, etc.) of varying degrees of maintenance |

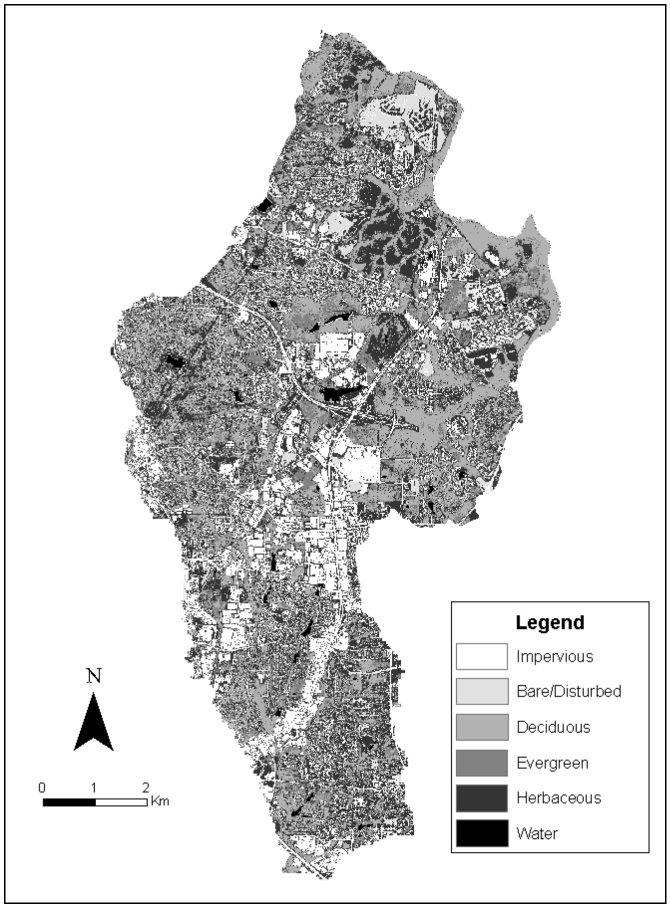

**Figure 5-2. Study area land cover map.**

Other data utilized in this study were GIS files for roads, property parcels, building footprints, and streams, all available from Wake County iMAPS server. The property parcel database includes a variety of individual lot data, including 2002 zoning classification, property value, and development build date. Raleigh utilizes Euclidean zoning and delineates residential lots by permissible density of dwelling units. It also sets minimum street setback requirements. Parcel types are sub-categorized by use such as restaurant, retail-type buildings, and gas stations. The road database is a street segment file and does not characterize roads as residential or commercial. All GIS processing was performed in ArcGIS® 9.0 by Environmental Systems Research Institute, and remote sensing analyses were conducted in Leica Geosystems' ERDAS IMAGINE®

8.7.

## 5.4. Methods

### *5.4.1. Estimating the extent of study area imperviousness from low-density roads and driveways*

As an initial step in evaluating the contribution of suburban roads to study area imperviousness, residential road segment features in the study area were manually identified from the study area roads GIS layer using the QuickBird image as a backdrop. Road segments included in this selection were two-lane features weaving in and through single-family residential zones limited to six dwelling units per acre (14.8 dwelling units/ha) or less, including four- and two-unit per acre zones. This density threshold was utilized because it isolated the study area's most homogeneous and contiguous clusters of single-family residential development. The selected road segments exclusively served detached single-family dwellings, although segments constituting a unique through passage between major roads were not selected.

The total length of these road segments was multiplied by an average road width generated from a random sample of 30 road segments in the study area measured curb-to-curb. This calculation gave an estimate of the amount of impervious surface contributed by roads exclusively serving low-density residential housing. In order to reflect the road impervious surface obscured by tree canopy overhang, a ten percent deduction was applied to the calculated estimate of road imperviousness. This deduction was intended to accord this estimate with the other calculations in this study, all of which were based on "above-the-canopy" satellite views, and it only incidentally implicates a potential effect of rainfall interception (Sanders, 1986). This reduced figure was then used to calculate the percent contribution to overall impervious surface made by residential roads.

To estimate the percentage contribution of private, low-density residential driveways to the study area's total impervious surface area, a subset of residential parcels was selected. Selected parcels were those assigned an "R-4" zoning classification at the time of image capture, a designation that limits development to single-family detached housing not denser than four dwelling units per acre (9.9 dwelling units/ha). These parcels, exemplified by those in Figure 5-3, have the low density typically associated with suburban sprawl. Next, an unsupervised classification of the image data representing these parcels was performed, using 20 classes, the ISODATA algorithm, and a 95% convergence threshold in ERDAS IMAGINE® 8.7. These 20 classes were aggregated into three unique categories: impervious-building, impervious non-building, and other. The relatively discrete reflectance properties of these three categories was a key part of this analysis, since dark rooftops and non-impervious features, such as vegetation, have very different reflectance properties than impervious non-building features. The accuracy of the three-category unsupervised classification was evaluated using a visual interpretation of 50 randomly selected R-4 parcels. In addition, the contribution of paved sidewalks and patios to average non-building imperviousness was estimated using a random selection of ten R-4 parcels.


**Figure 5-3. Low-density residential development**

### *5.4.2. Comparing imperviousness in low-density and compact residential development*

In order to compare the extent of imperviousness in low-density neighborhoods and alternative New Urban-type developments, two representative neighborhood sections were selected. This analysis was not meant to be an exhaustive statistical comparison of these two forms of development but rather a closer look at questions of form raised by the preceding analysis. It generally addresses the question of whether compact residential development in fact incorporates less impervious surface per household than conventional low-density residential development after accounting for associated transportation features. Analyzed sections included part of a low-density, curvilinear neighborhood of single-family detached dwellings and a part of the denser Bedford New Urban development discussed *supra*. Housing construction completed in both areas between 1997 and 2001, and each is a relatively stand-alone residential area having internal road segments.  The low-density neighborhood section encompassed 21.9 ha (54.1 ac) and the New Urban section 15.8 ha (39 ac).  These areas are displayed in Figure 5-4.

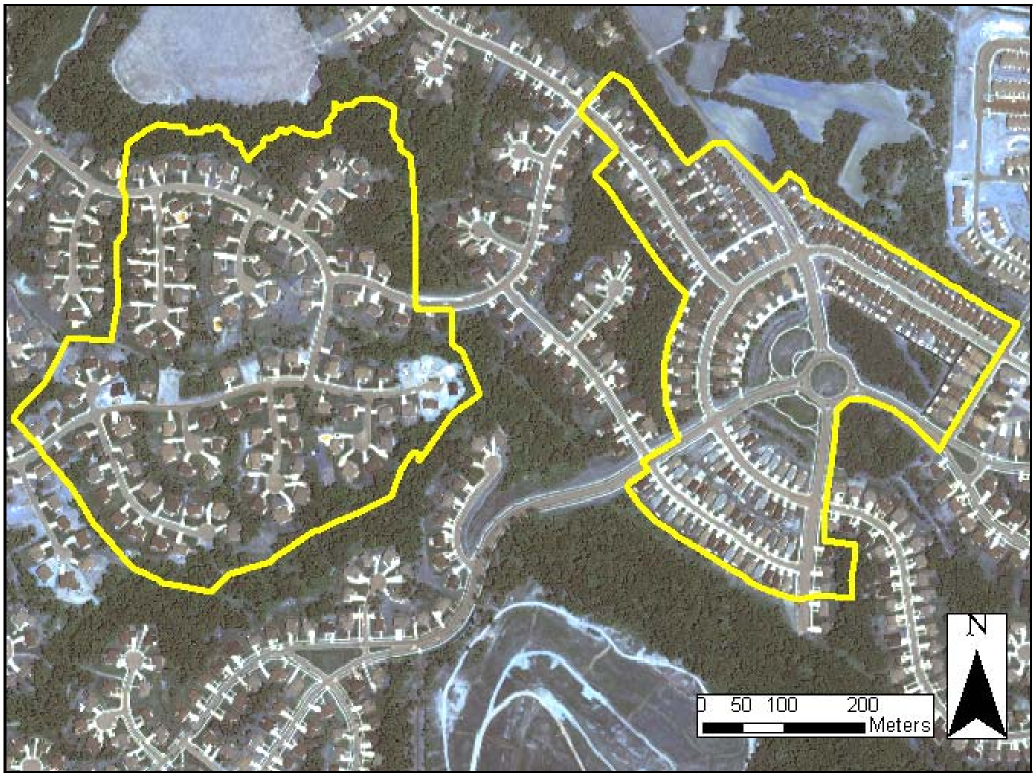


**Figure 5-4.  Low-density (left) and compact neighborhoods.**

Within these areas, total imperviousness was calculated using the QuickBird-derived land cover map.  The total number of households per area was extracted from the tax parcel database.  As above, the relevant road segments were selected, and their widths were measured as appearing on the QuickBird image.  This permitted the calculation of total imperviousness derived from roads in each neighborhood type.

*5.4.3.   Study area imperviousness from retail parking lots*

A subset of commercial parcels was selected for the retail parking lot imperviousness analysis.  Attributes in the parcel GIS layer were used to isolate retail parcels at which customer parking was provided. These 234 parcels were those occupied by restaurants, grocery stores, department stores, and similar retail uses. From these parcels, those for which the "year built" date was listed as 2001 or 2002 were excluded if construction appeared to be ongoing at the time of image capture. The final parcel selection included 195 parcels covering 1.4 $km^2$ of the study area. To summarize, development in these parcels was finished at the time of image capture, and they were being used for non-residential activity and related customer parking. Representative retail parcels are displayed in Figure 5-5.

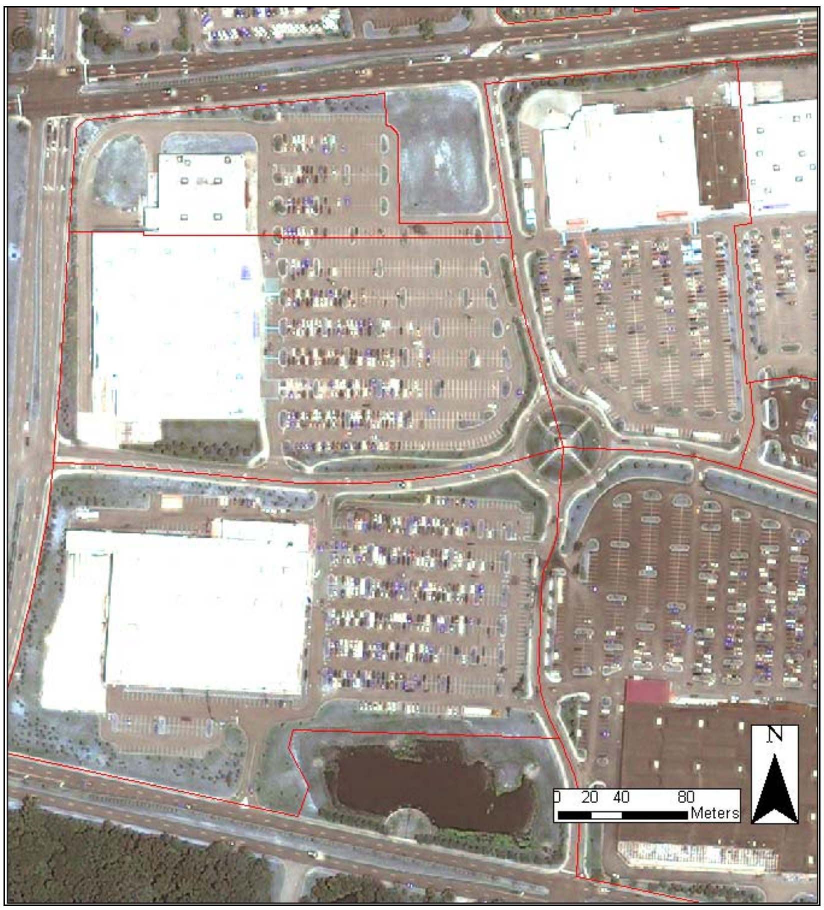

**Figure 5-5. Retail parcels and associated parking lots.**

After updating the building footprint GIS layer using the QuickBird image, the amount of impervious surface in each parcel constituted by buildings was tabulated using a GIS zonal function and the QuickBird image-derived land cover map. In addition, an estimate of the amount of non-building impervious surface devoted to loading, waste disposal, storage, or other uses necessary for commercial activity was generated through photointerpretation of the QuickBird image in a 30-parcel random sample. This sample included 10 parcels each from among the selected parcels with the 66 smallest, 65 intermediate-sized, and 65 largest building footprints, and it was used to derive an average value of such non-building, non-parking lot impervious surface within parcels of each building size class. Subtracting the building footprint and "loading" surfaces average developed for each building size class from the map estimate of non-building impervious surface, an average value for the percent of commercial imperviousness derived from retail parking surfaces was generated.

### 5.5. Results

The results of the low-density residential imperviousness analysis are summarized in Figure 5-6. In all, imperviousness from roads and driveways together with retail parking lots accounted for 14.3% of study area imperviousness and 58.8% of the imperviousness associated with low-density residential land use. Residential roads and driveways, retail parking lots, and the neighborhood comparison findings are presented by the corresponding sections below.

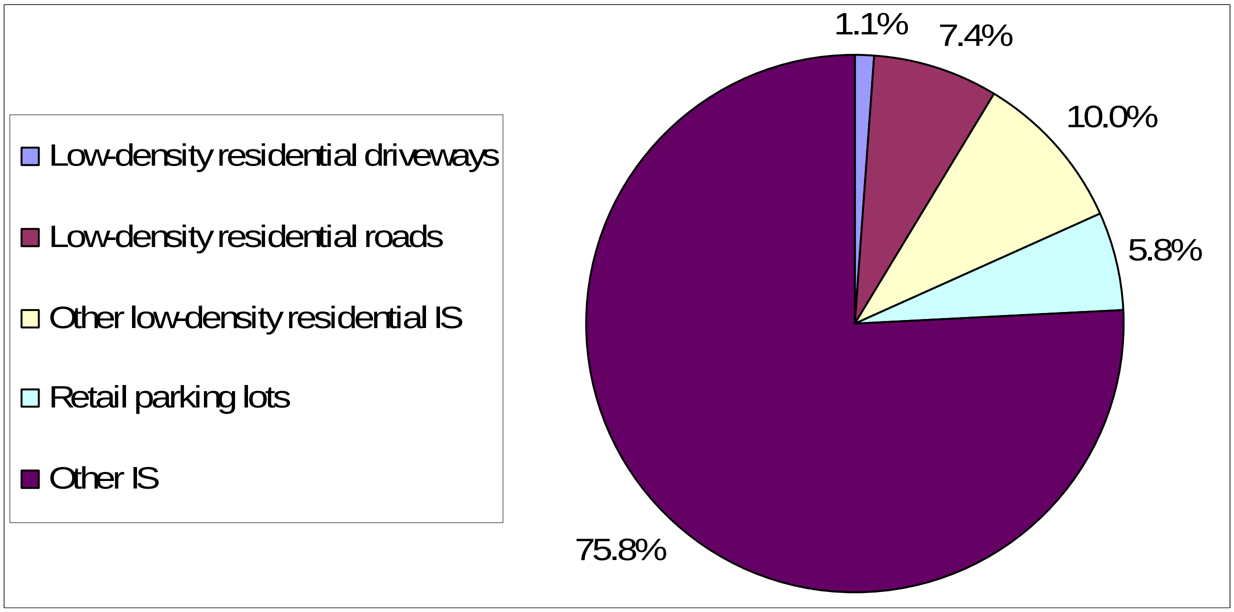


**Figure 5-6. Summary of study area impervious surface (read clockwise from top).**

### *5.5.1. Impervious surface from low-density residential roads and driveways*

The results of the residential road imperviousness analysis are reported in Table 5-2. The total length of the selected residential road segments was 182.3 km, which represents 47% of the total road length in the study area. Based on the 30-segment sample, the average residential road width in the study area was 7.7 m. These figures resulted in an estimated above-the-tree canopy impervious surface contribution from residential roads of 1.26 $km^2$. This is a contribution to total study area imperviousness (17.1 $km^2$) of 7.4%.

**Table 5-2. Results of residential road segment analysis (IS = impervious surface).**

| Residential road segment length (km) | Percent of study area road length made up of residential roads | Average residential road width (standard deviation) (m) | Estimated IS area from roads ($km^2$) | Estimated IS area from roads with tree canopy deduction ($km^2$) | Percent of study area occupied by residential road IS | Percent of study area IS made up of residential road IS |
|---|---|---|---|---|---|---|
| 182.3 | 47% | 7.7 (1.8) | 1.40 | 1.26 | 1.8% | 7.4% |

Of those parcels completely bounded by the study area, 7,704 parcels within the study area were zoned R-4 in 2002. A number of these parcels were excluded from analysis because they were either developed after the image date, contained more than 10% bare soil, were larger than 2.0 acres (0.81 ha) in size, or were being used for non-residential purposes. These exclusions left 5,436 parcels constituting 9.1 $km^2$ or 12.7% of the study area for this analysis. The impervious surface encompassed within these residential parcels totaled only 11.1% of total study area impervious surface, or 1.9 $km^2$.

A subset of the three-category land use map developed for this analysis is presented along with the corresponding QuickBird image in Figure 5-7. The accuracy assessment presented for this map is displayed in Table 5-3. Average parcel percent imperviousness was mapped with a positive difference from reference data of only 2.4%, while average parcel percent non-building imperviousness was underestimated by 4.1. Non-building, non-driveway paved surfaces made up an average of 16.1% of sampled residential parcel imperviousness. Subtracting this average from total imperviousness mapped as non-building (26.8%), a final estimate from this analysis is that driveway surfaces comprised 10.7% of low-density residential development imperviousness and only 1.1% of study area imperviousness.


**Figure 5-7. Low-density residential parcel land cover map example.**

**Table 5-3. Accuracy assessment of residential parcel land cover map (IS = impervious surface).**

| | Reference | Map | Percent error |
|---|---|---|---|
| Total IS | 15359.5 | 17337.4 | +12.8 |
| Average parcel % IS | 21.7 | 24.1 | +2.4 |
| Average parcel % building IS | 14.4 | 17.1 | +2.7 |
| Average parcel % non-building IS | 7.3 | 7.0 | -0.3 |
| Average % of parcel IS from buildings | 66.4 | 70.5 | +4.1 |
| Average % of parcel IS from non-buildings | 33.6 | 29.5 | -4.1 |

### *5.5.2. Low-density and compact neighborhood comparison*

The results of neighborhood comparison are presented in Table 5-4 and highlighted by Figure 5-8. As expected, residential density was higher in the New Urban neighborhood (22.8 households/ha) than in the low-density neighborhood (19.6 households/ha). Total percent imperviousness was nearly double in the New Urban neighborhood (45.6%), and a greater percentage of impervious surface area was contributed by roads there (31.9%). However, factoring in all sources of imperviousness, including rooftop, driveway, sidewalk, and road surfaces, impervious surface per household was higher in the low-density neighborhood (511.2 compared to 436.5).

**Table 5-4. Low-density and compact neighborhood comparison (IS = impervious surface).**

| | Low-density neighborhood | Compact neighborhood |
|---|---|---|
| Average parcel size (ha) | 0.16 | 0.05 |
| Total IS (ha) | 5.7 | 7.2 |
| Total area (ha) | 21.9 | 15.8 |
| Total area percent IS | 26.0% | 45.6% |
| Total roads (m) | 1899.0 | 2246.7 |
| Average road width (m) | 6.9 | 10.3 |
| Road IS (ha) | 1.3 | 2.3 |
| Percent of IS from roads | 22.8% | 31.9% |
| Households | 112 | 164 |
| Road IS per household ($m^2$/hh) | 116.1 | 140.2 |
| Households per hectare | 19.6 | 22.8 |
| Total IS per household ($m^2$/hh) | 511.2 | 436.5 |

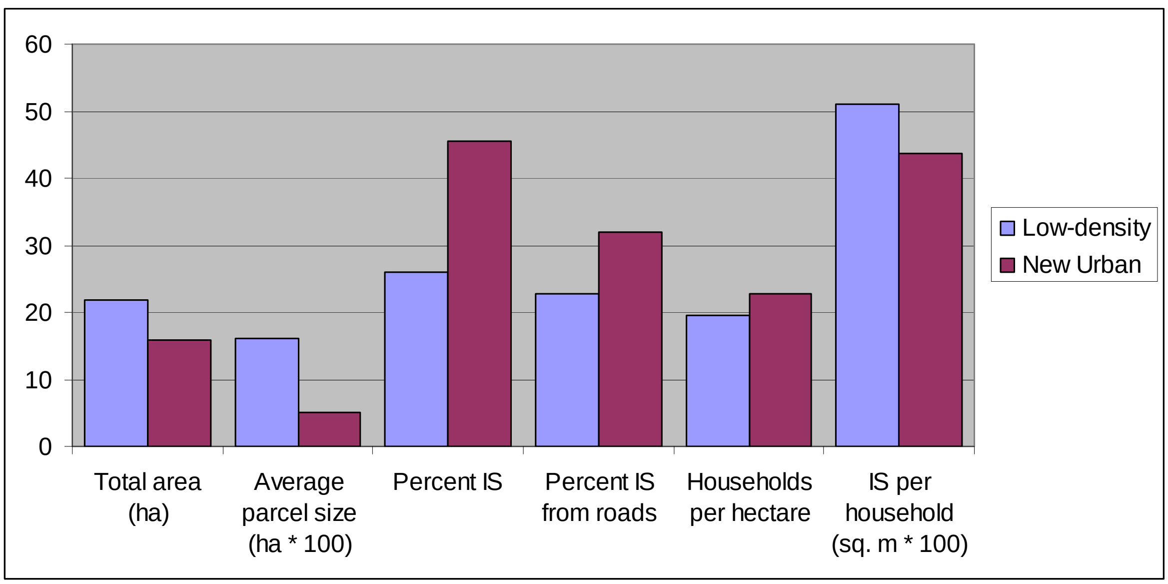


**Figure 5-8. Summary of neighborhood comparison (scaled by 100 where indicated, IS = impervious surface).**

### *5.5.3. Retail parking lot imperviousness results*

The selected commercial parcels constituted 2.4 $km^2$ or 3.4% of the study area but 1.4 $km^2$ or 8.1% of study area impervious surface. On average, these parcels were covered by 68.3% impervious surface. In the ten sampled commercial parcels from among those having the 66 smallest building footprints, an average of 7% of non-building imperviousness was devoted to loading, parking, and other non-building, non-parking land uses. Those figures for the intermediate-sized and largest building footprint parcels were 3% and 8%, respectively. When those average values were subtracted from each parcel's mapped percent non-building imperviousness, the resulting estimate of the average percent of commercial parcel imperviousness committed to retail parking lot surfaces was 68.0%. Thus, nearly 1 $km^2$ of the study area's 17.2 $km^2$ of impervious surface was comprised of retail parking lots. This represents 41.6% of the selected retail land usage itself. Figure 5-6 incorporates these results in summarizing the contribution of low-density residential imperviousness to overall study area imperviousness.

## 5.6. Discussion

### *5.6.1. Sprawl and transportation*

The analysis of roads exclusively serving low-density residential development reveals that, in suburban Raleigh, such roads constitute nearly one-tenth of total study area imperviousness. More significantly, these features accounted for more almost one-third of the imperviousness associated with low-density residential land use. Their role in watershed health may be even greater than those figures reflect for several reasons. First, cul-de-sac features, an additional source of road-related imperviousness, did not figure into this estimate. Additionally, overhanging tree canopy obstructed as much as 10% of residential road surfaces from satellite image view, although this overhang can substantially mitigate increases in stormwater volumes and velocity that may result from underlying impervious surface (Sanders, 1986). Finally, road surfaces are special conduits for pollutant transport given their collection of vehicle traffic contaminants and connectivity to streams via stormwater infrastructure ( Walsh et al., 2004; Van Bohemen and Van de Laak, 2003). Recent work has reinforced the related notion that the location of impervious surface may be determinative of watershed health than its extent ( Moglen and Kim, 2007; Snyder et al., 2005).

Low-density residential driveways contributed a trivial amount to total study area imperviousness. This result suggests that reduced street setback, a tenet of New Urban design, may not appreciably reduce overall impervious surface in the study area. Accordingly, Stone (2004) recommended this policy change as a way to reduce watershed imperviousness but emphasized that reductions in lot size and street frontage would more significantly advance that goal. Nonetheless, like roads, driveways are also often uniquely connected to ditches, storm drains, and other concentrated means of runoff transport. This connectivity gives these land uses a potential role in determining watershed health disproportionate to their contribution to overall imperviousness. In that sense, strategically reducing small amounts of impervious surface through a modest policy change such as reduced street setback may indeed be desirable.

Retail parking lots constituted an equally important source of study area imperviousness and pose an additional threat to water quality because they concentrate vast tracts of imperviousness. The average parking lot within the 195 parcels studied was 0.51 ha (1.3 ac) in size. Such large tracts of contiguous impervious surface can result in high volumes and velocities of stormwater runoff. In addition, parking lot runoff is highly concentrated in vehicle emitted pollutants such oil, grease, and heavy metals (Kim et al., 2007).

*5.6.2. Low-density residential imperviousness generally*

In total, the low-density residential development analyzed here represented 17.8% of the study area and 24.3% of its impervious surface when accounting for roads, driveways, and retail parking lots, sources which constituted nearly two-thirds of this imperviousness. These sources are distinct from the other one-third in that they are closely associated with the use of private automobiles. This is a distinction that should be considered when alternative residential development designs are evaluated as in the portion of this study comparing a low-density neighborhood with its compact, New Urban counterpart.

*5.6.3. Low-density and compact neighborhood comparison*

The results of this study provide some quantitative support for the potential environmental benefits of compact residential development as an alternative to the development patterns associated with sprawl. The New Urban subdivision's wider roads result in a higher percentage of imperviousness from those surfaces. Nonetheless, the compact neighborhood studied here has a lower level of impervious surface per household. This is primarily because its shorter street setbacks minimize non-road sources of impervious surface including driveways and sidewalks. On-street parking, in fact, replaces driveways in many New Urban designs. The denser development also required less street frontage per lot, a strategy identified by Stone (2004) as an effective way to reduce overall watershed imperviousness. The improved runoff management capacity of this type of development as compared to low-density designs have already been documented by Brander et al (2004) and Berke et al. (2003).

Additionally, this neighborhood design presents a variety of opportunities to indirectly reduce the environmental impact of residential land use through reduction in resident automobile dependence. Possible related environmental benefits include open space preservation and enhanced suitability of residential areas to alternative transportation, including mass transit, pedestrianism, and bicycling. Compact mixed use development can replace commercial parking lots outside residential areas with green spaces or parks because residents can walk to shopping destinations. A small grocery store, for example, built in the undeveloped portion of the New Urban neighborhood shown in Figure 5-4, may be able to replace substitute for both the store and the parking lot it would have required if built elsewhere, an open space savings measured in hectares. Such mixed use may even minimize the extent of new road construction. Residents may, however, prefer to have shared open space within their neighborhood, as it is in Figure 5-4.

Despite its potential environmental benefits, social critiques of New Urbanism cast it as being racially and socieconomically exclusive ( Clarke, 2005; Day, 2003; Al-Hindi, 2001). The touted environmental benefits have been questioned. In particular, analysts have tested the hypothesis that pedestrianism is indeed heightened in such communities (Patterson and Chapman, 2004). Greenwald (2003) found that New Urban development strategies did increase the substitution of walking for personal automobile usage in one city. Vojnovic (2006), however, observed that neighborhood self-selection may obscure the effect of such development on non-motorized travel behavior, since those inclined to make active travel choices might specifically seek out development friendly to it. Nonetheless, mixed-use development, of which some analysts have identified New Urbanism as a remarketed form, is an economic and perhaps social necessity in areas where open space is precious, such as Hong Kong (Lau et al., 2005). This may be instructive to municipalities experiencing rapid growth and considering such development strategies but not yet approaching build-out.

## 5.7. Conclusions

This study quantified the substantial contribution of the low-density residential development associated with sprawl to one suburban area's total imperviousness. This development was itself heavily vegetated but accounted for 18.5% of total study area imperviousness when both paved surfaces inside residential parcels and roads serving those parcels were considered. Additionally, these residential neighborhoods were associated with retail parking surfaces that also contributed significantly to watershed imperviousness. In all, low-density residential roads, driveways, and lots together with retail parking lots constituted 17.8% of the study area but 24.3% of its imperviousness.

The results of this study indicate that, while the compact development strategies incorporated by New Urbanism may only slightly reduce residential impervious surface area, related decreases in required retail parking space may significantly reduce overall watershed imperviousness. Moreover, these findings suggest that carefully planned compact mixed-use development can arrange impervious surface in a way that enhances suburban environmental quality. Related reductions in suburban parking lot, road, and driveway surfaces should, of course, be considered in light of the non-transportation community functions and interests these land uses may also serve.

Municipalities reluctant to approve large New Urban development projects but interested in water quality-friendly design may wish to merely decrease street setback requirements for residential development and minimum parking space requirements for retail development. Coupled with mixed use or increases in density, these changes may minimize the role of parking surfaces as concentrated sources of impervious surface and vehicle pollutants. Incidentally, the results of this study support the continued use of population density as a measure of sprawl inasmuch as it inversely relates to the extent of transportation infrastructure and segregated land use.

Although the empirical findings of this study most reliably characterize the suburban Raleigh area, they are of broader interest for at least two important reasons. First, the study area is fairly representative of suburban areas throughout the United States (Bjelland et al. 2006). In that light, the estimates of the percent of suburban imperviousness comprised by residential roads, driveways, and retail parking lots may be relevant to a discussion of land use in many places. These estimates may be directly transferable to similar empirical studies. On the other hand, these specific results may not precisely characterize areas outside the temperate deciduous forest region in which this study was set. Akbari (2003), for example, studied a city in the Western United States and found that roads in residential areas accounted for as much as 31.8% of above-the-tree canopy view impervious surface in those areas, a result which contrasts the 7.4% estimate calculated here.

The other broad value of this study is in its presentation of transferable methods for using novel high-spatial resolution satellite imagery such as QuickBird in urban land use analysis. In this study, methods were developed for studying the urban "microlandscape." Such a focus might be used in future studies to examine the relationship between discrete landscape features, such as driveways or parking lots, and highly localized environmental parameters such as water quality. This may uniquely inform the degree to which stormwater drainage infrastructure functions as a source of point-source pollution, an area of growing research interest (Walsh et al., 2004).

This new way to study urban land use is made possible by the resolution and consistency of high spatial resolution satellite imagery, and the methods described here permit a high level of analytical uniformity relative to traditional photointerpretation. The selection of a summer image even minimized complications due to shadowing, the negative image classification effects of which have been noted elsewhere (Dare, 2005). Moreover, for smaller geographic coverages, the cost of tasking new imagery has become comparable to that of contracting for new aerial photography. High-profile usage of such imagery by Internet mapping giants such as Google® will only increase its availability, especially for urban study areas, and a number of new high-resolution satellites are scheduled to launch during the next two years (Shalal-Esa, 2007). For these reasons, analysts and institutions currently buying and working with this imagery are developing databases and expertise that will exponentially increase in value. This is a promising sign of the continued synergy between remote sensing and landscape planning.

### 5.8. References

Akbari, H., L. S. Rose, and H. Taha, 2003. Analyzing the land cover of an urban environment using high-resolution orthophotos, *Landscape and Urban Plan.* 63 (1): 1-14.

Al-Hindi, K. F., 2001. The new urbanism: Where and for whom? Investigation of an emergent paradigm, *Urban Geogr.* 22 (3): 202-219.

Arnold, C., and C. Gibbons, 1996. Impervious surface coverage - The emergence of a key environmental indicator, *J. Am. Plann. Assoc.* 62 (2): 243-258.

Berke, P. R., J. MacDonald, N. White, M. Holmes, D. Line, K. Oury, and R. Ryznar, 2003. Greening development to protect watersheds - Does new urbanism make a difference? *J. Am. Plann. Assoc.* 69 (4): 397-413.

Bjelland, M. D., M. Maley, L. Cowger, and L. Barajas, 2006. The quest for authentic place: The production of suburban alternatives in Minnesota's St. Croix Valley, *Urban Geogr.* 27 (3): 253-270.

Borrego, C., H. Martins, O. Tchepel, L. Salmim, A. Monteiro, and A. T. Miranda, 2006. How urban structure can affect city sustainability from an air quality perspective, *Environ. Modell. & Software* 21 (4): 461-467.

Bowen, J. L., and I. Valiela, 2001. The ecological effects of urbanization of coastal watersheds: historical increases in nitrogen loads and eutrophication of Waquoit Bay estuaries, *Can. J. Fish. Aquat. Sci.* 58 (8): 1489-1500.

Brabec, E., S. Schulte, and P. L. Richards, 2002. Impervious surfaces and water quality: A review of current literature and its implications for watershed planning, *J. Plan. Lit.* 16 (4): 499-514.

Brander, K. E., K. E. Owen, and K. W. Potter, 2004. Modeled impacts of development type on runoff volume and infiltration performance, *J. Am. Water Resour. Assoc.* 40 (4): 961-969.

Brattebo, B. O., and D. B. Booth, 2003. Long-term stormwater quantity and quality performance of permeable pavement systems, *Water Res.* 37 (18): 4369-4376.

Burchell, R. W., and S. Mukherji, 2003. Conventional development versus managed growth: The costs of sprawl, *Am. J. Public Health* 93 (9): 1534-1540.

Burkholder, J. M., E. J. Noga, C. H. Hobbs, and H. B. Glasgow, 1992. New phantom dinoflagellate is the causative agent of major estuarine fish kills, *Nature* 358 (6385): 407-410.

Cakir, H. I., and S. Khorram, 2008. Pixel level fusion of panchromatic and multispectral images based on correspondence analysis, *Photogramm. Eng. Rem. S.* 74 (2): 183-192.

Clarke, P. W., 2005. The ideal of community and its counterfeit construction, *J. Archit. Educ.* 58 (3): 43-52.

Day, K., 2003. New urbanism and the challenges of designing for diversity, *J. Plann. Educ. Research* 23 (1): 83-95.

Dare, P. M., 2005. Shadow analysis in high-resolution satellite imagery of urban areas, *Photogramm. Eng. Rem. S.* 71 (2): 169-177.

de Cerreño, A. L. C., 2004. Dynamics of on-street parking in large central cities, *Transport Res. Rec.* 1898: 130-137.

Deakin, E., A. Bechtel, A. Crabbe, M. Archer, S. Cairns, A. Kluter, K. Leung, and J. Ni, 2004. Parking management and downtown land development in Berkeley, California, *Transport Res. Rec.* 1898: 124-129.

Ewing, R., R. C. Brownson, and D. Berrigan, 2006. Relationship between urban sprawl and weight of United States youth, *Am. J. Prev. Med.* 31 (6): 464-474.

Feitelson, E., and O. Rotem, 2004. The case for taxing surface parking, *Transp. Res. D-Tr. E.* 9 (4): 319-333.

Galster, G., R. Hanson, M. R. Ratcliffe, H. Wolman, S. Coleman, and J. Freihage, 2001. Wrestling sprawl to the ground: Defining and measuring an elusive concept, *Hous. Policy Debate* 12 (4): 681-717.

Gamba, P., F. Dell'Acqua, and G. Lisini, 2006. Improving urban road extraction in high-resolution images exploiting directional filtering, perceptual grouping, and simple topological concepts, *IEEE Geosci. Remote S.* 3(3): 387-391.

Garde, A. M., 2004. New urbanism as sustainable growth? A supply side story and its implications for public policy, *J. Plann. Educ. Research*, 24(2): 154-170.

Greenwald, M. J., 2003. The road less traveled - New urbanist inducements to travel mode substitution for nonwork trips, *J. Plann. Educ. Research*, 23(1): 39-57.

Handy, S., 2005. Smart growth and the transportation - Land use connection: What does the research tell us? *Int. Regional Sci. Rev.* 28(2): 146-167.

Hester, D. B., H. I. Cakir, S. A. C. Nelson, and S. Khorram, 2008. Per-pixel classification of high spatial resolution satellite imagery for urban land cover mapping, *Photogramm. Eng. Rem. S.* 74 (4): 464-471.

Interlandi, S. J., and C. S. Crockett, 2003. Recent water quality trends in the Schuylkill River, Pennsylvania, USA: A preliminary assessment of the relative influences of climate, river discharge and suburban development, *Water Res.* 37 (8): 1737-1748.

Jennings, D., S. Jarnagin, and D. Ebert, 2004. A modeling approach for estimating watershed impervious surface area from national land cover data 92, *Photogramm. Eng. Rem. S.* 70 (11): 1295-1307.

Kasperson, J., 2001. The stormwater utility: Will it work in your community? *Stormwater* 1 (1).

Kim, L. H., S. O. Ko, S. Jeong, and J. Yoon, 2007. Characteristics of washed-off pollutants and dynamic EMCs in parking lots and bridges during a storm, *Sci. Total Environ.* 376 (1-3): 178-184.

Lau, S. S. Y., R. Giridharan, and S. Ganesan, 2005. Multiple and intensive land use: case studies in Hong Kong, *Habitat Int.* 29 (3): 527-546.

Lee, J. G., and J. P. Heaney, 2003. Estimation of urban imperviousness and its impacts on storm water systems, *J. Water Res. Pl.-ASCE* 129 (5): 419-426.

Levine, J., and A. Inam, 2004. The market for transportation-land use integration: Do developers want smarter growth than regulations allow? *Transportation*, 31 (4): 409-427.

Lu, D. S., and Q. H. Weng, 2005. Urban classification using full spectral information of Landsat ETM+ imagery in Marion County, Indiana, *Photogramm. Eng. Rem. S.*, 71 (11): 1275-1284.

Lu, D. S., and Q. H. Weng, 2006. Use of impervious surface in urban land-use classification, *Remote Sens. Environ.* 102 (1-2): 146-160.

Manville, M., and D. Shoup, 2005. Parking, people, and cities, *J. Urban Plan. D.-ASCE* 131 (4): 233-245.

McCauley, S., and S. Goetz, 2004. Mapping residential density patterns using multi-temporal Landsat data and a decision-tree classifier, *Int. J. Remote Sens.* 25 (6): 1077-1094.

M McMahon, G., and O. Lloyd, 1995. Water Quality Assessment of the Albemarle-Pamlico Drainage Basin, North Carolina and Virginia: Environmental Setting and Water-Quality Issues. *U. S. Geological Survey Open File Report* 95-136. U. S. Geological Survey, Raleigh, North Carolina, 72p., abstract available at http://nc.water.usgs.gov/reports/abstracts/ofr95136.html (last accessed 25 Oct. 2007).

Mildner, G. C. S., J. G. Strathman, and M. J. Bianco, 1997. Parking policies and commuting behavior, *Transport. Q.* 51 (1): 111-125.

Moglen, G. E., and S. Kim, 2007. Limiting imperviousness - Are threshold-based policies a good idea?, *J. Am. Plann. Assoc.*, 73 (2): 161-171.

Moudon, A. V., S. E. Kavage, J. E. Mabry, and D. W. Sohn, 2005. A transportation-efficient land use mapping index, *Transport. Res. Rec.* 1902: 134-144.

North Carolina Department of Environment and Natural Resources (NCDENR), 2006, *Final North Carolina Water Quality Assessment and Impaired Waters List (2004).* Available online at http://h2o.enr.state.nc.us/tmdl/documents/2004IRCategories4-7.PDF (last accessed: 07 Oct 2007).

North Carolina Department of Environment and Natural Resources (NCDENR), 2007. *Final North Carolina Water Quality Assessment and Impaired Waters List (2006).* Available online at http://h2o.enr.state.nc.us/tmdl/documents/303d_Report.pdf (last date accessed: 07 Oct 2007).

Paerl, H. W., J. L. Pinckney, J. M. Fear, and B. L. Peierls, 1998. Ecosystem responses to internal and watershed organic matter loading: consequences for hypoxia in the eutrophying Neuse river estuary, North Carolina, USA, *Mar. Ecol. Prog. Ser.* 166: 17-25.
Patterson, P. K., and N. J. Chapman, 2004. Urban form and older residents' service use, walking, driving, quality of life, and neighborhood satisfaction, *Am. J. Health Promot.*

19 (1): 45-52.

Pendola, R., and S. Gen, 2007. BMI, auto use, and the urban environment in San Francisco, *Health Place* 13 (2): 551-556.

Ross, N. A., S. Tremblay, S. Khan, D. Crouse, M. Tremblay, and J. M. Berthelot, 2007. Body mass index in urban Canada: Neighborhood and metropolitan area effects, *Am. J. Public Health* 97 (3): 500-508.

Sanders, R. A., 1986. Urban Vegetation Impacts on the Hydrology of Dayton, Ohio, *Urban Ecol.* 9 (3-4): 361-376.

Shalal-Esa, A., 2007 (Sept. 14), *New satellite to sharpen Google Earth*, Reuters, available at http://www.reuters.com/article/newsOne/idUSN1445933620070914 (last accessed: 21 Oct. 2007).

Shoup, D. C., 1999. The trouble with minimum parking requirements, *Transport. Res. A-Pol.* 33 (7-8): 549-574.

Snyder, M. N., S. J. Goetz, and R. K. Wright, 2005. Stream health rankings predicted by satellite derived land cover metrics, *J. Am. Water Resour. As.* 41 (3): 659-677.

Speir, C., and K. Stephenson, 2002. Does sprawl cost us all? Isolating the effects of housing patterns on public water and sewer costs, *J. Am. Plann. Assoc.* 68(1): 56-70.

Stone, B., 2004. Paving over paradise: how land use regulations promote residential imperviousness, *Landscape and Urban Plan.* 69 (1): 101-113.

Thomas, N., C. Hendrix, and R. Congalton, 2003. A comparison of urban mapping methods using high-resolution digital imagery, *Photogramm. Eng. Rem. S.* 69 (9): 963-972.

Thompson-Fawcett, M., and S. Bond, 2003. Urbanist intentions for the built landscape: examples of concept and practice in England, Canada and New Zealand, *Prog. Plann.* 60: 147-234.

Torres, H., H. Alves, and M. A. De Oliveira, 2007. Sao Paulo peri-urban dynamics: some social causes and environmental consequences, *Environ. Urban.* 19 (1): 207-223.

Tu, J., Z. G. Xia, K. C. Clarke, and A. Frei, 2007. Impact of urban sprawl on water quality in eastern Massachusetts, USA, *Environ. Manage*. 40 (2): 183-200.

U.S. Census Bureau, 2003. *Table HU-EST2002-07 - County Housing Unit Estimates*. http://www.census.gov/popest/archives/2000s/vintage_2002/HU-EST2002-07.html (last accessed: 26 Nov. 2007).

Van Bohemen, H. D., and W. H. J. Van de Laak, 2003. The influence of road infrastructure and traffic on soil, water, and air quality, *Environ. Manage*. 31 (1): 50-68.

Vojnovic, I., 2006. Building communities to promote physical activity: A multi-scale geographical analysis, *Geogr. Ann. B.* 88B (1): 67-90.

Walsh, C. J., P. J. Papas, D. Crowther, and J. Yoo, 2004. Stormwater drainage pipes as a threat to a stream-dwelling amphipod of conservation significance, Austrogammarus australis, in southeastern Australia, *Biodivers. Conserv.* 13 (4): 781-793.

Yang, R., and P. A. Jargowsky, 2006. Suburban development and economic segregation in the 1990s, *J. Urban Aff.* 28(3): 253-273.

Zhu, C., W. Shi, M. Pesaresi, L. Liu, X. Chen, and B. King, 2005. The recognition of road network from high-resolution satellite remotely sensed data using image morphological characteristics, *Int. J. Remote Sens.* 26 (24): 5493-5508.

# 6. CONCLUSION

## 6.1. Summary of findings

### *6.1.1.* An overview

The research described here developed methods for analyzing land use and land cover with high spatial resolution QuickBird satellite imagery. It is presented in three substantive chapters, each one a stand-alone manuscript submitted for peer-review publication. In the first chapter, a land cover classification method is developed and used to produce an accurate 61-cm land cover map for a suburban Raleigh, NC, study area. This method was used to produce a second land cover map of the same study area at a later date, and a change detection method is developed. In the final manuscript, the land cover map generated in the first chapter is used in an urban planning and watershed management application with land use policy implications. The following three sub-sections summarize the findings of these three chapters.

### *6.1.2.* Land cover classification using high spatial resolution imagery

In the work described here, per-pixel classification, image fusion, and GIS-based map refinement techniques were tailored to pan-sharpened 0.61 m QuickBird imagery to develop a six-category urban land cover map with 89.3 percent overall accuracy ($\kappa$ = 0.87). The study area was a rapidly developing 71.5 $km^2$ part of suburban Raleigh, North Carolina, U.S.A., within the Neuse River basin. “Edge pixels” were a source of classification error as was spectral overlap between bare soil and impervious surfaces and among vegetated cover types. Shadows were not a significant source of classification error. These findings demonstrate that conventional spectral-based classification methods can be used to generate highly accurate maps of urban landscapes using high spatial resolution imagery.

### *6.1.3.* High spatial resolution land cover change detection

The primary objective of this research was to develop a change detection method that incorporated spatial and classification uncertainty in generating an accurate map of land cover change. As a secondary objective, this method was designed to facilitate the mapping of particular types and locations of change based on specific study goals. Urban land cover change pertinent to surface water quality in Raleigh, North Carolina, was evaluated using land cover classifications derived from pan-sharpened, 0.61 m QuickBird images from 2002 and 2005. A "from-to" change map had an overall accuracy of 78.9% ($\kappa = 0.747$) and effectively mapped land cover changes posing a threat to water quality, including increases in impervious surface. This work presents an efficient fuzzy framework for transforming map uncertainty into accurate and meaningful change analysis.

### *6.1.4.* Analysis of impervious surface using high spatial resolution imagery

Sources of impervious surface in suburban areas include roads, houses, buildings, parking lots, and driveways, and the arrangement and extent of these features are critical urban planning variables. The study used high spatial resolution satellite imagery to quantify the contribution of suburban imperviousness from sources closely associated with private automobile usage. Specifically, in a 71.5 $km^2$ study area in suburban Raleigh, NC, USA, QuickBird satellite image data were used to quantify the extent of imperviousness from low-density residential roads and driveways and from retail parking lots. These landscape features constituted only 14.3% of overall study area imperviousness but 58.8% of the imperviousness associated with low-density residential land use. Retail parking lots constituted 5.8% of study area impervious surface. A compact New Urban development within the study area was compared to a conventional low-density neighborhood in order to frame these findings within the context of contemporary urban planning and design. This study empirically documents the connections between conventional suburban form, private automobile-oriented transportation infrastructure, and watershed imperviousness, and it demonstrates the continuing synergy between remote sensing and landscape planning.

### 6.2. Recommendations for future studies

The research described here developed methods for using next-generation high spatial resolution satellite imagery to map urban land cover and its change. Given its novelty, future research directions using this imagery and these methods are numerous, and the following recommendations are made with the hope of informing that work:

- An inherent characteristic of digital data rich in information content is large file size. The QuickBird image files featured in this work were each over 4 GB in size, a fact that had substantial processing time, storage, and transfer implications. Analysts are advised to consider computing hardware needs before purchasing this imagery. In completing the work described here, a 2.41 GHz processor with 1 GB RAM was minimally sufficient.
- Using the methods described here, a robust water quality study using high spatial resolution land cover data and *in situ* water quality data could be developed. Such a study would exploit the potential of such land cover products to analyze the hydrologic effect of spatially-explicit landscape features such as stormwater infrastructure, tree canopy, and riparian land cover.

- Object-oriented and textural methods of analyzing high spatial resolution imagery should continue to be explored and may benefit from integration with successful per-pixel classification such as is described here. Non-distinct image elements, such as shadow regions, may particularly benefit from the intersection of per-pixel and object-oriented classification.
- Accuracy assessment methods well-suited to high spatial resolution land cover products are not evolving in the literature as quickly as methods for their generation. Future work exploring high resolution accuracy assessment would be a valuable research contribution.
- Image acquisition parameters should be of utmost importance to analysts considering the use of high spatial resolution satellite imagery. In the work described here, the effect of shadows was minimal because of the mid-day, summer season high sun angle. As a corollary to this recommendation, the work described here largely does not speak to leaf-off image analysis, a promising research subset of shadow analysis.
- High spatial resolution satellite imagery will become an increasingly cost-effective data source as additional platforms are launched, and high-profile Internet map applications such as Google Maps have rendered its usage at least as a backdrop a virtual given, even in mainstream applications. As a result, analysts are advised that academic, industry, and lay audiences alike will probably begin to expect its inclusion in a wide variety of research presentations.